Biopolymers and -oligomers of (*R*)-3-Hydroxyalkanoic Acids – Contributions of Synthetic Organic Chemists –

D. Seebach, A. Brunner,
B. M. Bachmann, T. Hoffmann,
F. N. M. Kühnle, U. D. Lengweiler

Ernst Schering Research Foundation

28

Lecture

Biopolymers and -oligomers of (*R*)-3-Hydroxyalkanoic Acids – Contributions of Synthetic Organic Chemists –

D. Seebach*, A. Brunner, B. M. Bachmann, T. Hoffmann, F. N. M. Kühnle, U. D. Lengweiler

*Laboratorium für Organische Chemie
Eidgenössische Technische Hochschule Zürich
Universitätstrasse 16
CH-8092 Zürich

Dedicated to Prof. Dr. Albert Eschenmoser at the occasion of his 70th birthday

Ernst Schering Research Foundation

Lecture

Published by
Ernst Schering
Research Foundation

All rights reserved.
No part of this publication may be translated into other languages, reproduced or utilized in any form or by any means, electronic or mechanical, including photocopying, recording, microcopying, or by any information storage and retrieval system, without permission in writing from Ernst Schering Research Foundation.

Editor: Information and Standards Medical Scientific Publications R.A. Henry A. Schlemmer
Design: Corporate Design Management
Composition and print: Druckerei Hellmich KG, Berlin
Printed in Germany
© Copyright 1995 by Ernst Schering Research Foundation 13342 Berlin, Germany
ISSN 0940-9300

Lectures Published

Vol. 1 (1991):
Gary D. Hodgen, Norfolk
The Physiology of Ovarian Follicular Maturation

Vol. 2 (1991):
D.M. Kolb, Ulm
The Initial Stages of Metal Deposition: An Atomistic View

Vol. 3 (1992):
Stephen I. Katz, Bethesda
The Skin Immune System. Allergic Contact Dermatitis as a Paradigm

Vol. 4 (1992):
Peter Dawson, London
Some Current Issues in Iodinated Contrast Agent Research

Vol. 5 (1992):
P. M. Vanhoutte, Houston
Endothelium-Derived Vasoactive Factors, Platelets and Coronary Disease

Vol. 6 (1992):
Jeff Schell
Jürgen Logemann, Köln
Pflanzliche Gentechnologie – Perspektiven für die praktische Anwendung in der Landwirtschaft

Vol. 7 (1992):
Hans J. Müller-Eberhard, Hamburg
The Molecular Basis of Target Cell Killing by Human Lymphocytes and of Killer Cell Self-Protection

Vol. 8 (1992):
Désiré Collen, Leuven
Thrombolysis: is there a Future for Thrombolytic Therapy in Acute Myocardial Infarction?

Vol. 9 (1992):
Egon Diczfalusy, Stockholm
Contraceptive Prevalence and the 1990s – a Critical Issue, a Critical Decade

Vol. 10 (1992):
Helmut Schwarz, Berlin
Chemie „nackter" Moleküle – oder das Massenspektrometer als Laboratorium

Vol. 11 (1992):
Paul M. Wassarman, Nutley
Early Events in Mammalian Fertilization

Vol. 12 (1992):
Wolf Singer, Frankfurt/Main
The Formation of Representations in the Cerebral Cortex

Vol. 13 (1993):
Peter Gruss, Göttingen
Partitur der Kontrollprozesse zur Entwicklung von Säugern

Vol. 14 (1993):
Rainer Hegselmann, Bremen
Eike von Savigny, Bielefeld
Über die Herkunft menschlicher Werte

Vol. 15 (1993):
Geoffrey Thomas, Oxford
Science in the Public Mind: A Cause for Concern?

Vol. 16 (1993):
Ludwig Missiaen, Leuven
Role of Ins(1,4,5)P_3-Sensitive Ca^{2+} Stores in Setting up Spatiotemporally Organized Ca^{2+} Signals in Mammalian Cells

Vol. 17 (1993):
Johann Mulzer, Berlin
Das Phänomen der Chiralität – Laune oder Fundamentalprinzip der Natur?

Vol. 18 (1993):
Walter Wahli, Lausanne
Fatty Acids Control Gene Expression through Members of the Nuclear Receptor Superfamily

Vol. 19 (1994):
Günter Schultz, Berlin
G Proteins Involved in Hormonal Regulations of the Cytoplasmic Calcium Concentration

Vol. 20 (1994):
Charles T. Esmon, Oklahoma
Cell Mediated Events that Control Blood Coagulation and Vascular Injury

Vol. 21 (1994):
Lothar Willmitzer, Berlin
New Developments in Plant Biotechnology

Vol. 22 (1994):
Gerald R. Cunha, San Francisco
Development of the Urogenital Tract: The Interface Between Developmental Biology and Endocrinology

Vol. 23 (1994):
Peter W. Vaupel, Mainz
Blood Flow, Oxygenation, Tissue pH Distribution, and Bioenergetic Status of Tumors

Vol. 24 (1994):
Wolfgang Steglich, München
Mushrooms –
Seen through the Eyes
of an Organic Chemist

Vol. 25 (1995):
H. Ringsdorf, W. Müller,
E. Rump, Mainz
Attempts to Mimic
Docking Processes of
the Immune System:
Formation and
Competitive Replacement
of Protein Multilayers

Vol. 26 (1995):
S. J. Danishefsky, J. T. Randolph,
J. Y. Roberge, K.F. McClure, R. B. Ruggeri,
New York
Recent Applications of the
Glycal Assembly Method:
Solid-Phase Synthesis of
Oligosaccharides and Glycoconjugates

Vol. 27 (1995):
Bruce S. McEwen, New York
Steroid Actions on Neuronal Signalling

Contents

Introduction	7
Polyhydroxyalkanoates as Cellular Storage Materials	8
Physical Properties of Poly-(*R*)-3-hydroxybutyrate	10
Crystalline Structure of Poly-(*R*)-3-hydroxybutyrate	11
Poly-(*R*)-3-hydroxybutyrate Metabolism	12
Cloning and Expression of the P(3-HB) Biosynthetic Pathway of *A. eutrophus*	13
Industrial Production of Polyhydroxyalkanoates	14
Use of Polyhydroxyalkanoates	17
PHAs as Biologically Degradable Plastics	17
Other Applications of Poly-(R)-3-hydroxybutyrate	20
Extracellular Biological Degradation of Poly-(*R*)-3-hydroxybutyrate	21
Polyhydroxy Acids as Chiral Synthetic C_4 Building Blocks	21
Chemical Degradation of Poly-(R)-3-hydroxybutyrate	22
Derivatives of the Cyclic 3-HB Trimer	23
Poly-(*R*)-3-hydroxybutyric Acid as a Component of a Natural, Nonproteinogenic Ion Channel?	27
Isolation and Characterization by ^{1}H-NMR Spectroscopy of *c*-P(3-HB) from Eukaryotic and Prokaryotic Organisms	34
Partial Depolymerization of Poly-(*R*)-3-hydroxybutyrate	39
Synthesis of Nearly Monodisperse Oligomers of 3-HB	42
Synthesis of Entirely Monodisperse 3-HB Oligomers	47
Solid State Structures of P(3-HB) and of Oligo(3-HB) Derivatives	50
Results from Transmission Electron Microscopy, from Small and Wide Angle X-Ray Scattering (WAXS) and from Atomic Force Microscopy	53
Preparation of Cyclic Oligomers from (*R*)-3-Hydroxybutyric, -valeric, and -octanoic Acid	56
Structural Studies – the Cyclic Oligomers as Model Compounds for the Polymer	60
Cation Transport across Bulk Liquid Organic Membranes	72

Electrophysiological Investigations on the Native P(3-HB)/Ca·PP_i Complex from Competent *E. coli*	77
Patch Clamp Experiments on Planar Bilayers with the Synthetic Oligomers of 3-HB	80
An Alternative Model for the P(3-HB) Ion Channel	82
Degradation Studies with 3-HB Oligolides and with Linear 3-HB Octamers Bearing Various End Groups	85
Degradation Studies on Linear 3-HB Octamers with a Specific Sequence of (*R*)- and (*S*)-Configurations	88
Conclusions and Outlook – PHAs, a Fifth Class of Physiologically Important Biopolymers	89
Acknowledgements	91
References	92
Curriculum Vitae Dieter Seebach	99
Curricula Vitae A. Brunner, B. M. Bachmann, T. Hoffmann, F. N. M. Kühnle, U. D. Lengweiler	105

Introduction

Polyhydroxyalkanoates (PHAs) are known as microbial storage compounds. They are polyesters with the general structure shown in Figure 1, the monomeric units being (*R*)-3-hydroxyalkanoic acids.

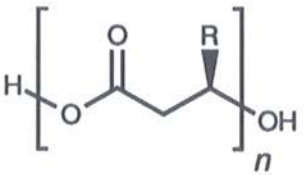

Fig. 1: General chemical structure of PHAs.

PHAs are synthesized by microorganisms, under conditions of nutrient limitation, in the presence of excess carbon and energy sources. Due to the low aqueous solubility and the high molecular weight, they do not cause an increase in osmotic pressure and are therefore ideal storage compounds [1]. In this role, PHAs are much more common in microorganisms than compounds such as glycogen or polyphosphates [2]. The most prominent example of the PHAs, poly-(*R*)-3-hydroxybutyrate [P(3-HB)], is a linear, unbranched homopolymer built up of (*R*)-3-hydroxybutyric acid units. The molecular weight values given in the literature vary considerably and are dependent upon microorganism, cultivation conditions and the method of isolation. Typically, they lie between 100,000 and 750,000 g/mol (n = 1000-9000, polydispersity (M_w/M_n) = 1.7-2.9 [3]), but they can be greater than one million. The copolymer poly-[(*R*)-3-hydroxybutyrate-(*R*)-3-hydroxyvalerate] [P(3-HB/3-HV)] has acquired some economic importance because it has properties similar to those of polypropylene. It is now marketed under the tradename BIOPOL™ by ZENECA Bio Products, a company resulting from the demerger of ICI [4]. The "microbial plastics", P(3-HB) and P(3-HB/3-HV), are biodegradable and their synthesis is based on renewable materials [5, 6]. Because of these qualities, an ever increasing interest in P(3-HB) within both the science community and the general public has developed; this is apparent by their regular appearances in the press [7–11], in review articles [3, 12–23], which are published increasingly frequently and in an increasing number of patents.

P(3-HB) was first described by *Lemoigne* in 1925 [24]. He later isolated and identified the material from *Bacillus megaterium* [25]. Since then, it has been identified in a large number of different microorganisms [18], a survey of microorganisms known to form intracellular PHAs is given in Table 1.

Acinetobacter	*Alcaligenes*	*Aphanothece*	*Aquaspirillum*
Azospirillum	*Azotobacter*	*Bacillus*	*Beggiatoa*
Beijerinckia	*Caulobacter*	*Chloroflexus*	*Chlorogloea*
Chromatium	*Chromobacterium*	*Clostridium*	*Derxia*
Ectothiorhodospira	*Gamphosphaeria*	*Halobacterium*	*Hyphomicrobium*
Lamprocystis	*Lampropedia*	*Leptothrix*	*Methylobacterium*
Methylocystis	*Methylosinus*	*Micrococcus*	*Microcoleus*
Microcystis	*Moraxella*	*Mycoplana*	*Nitrobacter*
Nitrococcus	*Nocardia*	*Oceanospirillum*	*Paracoccus*
Photobacterium	*Pseudomonas*	*Rhizobium*	*Rhodobacter*
Rhodospirillum	*Sphaerotilus*	*Spirillum*	*Spirulina*
Stroptomyces	*Syntrophomonas*	*Thiobacillus*	*Thiocapsa*
Thiocystis	*Thiodictyon*	*Thiopedia*	*Thiosphaera*
Vibrio	*Xanthobacter*	*Zoogloea*	

Table 1: Microorganisms known to accumulate poly-(*R*)-3-hydroxyalkanoates. (Table taken from [18]).

P(3-HB) is present in archaebacteria, in both *Gram*-negative and *Gram*-positive bacteria and in cyanobacteria. Apart from a few phototrophic microorganisms, *Clostridium* and *Syntrophomonas* are the only strict anaerobes in which P(3-HB) has been found. Interestingly, enterobacteria (gut bacteria) such as *Escherichia coli* do not normally synthesize P(3-HB) as a storage compound [18, 26]. Certain strains, however, are reported to accumulate small quantities of P(3-HB) under the appropriate conditions [27].

Polyhydroxyalkanoates as Cellular Storage Materials

The role of polyhydroxyalkanoates is to store carbon-containing material and reducing equivalents in the cells of prokaryotic microorganisms (up to 90% of cell dry weight!). It has been demonstrated that microorganisms with PHA storage materials can survive "starvation periods" much better than those without them. This ability to survive is often directly proportional to the initial PHA content [14]. The biosynthesis of high molecular weight P(3-HB) has been the subject of the most intensive studies. These have shown which other hydroxy acids can be incorporated into the polymer, in both natural or synthetic growth media. The enzymes involved have been identified and they have been expressed in other microorganisms using genetic technology.

P(3-HB) accumulation in the microorganism begins when the limitation of a nutrient (either nitrogen, oxygen or phosphorus, dependent upon bacterium [18]) occurs. Degradation is initiated if too little carbon source is present and hence, acetyl-CoA units can be released from P(3-HB).

PHAs occur in the cytoplasm of the cell in the form of inclusion bodies, or so-called granules (see Fig. 2). Typically, these have a diameter of 100-800 nm and have been shown to be surrounded by a kind of micelle ("monolayer") but not by a double layered structure (typical membrane, lipoprotein bilayer) [28]. Depending on the bacterium, the PHA-synthase and depolymerase system may also be bound to this envelope. Purified granules from *B. megaterium* consist of 97.7% P(3-HB), 1.8% protein and 0.5% lipid [3, 29].

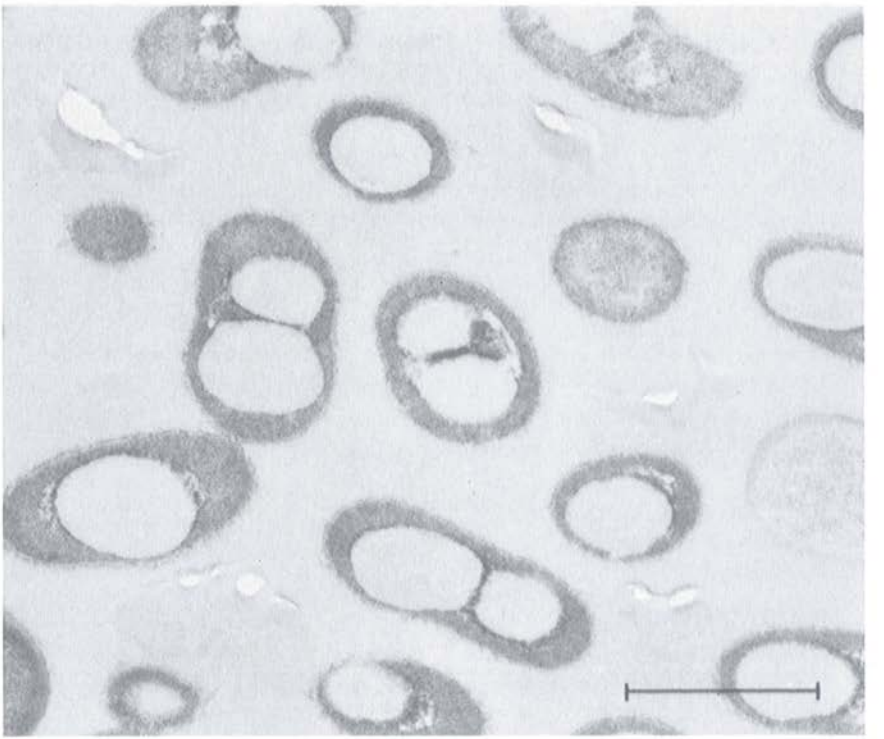

Fig. 2: Electron micrograph of ultrathin sections of *A. eutrophus* showing P(3-HB) inclusions, scale bar 1 µm. (Figure taken from [3]).

Until recently, the structure of P(3-HB) within the granules has been the subject of great debate. All that was previously known was that treatment with solvents, bases or acids, cooling or heating inhibited their enzymatic digestion [30]. More

recently, *Doi et al.* [31] (by X-ray diffraction) and *Sanders et al.* [32, 33] (by high resolution ^{13}C-NMR spectroscopy) have shown that the P(3-HB) within the native granules is present in an amorphous form. This is surprising, since isolated P(3-HB) normally reveals between 60 and 70% crystallinity. Many different explanations for the amorphous state of the native P(3-HB) granules have been given, including water as plasticizer or the presence of an unknown lipid that acts as an inhibitor for crystallization. Recently, it has been shown that stable amorphous polymer granules can be prepared *in vitro* [34], supporting the hypothesis that only the slow nucleation kinetics, which are operative for small particles, are responsible for the metastable amorphous state of the PHAs *in vivo* [33, 35].

Physical Properties of Poly-(*R*)-3-hydroxybutyrate

P(3-HB) is a stereoregular polyester. The absolute configuration of all the β-carbons in the polymer are identical, so the polymer is completely isotactic [36] (it should be noted that a strain of *Rhodococcus* is reported to produce P(3-HB/3-HV) that is not optically pure when grown on glucose as the sole carbon source [37]).

The physical properties of PHA copolymers can be regulated by variation of the monomer structure and copolymer composition.

A survey of the most important physical properties of P(3-HB) is given in Table 2.

Melting point T_m	173 - 180 °C
Glass transition temperature T_g	5 - 10 °C
Density	1.25 g/cm^3
Crystallinity	65 - 80%
Molecular weight M_w	10000 - 8x10^5
Tensile strength	40 MPa
Flexural modulus	3.5 GPa
Piezoelectric coefficient	1.67 pC/N

Table 2: Physical and mechanical properties of P(3-HB). (Data taken from [20]).

The physical and mechanical properties of PHAs with side chains other than methyl (homo- or copolymers) can vary considerably from the data given above. Normally, the crystallinity of the polymer decreases as the length of the side chain increases. The melting point of P(3-HB/3-HV) is also reduced as the percentage of valerate incorporated is increased.

While P(3-HB) is a relatively stiff and brittle material, P(3-HB/3-HV) has greatly improved mechanical properties (in particular, the flexibility and toughness improve with increasing 3-HV content), which are somewhat similar to polypropylene as shown in Table 3. The oxygen permeability of the PHAs are similar to PET, which is used as packaging material.

Additionally, the mechanical properties of P(3-HB) can be considerably improved by a simple annealing process [38].

	P(3-HB)	P(3-HB/3-HV)	PP	PET
Melting point [°C]	180	145	176	267
Crystallinity [%]	60 - 80	50 - 60	50 - 70	30 - 50
Flexural modulus [GPa]	3.5	1.2	1.7	2.9
Tensile strength [MPa]	40	32	38	70
Extension to break [%]	8	50	400	100
Oxygen permeability[a)]	45	60[b)]	1700	70

a) [$cm^3/m^2/atm/day$] normalized for 25 µm thick film

b) 17 mol% 3-HV

Table 3: Mechanical properties of P(3-HB) and P(3-HB/3-HV) with 20 mol% 3-HV compared with polypropylene (PP) and polyethyleneterephthalate (PET) [3,39].

The modification of PHAs, after their extraction from bacteria, can lead to a wide range of polymers with interesting physical and mechanical properties. For example, cross-linking of PHA, which contains a certain percentage of unsaturated side chains, results in the formation of a rubber-like material that remains biodegradable [40].

Crystalline Structure of Poly-(*R*)-3-hydroxybutyrate

Cornibert and *Marchessault* have confirmed the structure of P(3-HB) in the crystalline state, using X-ray diffraction measurements (Fig. 3). The P(3-HB) molecules assume the structure of a left-handed 2_1 helix with a fibre period of 5.96 Å. The unit cell of the crystal contains two helices in an antiparallel arrangement [41].

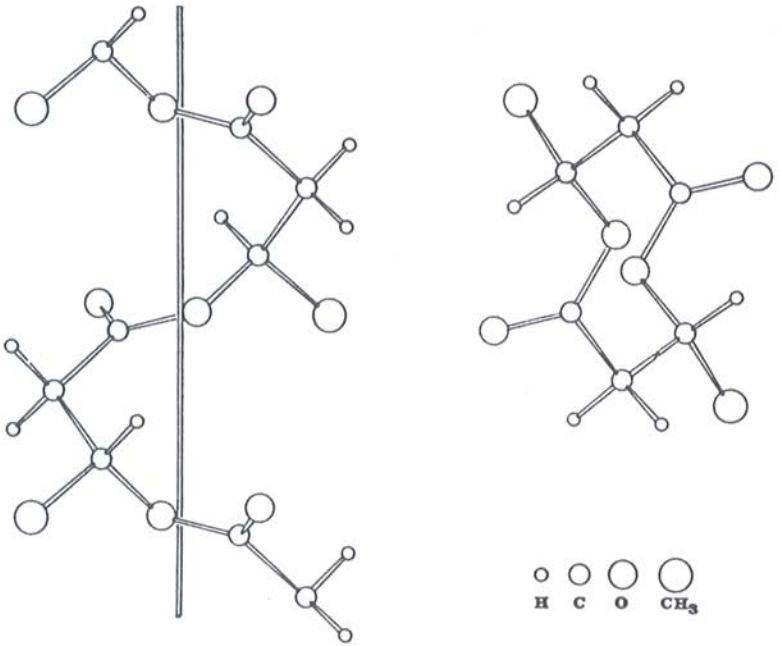

Fig. 3: Structure of P(3-HB) in the crystalline state as modelled from fibre X-ray diffraction measurements [42]. Left: View from a direction normal to the helix axis. Right: View along the helix axis.

Poly-(*R*)-3-hydroxybutyrate Metabolism

Intracellular P(3-HB) metabolism is a cyclic process, which involves seven enzymes. This process has been investigated in a variety of microorganisms by different groups. The best known and probably most widely distributed P(3-HB) metabolic pathway, which also occurs in *Alcaligenes eutrophus, Zoogloea ramigera* and *Azotobacter beijerinckii,* is shown in Figure 4. The key step of the polymer synthesis is the polymerization reaction by the P(3-HB) synthetase with (*R*)-3-hydroxybutyryl-CoA as substrate.

In other bacteria, variations of the metabolic pathway have been found. For a survey of the biosynthesis and enzymatic depolymerization of P(3-HB) see [22].

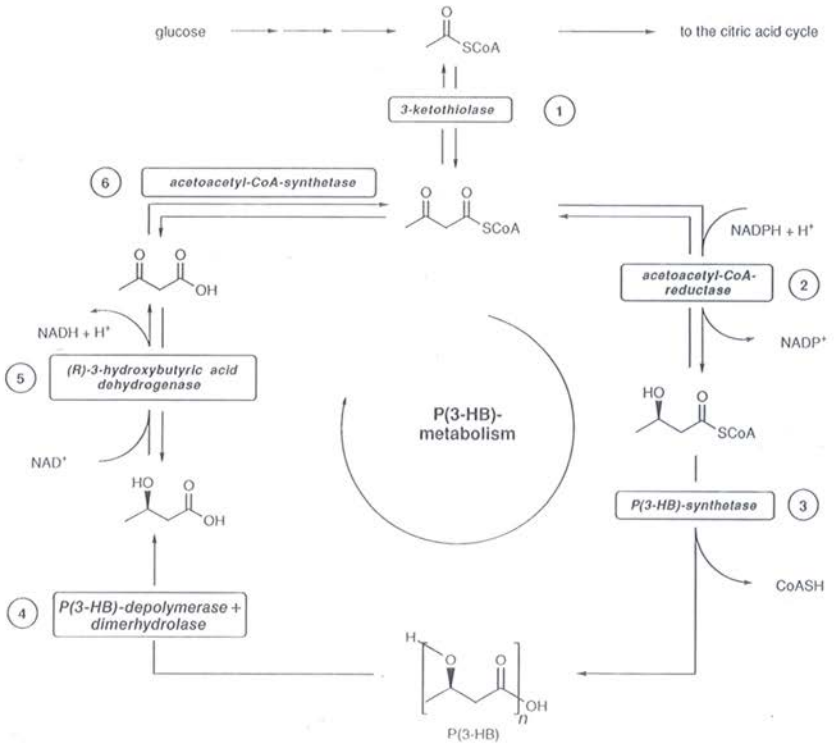

Fig. 4: The best known and most common P(3-HB) metabolic pathway [22].

Cloning and Expression of the P(3-HB) Biosynthetic Pathway of *A. eutrophus*

In order to obtain a more convenient and robust means of microbial product formation, the genes coding for the biosynthetic pathway may be transferred from the original organism. This allows for alternative (cheaper) raw materials to be used and mechanistic questions to be investigated [43]. Often the genes coding for the biosynthesis lie close to each other on the DNA strand, making transfer to another organism somewhat simpler. When the great expectations placed on PHAs are considered, it is hardly surprising that several research groups have cloned and expressed the *A. eutrophus* P(3-HB) biosynthetic genes (Steps 1-3, Fig. 4) in *E. coli* [26, 44–46]. The wild type of *E. coli* does not normally synthesize PHAs. However, the mutant with the P(3-HB) biosynthetic genes expressed can produce ca. 50% of its dry weight as P(3-HB) (with some strains up to 80%). Here too, it appears in the form of intracellular granules.

Other projects are, at present, probably more visions of the future than reality. It is planned to insert the P(3-HB) synthesis genes of *A. eutrophus* into potatoes or other plants, in order to harvest a type of "plastic potato" after expression of the genes. A first realization of this idea has been reported by *Somerville et al.*, they were able to transfer the genes responsible for P(3-HB) synthesis into the higher plant *Arabidopsis thaliana,* where a P(3-HB) synthesis of up to 14% of the dry mass could be achieved [39, 47, 48].

Fig. 5: Future prospect of agricultural plastic production as seen by the cartoonist *Y. Rook* (from Science 1989, 245:1187).

Industrial Production of Polyhydroxyalkanoates

P(3-HB) and P(3-HB/3-HV) (BIOPOL) are produced by ZENECA from renewable feed stocks by a fermentation process. The microorganism that was chosen by ZENECA for the production of BIOPOL is a nonpathogenic *A. eutrophus*

strain that grows on glucose. In the first stage of fermentation, the microorganism is grown in a medium, where the phosphate content is such, that only a certain amount of cell growth is allowed. When the cell concentration has reached a defined value, the phosphate supply becomes depleted and the culture enters phosphate limitation. During the second stage, glucose is fed and the dry weight of the biomass rises due to massive PHA accumulation. Concentrations of PHA of up to 80% of the total dry cell weight can be achieved. The 3-HV content of the PHA accumulated in the cell can be regulated between 0 and 30% by addition of the appropriate amount of propionic acid to the nutrient solution. At the end of the fermentation process, the plastic is harvested by an aqueous extraction process which removes the cell components and leaves behind purified polymer that is dried to a fine, white powder [49, 50].

For the production of P(3-HB) by fermentation, a lot of substrates can be used. Table 4 gives an overview of different substrate prices and the corresponding costs of P(3-HB) production.

Substrate	Approximate price $/t	Yield (wt/wt) of P(3-HB)/substrate	Substrate costs $/t P(3-HB)
Methanol	184	0.18	1020
Ethanol	502	0.50	1005
Acetic Acid	705	0.33	2135
Sucrose	790	0.33	2395
Glucose	493	0.33	1495
Fructose	517	0.33	1565
Cane molasses	220	0.42	524
Lactose (cheese whey)	71	0.33	215

Table 4: Substrate prices, yields of P(3-HB) and costs (dependent on substrates) of P(3-HB) production [51].

Besides glucose, a range of carbohydrates obtained from a wide variety of crops may be used as substrates for the production of P(3-HB) by fermentation. As the overall production costs are not only substrate dependent (rate of polymer accumulation, polymer content and ease of P(3-HB) extraction must also be considered), ZENECA has chosen to use glucose as the substrate for the fermentation process [52]. Nevertheless, fermentation processes are in development, which use cheaper substrates such as beet molasses [53, 54] or methanol [55, 56] for PHA production.

Until recently, P(3-HB) was also industrially produced by Chemie Linz GmbH in Austria on a 50 tons per annum scale. For the fermentation process, they used the microorganism *A. latus* [57]. The production of P(3-HB) by this fermentation process will be continued by the Biomer company on the same scale [58].

To date, the polyesters P(3-HB) and P(3-HB/3-HV) are the only PHAs that have been produced by biotechnological methods on a large scale. Using these methods, about 1 kg P(3-HB) can be made from 2.5 kg glucose [59]. The annual production of BIOPOL by ZENECA is approximately 1000 tons. The production costs at present constitute about $15 per kilogram; the future aim is a kilo-price of $5. This is achievable if the production rate can be increased to ca. 10,000 tons or more per year [47].

By employing phototrophic microorganisms, it is possible to utilize sunlight as an energy source. Thus, *Rhodobacter sphaeroides* synthesizes up to 70% of its dry weight as P(3-HB) [60].

Beside the PHAs containing (*R*)-3-hydroxybutyric and (*R*)-3-hydroxyvaleric acid as monomeric units, PHAs with a variety of unfunctionalized and functionalized side chains have been produced by fermentation processes with the appropriate microorganisms and substrates. Surveys covering the different PHAs isolated so far can be found in the literature [17, 18, 20, 22].

One interesting organism is the bacterium *Pseudomonas oleovorans*. When grown on aliphatic hydrocarbons (*n*-hexane to *n*-decane) in a two-phase fermentation process, PHAs with 3-hydroxyalkanoate monomeric units from the corresponding alkanes are formed [61].

Microbiological production of PHAs with a great variety of compositions and material properties is therefore possible, even if at present the yields are unsatisfactory and the starting materials are derived from oil. How far these disadvantages can be countered by the use of organisms, which have been modified by genetic engineering, remains to be determined.

Synthetic methods are at present not well enough developed to compete with biotechnological production, at least in the case of BIOPOL. On the other hand, a broad range of (*R*)- and (*S*)-3-hydroxy acids is now readily available by enantioselective hydrogenation of the corresponding 3-keto esters [62–64]. It can therefore be expected that in the future, synthetic processes will be developed which will be a match for microbial methods [48]. With such a procedure, a variety of polymers will probably become accessible without great changes in the reaction conditions. In addition, work-up of these reactions is likely to prove far simpler than those used for biotechnological production methods, since it will be possible to work at high concentrations and in organic solvents.

Use of Polyhydroxyalkanoates

PHAs as Biologically Degradable Plastics

Plastics make up about nine percent by weight and over thirty percent by volume of the total waste produced in the USA as estimated for the year 2000 (Fig. 6a) [65], similar distributions are to be found in Europe. This can be explained, in part, by the fact that the replacement of glass, paper or metal as packaging materials by plastic is seen more and more frequently. In practice, there are four possibilities for the disposal of municipal waste: incineration, landfill, recycling and composting. In Europe, 60% of the municipal waste is disposed of in landfills, so most of the used plastics are disposed of in the environment (Fig. 6b).

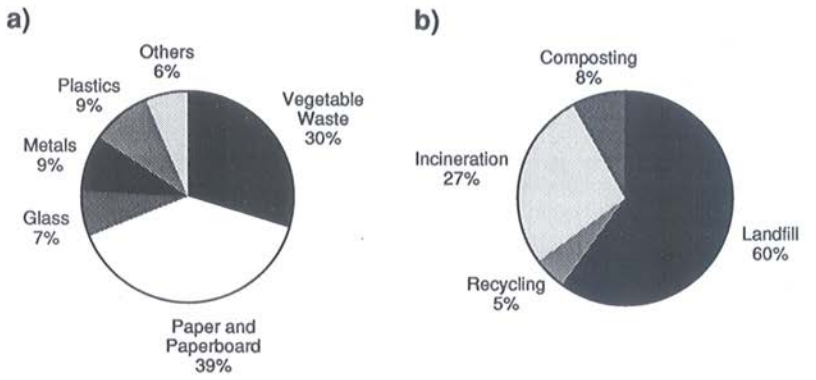

Fig. 6: a) Municipal waste distribution in USA as estimated for the year 2000 [65] and b) Municipal waste disposal in Europe 1995 [66].

Although most of the waste deposited on landfills is biodegradable, it is the smaller nonbiodegradable part that will be accumulated over the years without being degraded (Fig. 7). By replacing conventional plastic goods by biodegradable plastics, the percentage of nonbiodegradable materials found in landfill sites could be reduced. Biodegradable plastics would also be suitable for composting.

PHAs are able to replace conventional plastics in a variety of applications. The higher production costs of PHAs compared with undegradable plastics means that their increasing application will be seen only if governments pass laws with the aim of reducing the use of nondegradable plastics.

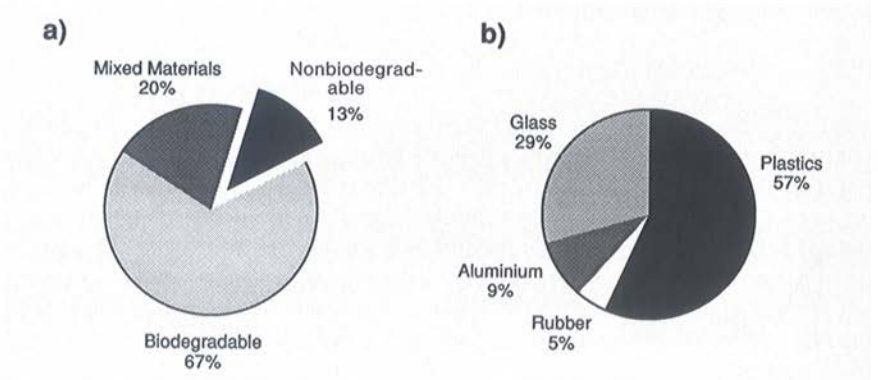

Fig. 7: a) Landfill composition and b) Breakdown of the nonbiodegradable part of the landfill composition. All data for USA in 1988 [65].

Several countries, such as Italy for example, have introduced legislation which requires plastic packaging materials to be degradable. Further actions against nondegradable plastics in western countries are listed in Table 5.

Country	Action
United States	Effective January 1, 1994, based on the MARPOLE treaty and the Marine Plastic Pollution Act of 1987 (Public Law 100-220), the U.S. Navy can no longer dispose of its plastic waste into oceans. Most of the States have bans on nondegradable plastics.
Italy	By 1991, all plastics used for nondurable goods must be degradable.
Denmark	Banned nonrecycable plastic beverage containers and PVC in 1987.
United Nations	The 1973 MARPOLE Convention, Annex 5, prevents ocean dumping of plastic waste.

Table 5: Selection of governmental actions against nondegradable plastics [67, 68].

The market for degradable polymers is expected to grow by 75% per year, representing a turnover in 1992 of about 400,000 tons and approximately US$ 340,000,000 [67].

"Degradable plastics" is a term including a variety of different types of plastics. First, they can be split up by the method of degradation. The most important

types of degradation are photodegradation (sunlight), autooxidation (reaction with oxygen), hydrolysis (cleavage of the polymer by water) and biodegradation (by the action of microorganisms).

Biodegradable plastics, the category to which PHAs belong, are a broad family of different types of biopolymers [68]. On an industrial scale, the most important representatives are starch and PHA derivatives. Starch is a commodity that is available at low cost in large quantities. Therefore starch based plastics are on the market at relatively low costs of 3 – 6 $/kg [69]. Because starch can take up a considerable amount of water, the use of starch derivatives is restricted by their moisture sensitivity. As many applications demand water resistant materials, the hydrophobic BIOPOL is able to compete against starch despite its high price.

With respect to molecular weight, melting region, crystallinity, flexibility and tensile strength, BIOPOL and polypropylene are quite similar. However, the former has disadvantages in its low tensile strength, poor solvent resistance, limited resistance to acids, bases and heat and, last but not least, its high price. It can be moulded thermoplastically and processed to sheets and fibres [70] but it has been used primarily for the production of shampoo bottles (Fig. 8).

Fig. 8: Shampoo bottles made of BIOPOL, after 3 and 9 months in compost. The slower degradation of the printed areas is clearly visible.

Recently, attempts have been made to extend the field of application of P(3-HB) and P(3-HB/3-HV) by preparing degradable block-copolymers with polystyrene and polyethers [71], or "blends" with polyethylene, polystyrene, polyvinyl chloride or polyethylene oxide. Films of P(3-HB) act as a gas barrier in a similar way to polyvinyl chloride or polyethylene terephthalate [72]. Because of these properties, P(3-HB) may play an important role as a packaging material of the future.

Judging by the increasing number of publications, the area is in the midst of great developments. How well PHAs can assert themselves against other biopolymers remains to be seen.

*Other Applications of Poly-(*R*)-3-hydroxybutyrate*

Apart from the use as biodegradable plastic for mass consumers, PHAs are also discussed as a substitute for implants in reconstructive surgery or as a biologically degradable drug carrier. *In vivo* experiments with P(3-HB) tablets implanted in tissue have shown that the biological degradation of P(3-HB) is relatively slow and is directly proportional to elapsed time. P(3-HB) is not repelled from animal tissue after implantation and no necrotic tissue is formed; it shows an outstandingly high biocompatibility. The only degradation product of P(3-HB) is the monomeric unit (*R*)-3-hydroxybutyric acid, which is a normal metabolite in mammals. Furthermore, the rate of liberation of drugs loaded in P(3-HB) tablets can be controlled, for example by choosing the appropriate particle size and the molecular weight of the P(3-HB) employed [15].

Other possible medical applications of PHA may be surgical swabs, wound dressings, as lubricant for surgeons' gloves or as artificial vascular grafts and blood vessels acting as temporary scaffolds for new tissue ingrowth [73].

Applications for PHAs or their blends with nondegradable polymers can be found in agriculture (e.g. as cold frame sheeting, seed capsules, or preparations for the controlled release of pesticides or herbicides [20]). A biological process for elimination of nitrate from drinking water using P(3-HB) as immobilized carbon-source for microorganisms has also been developed [74, 75].

PHAs have been patented by Nutrasweet as cream substitutes. By addition of macrocolloidal PHA particles to foods, the feel of fat or cream is simulated within the mouth [76]. Porous PHA can also act as flavor delivery system in low-fat or no-fat food [77].

A completely biodegradable composite based on cellulose fibres embedded in a thermoplastic BIOPOL matrix has also been reported [78].

Extracellular Biological Degradation of Poly-(*R*)-3-hydroxybutyrate

Many bacteria and fungi possess extracellular depolymerases [79], with which they can degrade PHAs and, if necessary, utilize them as a sole carbon source. The enzymes of *A. faecalis* [80–83] and *P. lemoignei* [84–88] have received the most attention. *A. faecalis* has two extracellular esterases, a P(3-HB) depolymerase and an oligomer hydrolase. The depolymerase degrades both P(3-HB) and water soluble oligomers. However, it displays significantly higher activity towards the longer oligomers and attacks in an *endo* fashion at the second ester bond from the hydroxy terminus [80]. The oligomer hydrolase attacks only water soluble oligomers, with approximately ten times higher activity than the depolymerase. Longer chains are more rapidly degraded than the dimers. Of the four possible stereoisomers of 3-hydroxybutyrate dimers, only the (*R,R*)-form and the (*R,S*)-form are hydrolyzed, the latter rather more slowly. The monomeric methyl ester is also attacked, while the corresponding ethyl and benzyl esters are practically inert. Degradation occurs in an *exo* manner from the acid end [81].

The *Gram*-negative organism *P. lemoignei* also contains two enzymes which are involved in extracellular degradation. However, they differ from those of *A. faecalis* in that only the depolymerase is exported from the cell. P(3-HB) is degraded outside the cell to a trimer/dimer/monomer mixture which is then transported through the cell wall and is only fully hydrolyzed to the monomer by a dimer hydrolase within the cell. Here too, the depolymerase attacks in an *endo* fashion at the second or third ester bond from the hydroxy terminus, although in this case both oligomers and P(3-HB) can be hydrolyzed [88]. In contrast to *A. faecalis,* the dimer hydrolase degrades the (*S,R*)-dimer as well as the (*R,R*)-form, while their enantiomers are not hydrolyzed. (*R*)-3-(butanoyloxy)-butyric acid is also attacked [85].

Despite numerous investigations, many questions remain unanswered. It is not clear, for instance, how the depolymerase can attack both the water soluble oligomers and the hydrophobic P(3-HB), which, in contrast to the intracellular material of the granules, is present here in a crystalline form. From our chemical point of view, it also seemed interesting to investigate the influence of various end groups, cyclization and specific sequences of (*R*) and (*S*) configurations on the degradability. Synthetically produced all-(*S*)-P(3-HB), for example, is known not to be biodegradable and neither is a stereoblock-P(3-HB) built up of (*R*)- and (*S*)-configuration segments [18].

Polyhydroxy Acids as Chiral Synthetic C_4 Building Blocks

The fact that microbially synthesized polyesters show an impressive stereoregularity brought our research group into contact with P(3-HB) for the first time a

decade ago. Since nature exclusively produces enantiomerically pure compounds, as it was pointed out recently in a *Schering* Lecture [89], compounds with a high enantiopurity and an economical availability are of considerable interest for synthetic chemists in general and the pharmaceutical industry in particular. (*R*)-3-hydroxybutyric acid was welcomed as a new member of the "pool of chiral building blocks" [90, 91]. However, in order to allow for the exploitation of the synthetic potential of P(3-HB), suitable procedures for the preparative degradation to its monomeric unit had to be found.

Chemical Degradation of Poly-(R)-3-hydroxybutyrate

The investigations carried out in this area were all limited to P(3-HB) or P(3-HB/3-HV) (BIOPOL), since these two polymers were the only two polyhydroxy esters available in large quantities at the time. Depending on the aims of the study, either the oligomer mixtures (*vide infra*) or the monomers could be of interest. The work of *Züger et al.* [92–94] and *Vanlautem et al.* [95] has led to the development of procedures for the formation of monomeric (*R*)-3-hydroxybutyric acid or its esters (**A** in Fig. 9) by acid-catalyzed hydrolysis or transesterification of

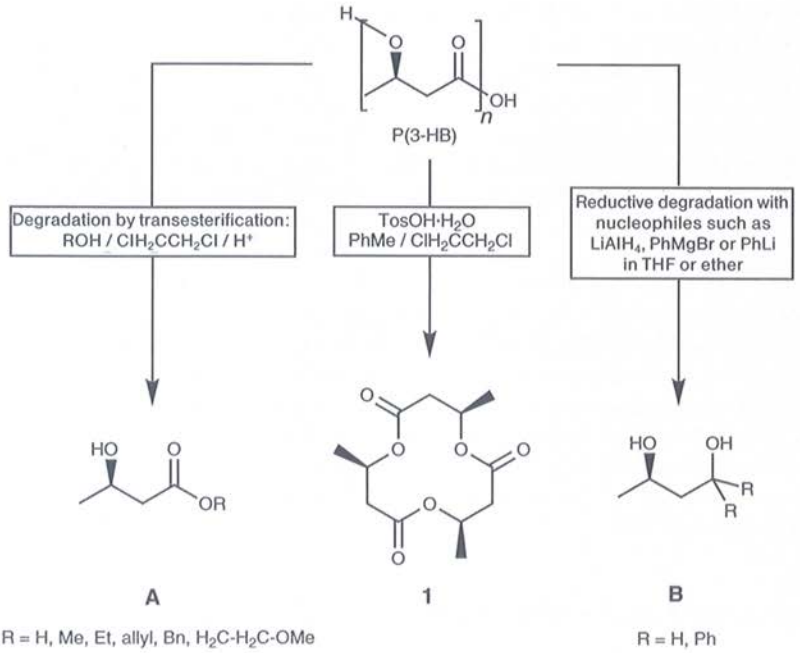

Fig. 9: Depolymerization of P(3-HB) by transesterification, direct acid-catalyzed cyclization or reduction of the ester functionality.

P(3-HB) [96]. The reaction conditions have been optimized by our group [97] and these facile methods allow the production of the monomeric acid derivatives in ca. 80% yield. A direct cyclization of P(3-HB) catalyzed by *p*-toluenesulfonic acid yields the all-(*R*) triolide **1**. Treatment of P(3-HB) with lithium aluminium hydride or organometallic reagents leads directly to the 1,3-butanediols of type **B**, with (*R*) configuration (Fig. 9).

Natural product syntheses starting from (*R*)-hydroxybutyric acid are being published continuously [98], as shown by recent syntheses of gloeosporon [99], grahamimycin A_1 [100], (*R*)-lasiodiplodin [101] and soraphen $A_1\alpha$ [102].

The transformation of (*R*)-3-hydroxybutyric acid (**2**) with triethyl orthoacetate in toluene leads to a cyclic orthoester (**3**) which gives, by thermolysis, (*S*)-β-butyrolactone **4** in about 30% yield [103]. In this manner, another important chiral building block is accessible through P(3-HB) (Fig. 10).

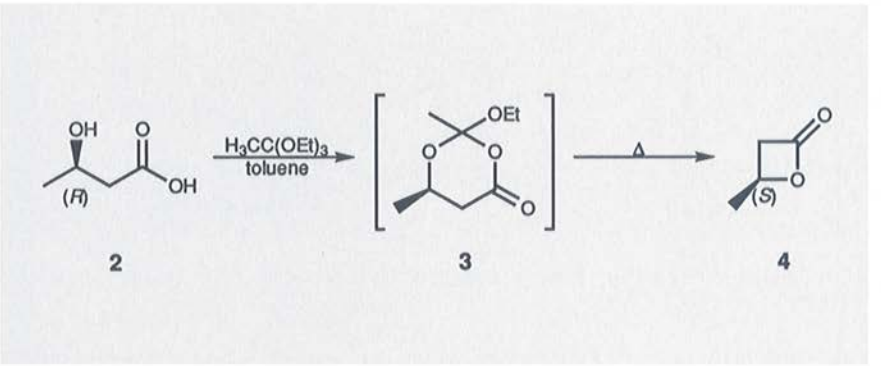

Fig. 10: Synthesis of β-butyrolactone (**4**) via a cyclic orthoester.

Additionally, it is now possible to replace any of the hydrogen atoms in (*R*)-3-hydroxybutyric acid by other groups [104, 105] (Fig. 11).

Derivatives of the Cyclic 3-HB Trimer

It is not only the monomeric derivatives of P(3-HB) which are accessible by chemical degradation, the cyclic trimer **1** can be obtained from P(3-HB) in large quantities. By simply heating the polymer in a mixture of toluene and dichloroethane in the presence of an acid catalyst and with removal of water from the reaction mixture, the triolide is formed as the major product [106]. In this way, pure triolide can be obtained in 40–50% yield directly from P(3-HB). Hence, the triolide can be used as a new enantiomerically pure starting material for diastereoselective reactions.

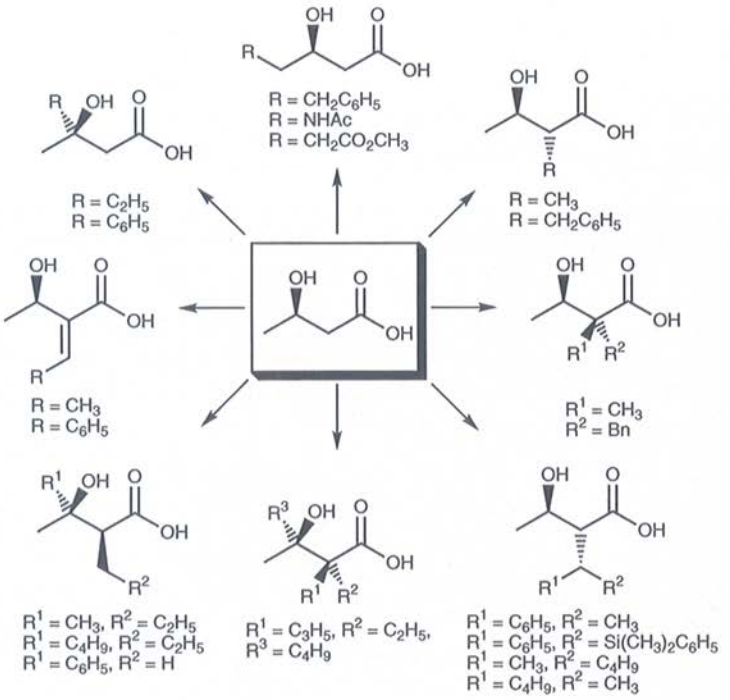

Fig. 11: Products of the transformation of (*R*)-3-hydroxybutyric acid while retaining the acid and alcohol functions.

One interesting feature of the triolide, which is revealed by X-ray crystal structure analysis, is its rather rigid structure with all three carbonyl oxygens pointing in the same direction. The structure of the triolide can be found also as the basic skeleton of naturally occurring macrolactones such as the siderophore enterobactin (see Fig. 12).

Initially, attempts were made at alkylation of the triolide at the position α to the carbonyl moiety. The triolide was treated with base at low temperature in order to generate the enolate and then quenched with electrophiles. Under a selected set of reaction conditions, no alkylation could be obtained; after work-up, only unreacted starting material or ring-opened products could be isolated [107]. Apparently, the triolide is not stable under the conditions applied; either β-elimination is favored over enolate formation at -78 °C or the enolate is unstable and decomposes with ring opening.

A second approach was to modify the ester functionality of the triolide. Reaction with *Lawesson's* reagent **6** led to a mixture of mono-, di- and trithionated triolide

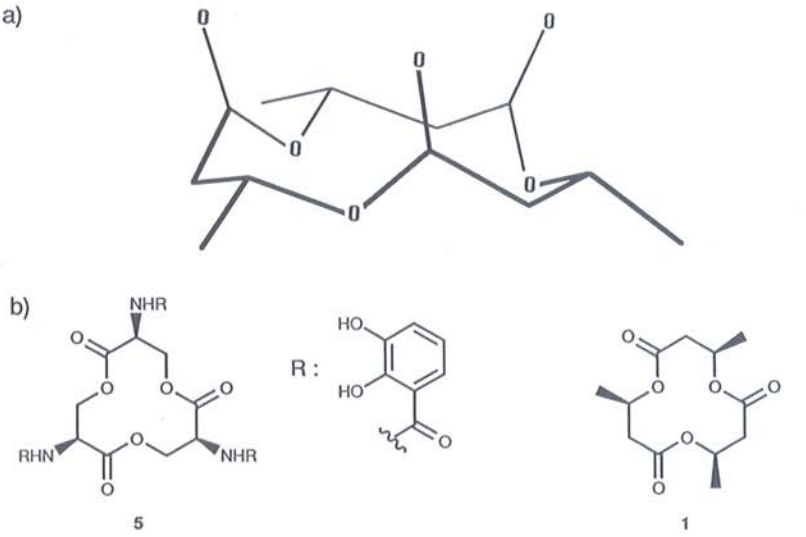

Fig. 12: a) MacMoMo representation of the crystal structure of triolide **1**. b) Comparison of the naturally occurring siderophore enterobactin **5** and the cyclic trimer **1** of the (*R*)-3-hydroxybutyric acid.

derivatives. The products are separable by flash chromatography on silica gel. The product distribution can be regulated by the amount of *Lawesson's* reagent added and by the reaction time (Fig. 13).

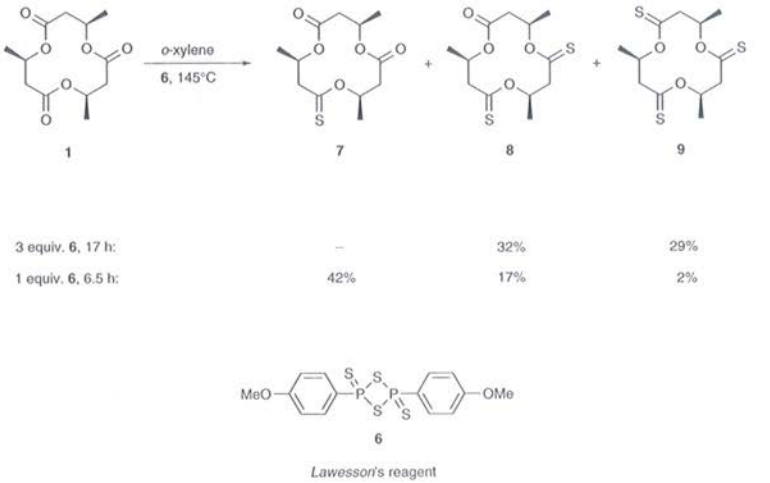

Fig. 13: Synthesis of the thiocarbonyl derivatives of the triolide **1**.

In both cases, a total of ca. 60% thionated products can be isolated. X-ray structure analysis showed that the rigid structure of the triolide **1** is still present in all thiocarbonyl derivatives **7–9.**

Thioesters can be converted to imidates by reaction with amines in alcohol [108]. With reaction at room temperature giving the corresponding imidates **C** in almost quantitative yields, this reaction works well for the monothiotriolide **7**, with ammonia or a primary amine (Fig. 14).

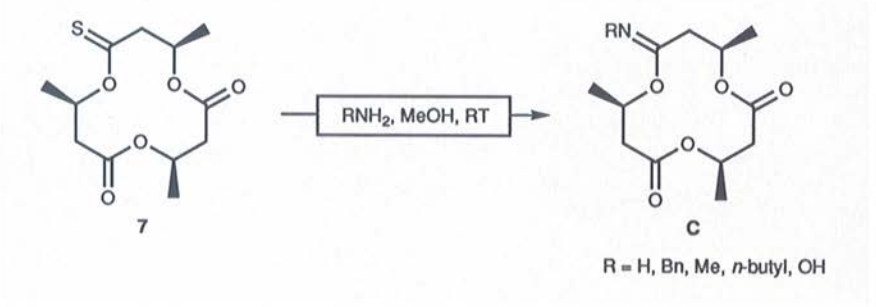

Fig. 14: Preparation of imidates **C** by treatment of the thiotriolide **7** with primary amines.

By reaction of the dithio- and trithiotriolides **8** and **9** with primary amines at 0 °C, the corresponding imidates **D** and **E** are formed in high yields. These imidates may be of particular interest as chiral catalysts. Imidates of type **F** (Fig. 15) were used by *Pfaltz* as ligands in various enantioselective reactions [109].

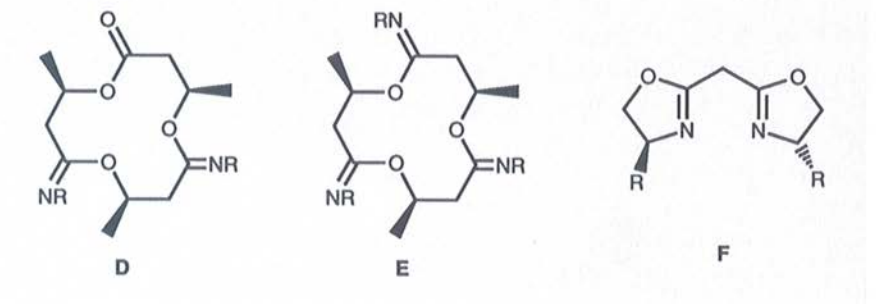

Fig. 15: Comparison of the imidates **D** and **E** with the imidate derivative **F** used by *Pfaltz* as ligand in catalytic enantioselective reactions.

The Pd-catalyzed allylic alkylation reaction often serves as a standard test reaction for nitrogen or phosphorus based ligands. Unfortunately, the imidate derivatives **D** and **E** were not catalytically active in this reaction. This result was not surprising after consideration of the crystal structure, which was solved by X-ray

analysis: the exocyclic substituents at the nitrogen atoms maintain a *trans* configuration, even if sterically more demanding benzyl substituents are introduced (Fig. 16 with **10**). A chelating effect of the lone pairs on the nitrogen atoms, as in the ligands of type **F**, is thus impossible. Nevertheless, introducing appropriate moieties on the benzyl residues could lead to compounds with high potential for complexation, as shown by the structural similarity of **10** and the natural siderophore enterobactin **5** [110] (Fig. 16).

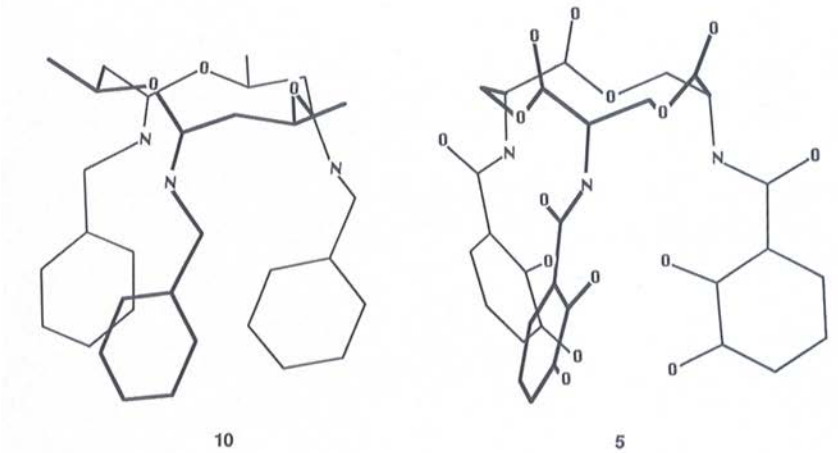

10 5

Fig. 16: MacMoMo representation of the tribenzylimidate **10** (left) and of the natural siderophore enterobactin **5** (right).

In order to attach a functionality with an improved complexing ability at the triolide backbone, the thioesters **7** and **8** were converted by reaction with aminophosphanes to give the *N*-(diphenylphosphanylalkyl)-imidates **11-13** in moderate to good yields.

Used as ligands in the palladium catalyzed allylation, these phosphinimines catalyzed the reaction and the product was formed in moderate to good yield, albeit with only low to moderate enantioselectivity (Fig. 17).

Poly-(*R*)-3-hydroxybutyric Acid as a Component of a Natural, Nonproteinogenic Ion Channel?

Almost all of the literature on P(3-HB) deals with the high molecular weight polymer that appears as inclusion bodies and is used as a biodegradable plastic. P(3-HB) has been implicated in biochemical processes such as sporulation [111] and encystment [112] and it has also been discussed as a possible energy source for nitrogen fixation in *Rhizobium* and *Bradyrhizobium* [17].

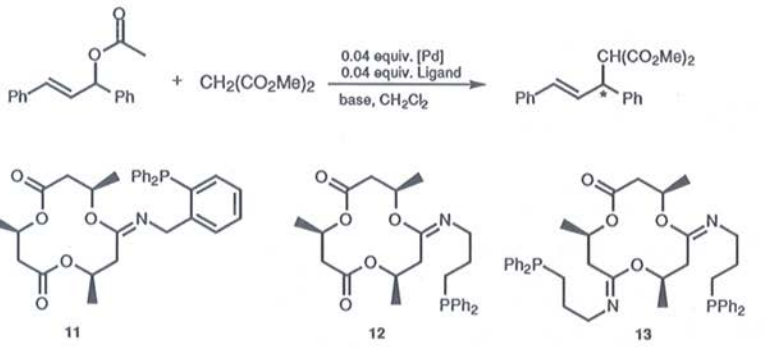

Ligand used	Yield	R/S
11	61%	1/2.7
12	92%	1.16/1
13	68%	1/3.4

Fig. 17: Palladium-catalyzed allylation using the phosphines **11-13** as chiral ligands.

Reports on 3-HB oligomers for microbial functions other than energy and carbon storage are rather scarce. For example, *Schulz* and *Toft* have shown that in certain species of spiders from the *Linyphia* family, 3-(*R*)-hydroxybutyrate monomers and dimers act as pheromones [113]. They cause the male to roll up the web of unfertilized females, possibly in order to demonstrate that the female is now occupied. This behavior is not observed with the webs of already fertilized females. 3-HB was further identified as a component of extracellular glycolipids of *P. aeruginosa* and *P. fluorescens*. Also, 3-HB has been detected as a constituent of extracellular polysaccharides of some *Rhizobium* strains [21].

Besides storage properties, no physiological significance has been given to P(3-HB) in microorganisms. It was, therefore, rather surprising when P(3-HB) was detected by *Reusch* and *Sadoff* in different types of *Gram*-negative and *Gram*-positive bacteria, albeit in minute amounts, when these bacteria were genetically transformable [114]. "Genetic transformation" indicates the ability of a cell to take up DNA from the external medium, leading to both a new genotype and – because of expression of the introduced DNA – a new phenotype [115]. Bacteria can be made genetically transformable (or competent) by a so-called chemical treatment with buffers containing bivalent cations at low temperature. In this state, the bacterial membranes are permeable to foreign DNA. *Reusch et*

al. also observed abrupt changes in the fluorescence intensity of *N*-phenyl-1-naphthylamine in the membranes of competent cells, indicating a major change in the lipid composition of the membranes. No such changes could be observed in noncompetent cells. A representative example of the lipid phase transition of competent bacteria is shown in Figure 18 with the bacteria *E. coli.*

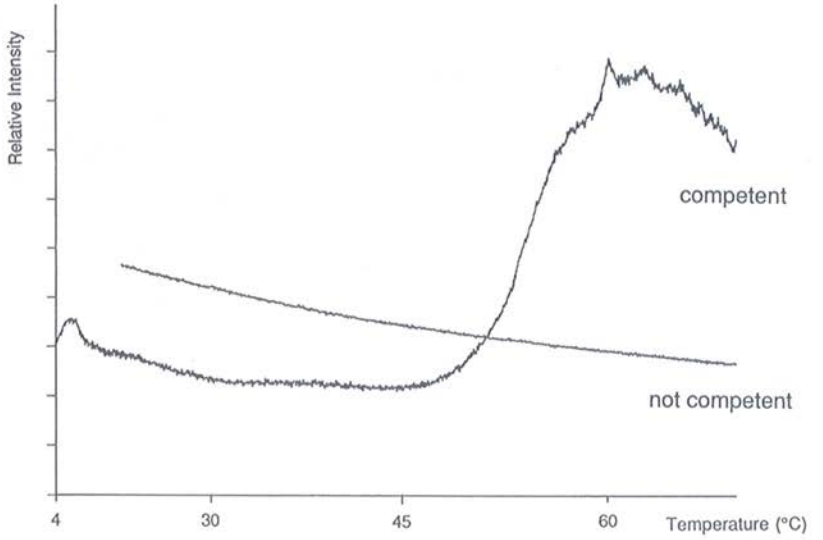

Fig. 18: Fluorimetric determination of the thermotropic lipid phase transition of competent and noncompetent *E. coli* DH5.

The P(3-HB) detected in these bacteria showed a molecular weight of about 13,000 g/mol, corresponding to ca. 150 monomeric units and was predominantly accumulated in the inner cell membrane. The highest increase in P(3-HB) content during competence could be detected in *A. vinelandii*. *E. coli* and *A. vinelandii* also showed a different structure of the inner cell membrane during the stage of genetic competence. This was detected by freeze-fracture electron microscopy [116] as shown in Figure 19. Small semiregular plaques in the inner cell membrane developed with increasing transformability. A relationship between competence and P(3-HB) content in *E. coli* cells has also been established [117].

Every biological cell is surrounded with membranes in order to preserve its special "microclimate" against the conditions of the environment. Biological membranes are essentially lipid bilayers interspersed with proteins. The thickness of a lipid bilayer is about 50 Å , where the hydrophobic part has a thickness of

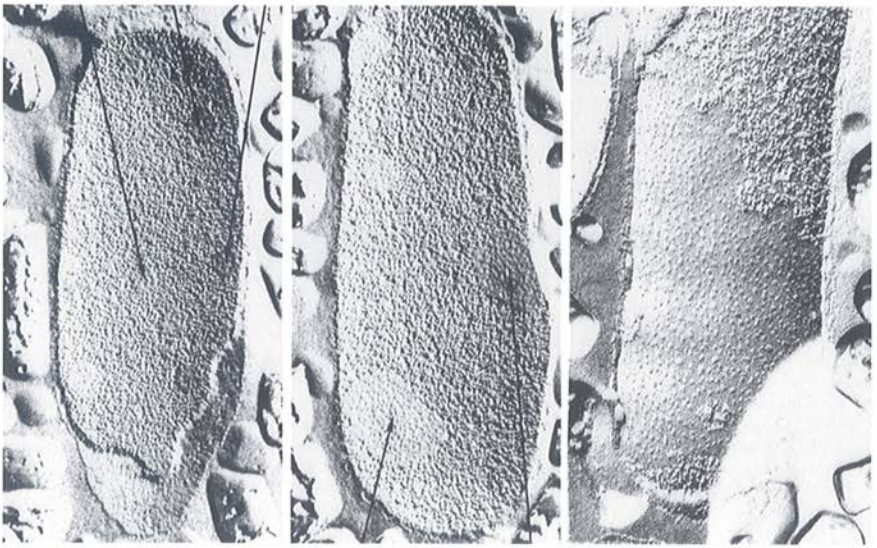

Fig. 19: Freeze-fracture electron micrographs of *E. coli* cells. The structure of the inner cell membrane is altered with increasing degree of competence. The arrows point to membrane plaques.

about 30–35 Å [118]. Lipid bilayers are practically impermeable to ions and most polar molecules. Nevertheless, somehow these must be able to pass through the membrane since they play an important part in many physiological processes. Proteins dispersed in the lipid bilayer are responsible for the interactions between the inside of the cell and the environment. A representative section of a typical biological membrane is shown in Figure 20.

The P(3-HB) isolated from competent bacteria by chloroform extraction has been found to be always accompanied by calcium polyphosphate ($Ca{\cdot}PP_i$, which is insoluble in $CHCl_3$!) of an estimated chain length of 130-170 monomeric units. This isolated complex has been shown to be very labile when removed from the naturally occurring environment. These findings led to the highly speculative postulation of a P(3-HB)/$Ca{\cdot}PP_i$ complex, which may be located in the inner cell membrane. On the basis of molecular modeling and energy minimization considerations (with the force field program Charmm), *Reusch et al.* proposed the exolipophilic/endopolarophilic structure shown in Figure 21. Because the complex components could only be detected in genetically competent bacteria, it was speculated that this complex could act as a nonproteinogenic transmembrane ion channel, which is responsible for Ca, PP_i or even DNA uptake of the cell [120].

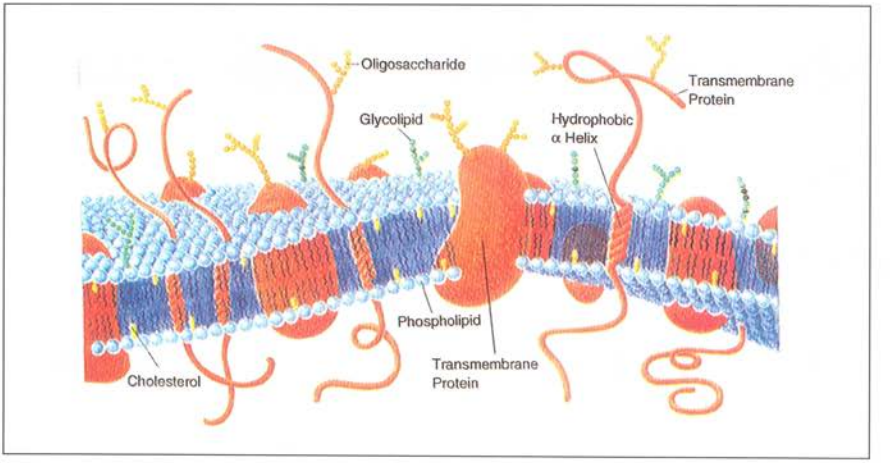

Fig. 20: Representative scheme of a typical biological membrane. (Figure taken from [119]).

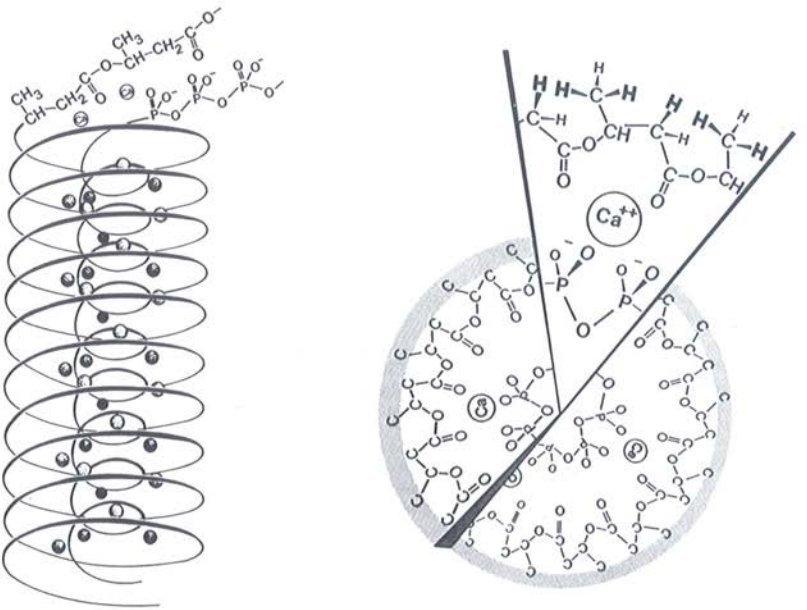

Fig. 21: Structure of a P(3-HB)/Ca-PP_i complex suggested by *Reusch* and *Sadoff* [120]. Left: View perpendicular to the channel axis. Right: View looking down the channel axis.

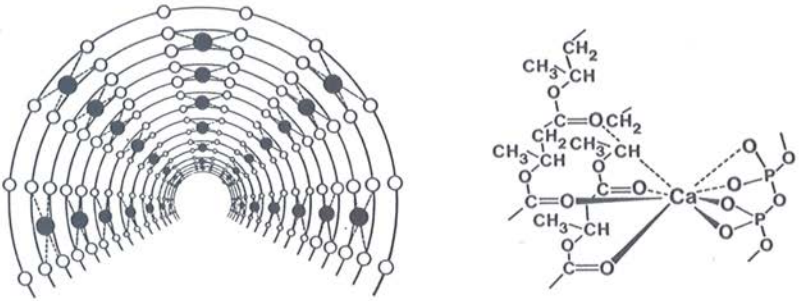

Fig. 22: Coordination of calcium ions in the postulated P(3-HB)/Ca·PP_i complex [121]. Left: View down the P(3-HB) cylinder showing calcium ions (closed circles) bound to carbonyl ester oxygens (open circles). Right: Coordination geometry of calcium ions in the helix.

It has to be mentioned that the mechanism of DNA uptake through the cell membranes of bacteria still remains to be resolved. For applications in genetic technology, many different protocols have been established, by trial and error, in order to get bacteria into a state, such that they can take up foreign DNA. One of the most common procedures is the treatment of a bacteria culture with ice-cold, nutrient-free salt buffers as developed by *Hanahan* [122] and used, with some changes, by *Reusch.* Other methods like electroporation (where the culture medium mixed with DNA is brought into an electric field that ruptures the cell membranes to some extent) are also quite common [123, 124].

In a later development, low molecular weight P(3-HB) has been detected in a variety of eukaryotic cells, although the concentrations were found to be lower than in competent *E. coli* (see Fig. 23). In beef liver, an accumulation of P(3-HB) in the mitochondria and the heavy liposomes could be detected.

As in the bacteria, P(3-HB), polyphosphate and calcium have been found to be present in a molar ratio of ca. 2:2:1. This leads to the conclusion that the former postulated complex should be present in the eukaryots. The high molecular weight storage P(3-HB) was not detected [121].

Finally, P(3-HB) was detected in human blood plasma [125]. The total content of P(3-HB) determined by chemical and immunological assays shows a mean value of 3.5 mg/l. The P(3-HB) is accumulated in the fraction containing the very low density and low density lipoproteins. Most of the P(3-HB) seems to be complexed to albumin, a serum protein.

The low molecular mass polymer always appears to be complexed with other large molecules [126]. Therefore, it is now designated *c*-P(3-HB) (*c* for complex-

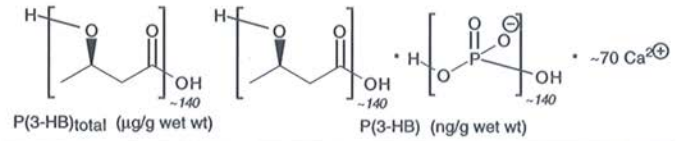

Sample	P(3-HB)total (µg/g wet wt)	P(3-HB) (ng/g wet wt)
E. coli		
Log phase	0.26	--
Competent	156.00	9600
Beef liver	9.20	662
Beef heart	6.50	435
Spinach leaves	0.86	163

Fig. 23: Occurrence of P(3-HB) as a component of a P(3-HB)/Ca·PP_i complex in prokaryotic and eukaryotic membranes according to *Reusch* [121].

ed) in order to distinguish it from the well-known high molecular mass storage P(3-HB) or *s*-P(3-HB) (*s* for storage).

Based on the broad variation of the samples examined, the conclusion that has to be drawn is that the low molecular weight *c*-P(3-HB) is almost omnipresent in living organisms.

Nothing is yet known about the physiological role of *c*-P(3-HB) found in eukaryotic cells. The monomeric unit, (*R*)-3-hydroxybutyric acid, is a well-known metabolite in fatty acid biosynthesis. (*R*)-3-hydroxybutyric acid, acetoacetate and acetone are known as ketone bodies and are synthesized by the liver from acetyl-CoA when carbohydrates are unavailable during, for example, starvation or diabetes. The level of ketone bodies found in the blood stream is low and normally does not exceed 2.0 mg/100 ml. However, patients with diabetes mellitus can show levels of up to 100 mg/100 ml. The smell of acetone is clearly perceptible when people have raised levels of ketone bodies [118, 127].

Ketone bodies are a product of abnormal metabolism but they also have important physiological functions. The most important role they play is probably their possible ability to provide alternative fuel to body tissues when carbohydrate is in short supply or cannot be efficiently utilized. In particular, the central nervous system is unable to use fatty acids as an energy source (in contrast to most

other tissues). Hence, the ketone bodies largely replace glucose as a fuel of respiration in the brain during starvation periods [128, 129]. A clinical application of 3-hydroxybutyrates is their use as an energy source for brain metabolism during periods of therapeutic starvation of obese patients for whom urgent and rapid weight loss is dictated by medical or surgical factors. A net body protein loss can be reduced by acute oral or intravenous administration of a daily dose of 18 g sodium *rac*-3-hydroxybutyrate [130]. Generally, the patients reported feeling less hungry when receiving hydroxybutyrate.

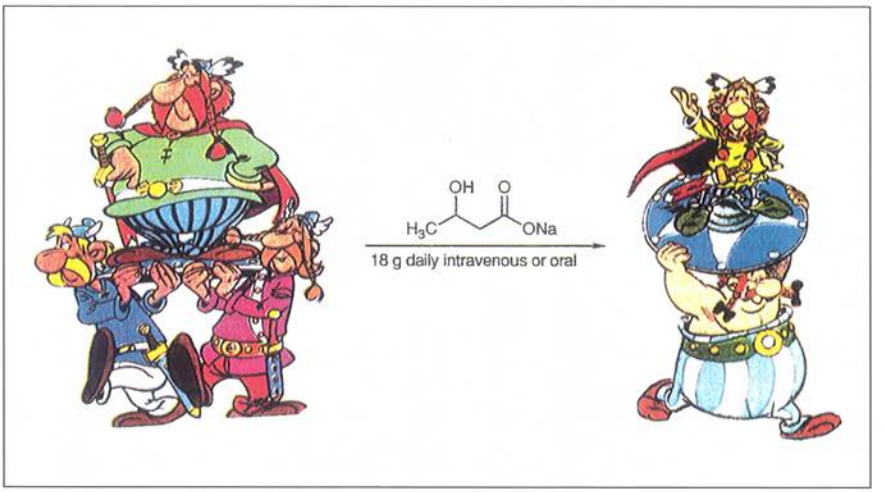

Fig. 24: Therapeutical use of 3-hydroxybutyrate as "brain-food" during starvation periods [130]. The cartoon characters are taken from Asterix and Obelix: "Le Bouclier Arverne", Dargaud Ed. SA Paris, 1968.

Isolation and Characterization by ^{1}H-NMR Spectroscopy of *c*-P(3-HB) from Eukaryotic and Prokaryotic Organisms

Given our knowledge about the chemistry of P(3-HB) and the intriguing proposal of a P(3-HB)/Ca·PP$_i$ transmembrane ion channel by *Reusch,* we decided to provide evidence for or against this speculation by synthetic means. We planned to synthesize P(3-HB) oligomers of the appropriate chain length and to look for possible complexing properties of these synthetic P(3-HB) oligomers with Ca·PP$_i$. As a starting point for our work, we tried to detect, isolate and characterize some *c*-P(3-HB), in order to have some reference material in hand.

Methods for the quantitative determination of P(3-HB) are well-known and have been developed in order to validate the production of high molecular weight *s*-P(3-HB) in bacteria. The most common and accurate methods are the chemical conversion of P(3-HB) to monomeric derivatives of crotonic acid [131] or

3-hydroxybutyric esters [132] and the determination of these derivatives by high performance liquid chromatography (crotonic acid) or gas chromatography (3-HB esters). The detection limit for the crotonic acid assay is reported to be in the 10 ng region [121]. The biggest disadvantage of these assays is the fact that not the polymer itself but a derivative is detected. This is not a problem as long as P(3-HB) is present as the major product of the mixture being analyzed. But when detecting P(3-HB) in the ppm region, a possible precursor other than P(3-HB) for the derivatives cannot be ruled out.

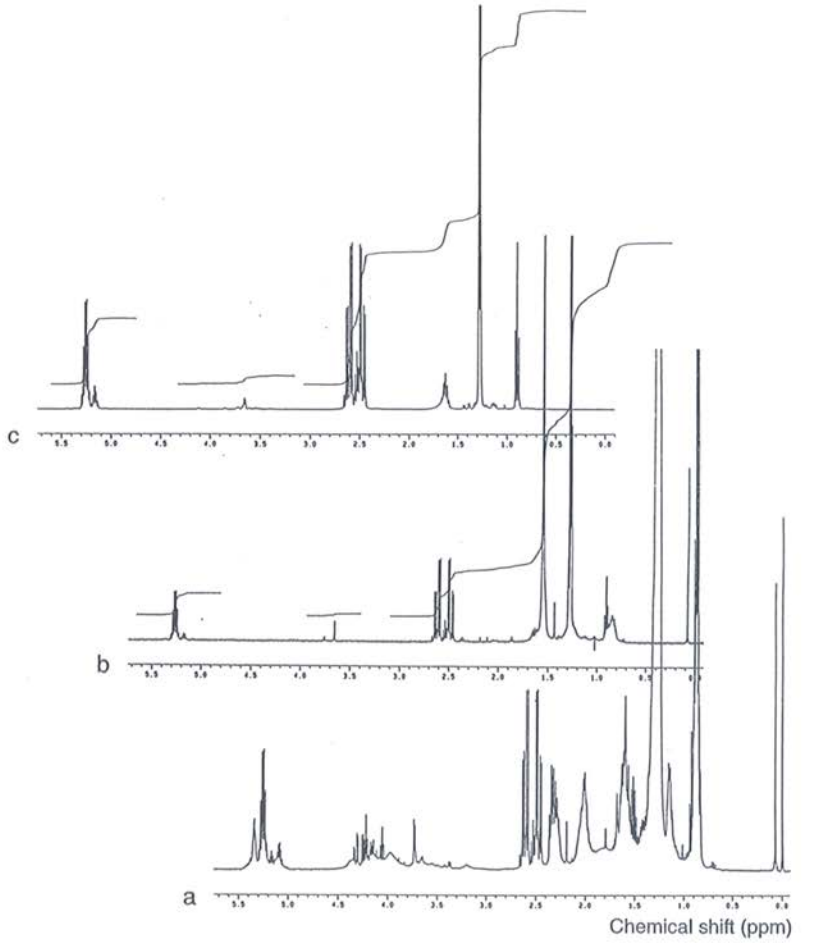

Fig. 25: 400 MHz ^{1}H-NMR spectra of the $CHCl_3$ extracts of competent *E. coli*. a) Crude extract and b) Extract purified by GPC. c) Reference spectrum of the commercial copolymer of P(3-HB/3-HV).

Most of the determinations of *c*-P(3-HB) by *Reusch et al.* have been performed using the crotonic acid assay. In the determination of P(3-HB) in blood serum, an immunoassay was also developed, ruling out the possibility that the monomeric metabolite hydroxybutyrate was interfering [125].

We, as synthetic organic chemists, wanted to detect the polymer directly without the need for any degradation step. P(3-HB) is difficult to detect in the presence of an excess of lipids by both chemical and spectroscopic means. P(3-HB) does show characteristic signals in ^{1}H-NMR spectroscopy and the methylene and methine protons can be detected at a frequency which is unusual for the protons of other lipids. The disadvantage of this method is the rather large amount needed ($\approx$ 50 µg). Although *Reusch* reported the characterization of *c*-P(3-HB) extracted from competent bacteria [120] and eukaryotic membranes [121] by ^{1}H-NMR spectroscopy, we were unable at first to reproduce these findings. After some initial pitfalls following the published protocols, we learned from personal collaboration with *Reusch* that larger culture volumes and modifications in the competence protocol were necessary in order to extract the amounts of *c*-P(3-HB) we were looking for from competent *E. coli* [133]. From a 5 liter culture of competent *E. coli,* we were able to extract enough *c*-P(3-HB) for ^{1}H-NMR spectroscopic analysis. The ^{1}H-NMR spectrum of the crude $CHCl_3$ extract is shown in Figure 25a, where the characteristic signals due to *c*-P(3-HB) are clearly visible. By gel permeation chromatography (GPC), the molecular weight distribution could be estimated and the average chain length was determined to be in the range of 90 to 130 monomeric units. No high molecular weight *s*-P(3-HB) was detected. The ^{1}H-NMR spectra of a sample purified by GPC, shown in Figure 25b, revealed the presence of some polyhydroxyvalerate as can be seen by comparing the ^{1}H-NMR spectrum of the purified extract with the reference spectrum of the commercial copolymer P(3-HB/3-HV) (Fig. 25c).

We decided to degrade the polymer to the methyl esters of the monomers and analyze them by gas chromatography in order to evaluate the 3-HV content quantitatively, using the method developed by *Braunegg et al.* [132]. As a suitable chiral GC column, which allows separation of the enantiomeric methyl esters of 3-hydroxybutyrate, had been found, it was possible to determine the absolute configuration of the building blocks in this *c*-P(3-HB). A modification of the method developed by *Seebach* and *Züger* [93], Figure 9, was used for the degradation of the polymer to the methyl esters.

The chromatograms in Figure 26 revealed the same absolute configuration (*R*) for both *c*- and *s*-P(3-HB). Furthermore, the presence of 3-HV units was confirmed and was approximately 14%, the absolute configuration appears also to be (*R*), although the separation was not as satisfactory as that for 3-hydroxybutyrate.

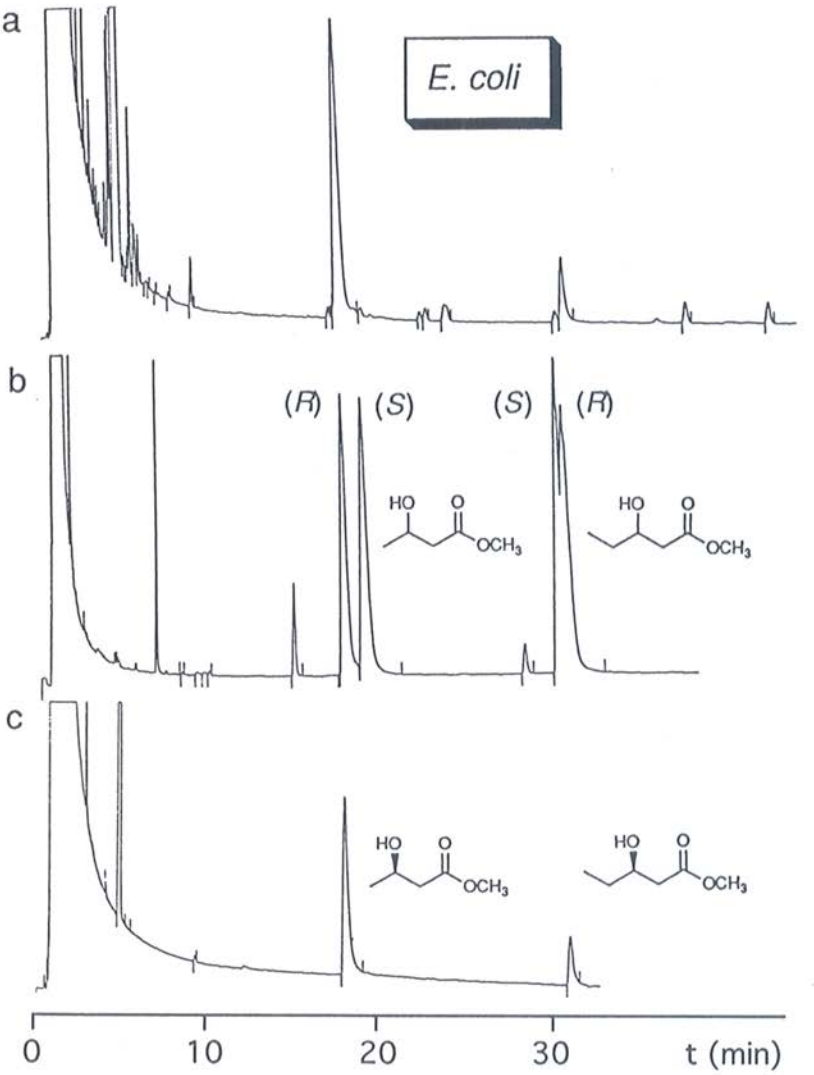

Fig. 26: Gas chromatographic analysis of the methyl esters of 3-hydroxybutyric acid and 3-hydroxyvaleric acid. a) From *E. coli* by acid-catalyzed methanolysis of the polymer. b) Racemic reference material. c) Methanolysis products of the commercial copolymer BIOPOL (19% 3-HV).

In the original procedures published by *Reusch et al.*, only *c*-P(3-HB) was detected by ^{1}H-NMR spectroscopy in bacterial samples as well as in the extracts from eukaryots [126].

By extraction of fresh dried spinach with a $CHCl_3$/MeOH mixture, it was again possible to isolate *c*-P(3-HB) in a quantity suitable for ^{1}H-NMR spectroscopy analysis. The presence of high molecular weight *s*-P(3-HB) could be ruled out by GPC purification, where only the fraction corresponding to a molecular weight below 20,000 g/mol contained amounts of P(3-HB) detectable by ^{1}H-NMR spectroscopy. It was again possible to determine the absolute configuration of the *c*-P(3-HB) building blocks by GC analysis of the methanolysis product of the extract. As in the storage material and in the *c*-P(3-HB) from *E. coli*, the *c*-P(3-HB) isolated from spinach had an all-(*R*) configuration. No 3-HV could be detected by ^{1}H-NMR spectroscopy or GC analysis.

In mammals, *c*-P(3-HB) has been reported to be located mainly in the mitochondria and in the heavy microsomes [121]. By extraction of mitochondria (prepared from beef heart) with hot $CHCl_3$ and subsequent purification of the crude extract by GPC, P(3-HB) could be detected by ^{1}H-NMR spectroscopy.

In the human blood stream, most of the *c*-P(3-HB) detected by crotonic acid assay or immunoassay seems to be complexed with albumin [125]. Therefore, we tried to extract P(3-HB) from commercially available bovine serum albumin. To our surprise, the *c*-P(3-HB) is bound so strongly to this transport protein, that only a fraction, which is too small for ^{1}H-NMR spectroscopic determination of the *c*-P(3-HB), can be extracted with $CHCl_3$. However, we were able to extract enough *c*-P(3-HB) for detection by ^{1}H-NMR spectroscopy by using a mixture of chloroform and methanol (9:1).

Although the majority of P(3-HB) in human blood serum is bound to albumin, the residual P(3-HB) was reported to be accumulated in the fractions of very low density lipoproteins (VLDL) and low density lipoproteins (LDL) when the plasma was separated by density gradient ultracentrifugation [125]. Because chronically elevated levels of LDL and VLDL plasma lipoproteins are associated with an increased incidence of arteriosclerosis [134], the question was raised whether P(3-HB) itself could be arterogenic. Patients with arteriosclerosis show depositions (so-called plaques) in the arteries, which cause heart disease and myocardial and cerebral infarction [135]. In a collaboration with the Department of Pathology at the University of Zürich, arteries and plaques of patients with differing degrees of arteriosclerosis were examined for their P(3-HB) content using the crotonic acid assay. With the rather small number of samples available to us (the sampling was not done systematically), we found no correlation between the amount of crotonic acid and the degree of arteriosclerosis and also no significant enrichment in the separated plaques as compared to the remaining aorta tissue. Nevertheless, we succeeded in isolating P(3-HB) in ^{1}H-NMR-detectable amounts from lyophilized whole aorta tissues by $CHCl_3$/MeOH extraction followed by gel chromatographic purification. Although the signals from the P(3-HB) are hardly visible in the spectrum shown (Fig. 27), the signals

due to the methylene and methine protons show the pattern characteristic for P(3-HB) [133].

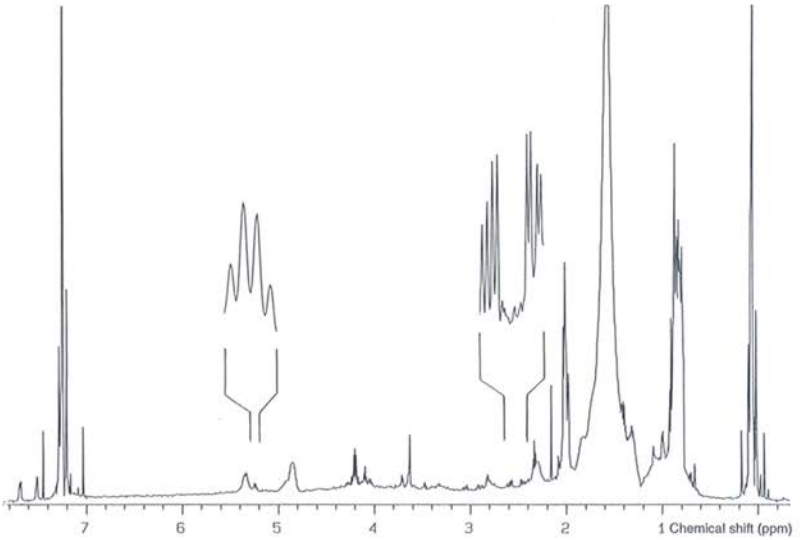

Fig. 27: ^{1}H-NMR spectrum of an extract from lyophilized whole aortae, purified by reprecipitation and chromatography.

In this way, the ubiquitous occurrence of *c*-P(3-HB) in prokaryotic and eukaryotic cells was confirmed using ^{1}H-NMR spectroscopy as an analytical tool, where P(3-HB) can be clearly distinguished from any other lipid components.

The only speculation about the physiological role of *c*-P(3-HB) at the time was the proposal of *Reusch*, that short-chain *c*-P(3-HB) could be part of a nonproteinogenic transmembrane ion channel as shown in Figure 21. In this channel, the *c*-P(3-HB) would be complexed with Ca·PPi, forming an aggregate, which, when removed from its native environment, would be highly unstable in aqueous systems.

To gain some structural information about a possible P(3-HB)/Ca·PP$_i$ complex, our initial goal as synthetic chemists was to prepare analytically pure 3-HB oligomers of the appropriate chain length (100–150 units) and examine the possible complexing properties of these polyesters with Ca·PP$_i$.

Partial Depolymerization of Poly-(*R*)-3-hydroxybutyrate

In order to obtain 3-HB oligomers of a defined chain length, initial attempts lay in the partial depolymerization of P(3-HB). Various mixtures of oligomers can be

formed by hydrolysis, alcoholysis or by ester pyrolysis at temperatures >175 °C, where the average molecular weight is determined by the length of the heating period [136, 137]. At the alcohol terminus, the pyrolysis products **G** all carry a crotyl group, as is to be expected for mechanistic reasons.

The treatment of P(3-HB) with lithium amide bases in THF at -78 °C leads, after work-up, to partial, but not total, degradation with formation of oligomers **G** also bearing crotyl groups at the hydroxy terminus [137, 138] (Fig. 28).

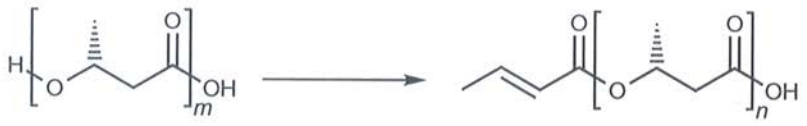

P(3-HB)
$m \approx 9000$

G

Fig. 28: Degradation of P(3-HB) by pyrolysis or treatment with strong bases leading to oligomers of type **G**.

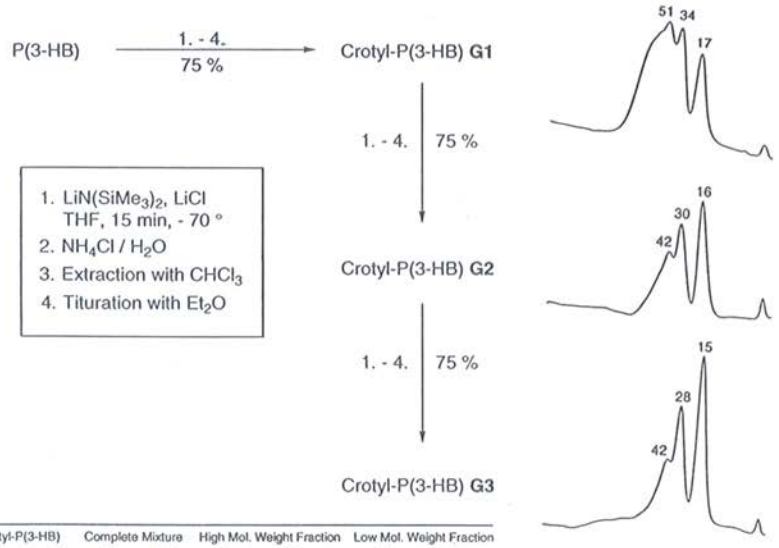

Crotyl-P(3-HB)	Complete Mixture		High Mol. Weight Fraction		Low Mol. Weight Fraction	
	$\overline{X}_n$	$\overline{X}_w$	$\overline{X}_n$	$\overline{X}_w$	$\overline{X}_n$	$\overline{X}_w$
G1	37	58	52	68	17	17
G2	25	34	38	44	15	16
G3	22	28	34	38	15	15

Fig. 29: Multiple degradation of P(3-HB) by a Li amide. The GPC analysis was performed on the methyl esters. Number and weight average degree of polymerizations were calculated for the complete mixture and also for the fractions above and below the trough separating the lowest molecular weight peak from the rest of the chromatogram.

The molecular weights of these oligomers have been established by ^{1}H-NMR spectroscopy end group determination (as methyl ester), by osmometric measurements in $CHCl_3$, by gel permeation chromatography (GPC, polystyrene standard) and by plasma desorption mass spectroscopy (PDI-MS). These methods gave somewhat conflicting results, with GPC giving particularly high values of molecular weight. More disturbing was the fact that both the chromatographic and the MS analysis indicated that the oligomer was composed of three major fractions (i.e. it had a trimodal distribution). The material obtained was subjected to exactly the same procedure two further times (see Fig. 29).

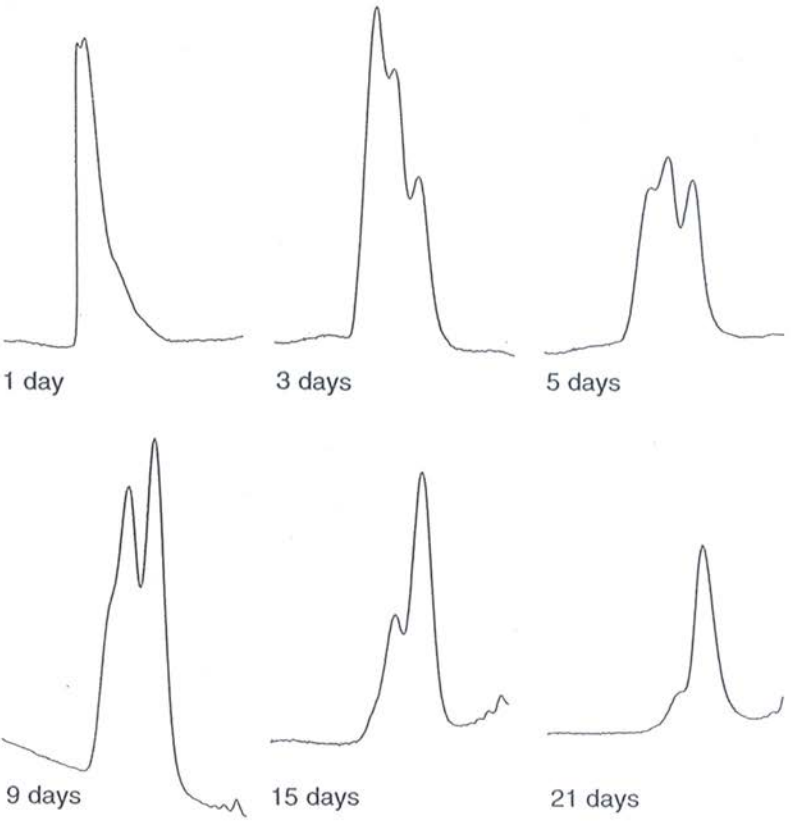

Fig. 30: GPCs of degradation products of P(3-HB), molecular weight ca. 10^7 g/mol, in boiling triethylamine. The shape of the curve obtained after treatment for one day indicates that a lot of the P(3-HB) is still of a high molecular weight, as the exclusion limit of the columns render this inseparable.

The mixtures were analyzed by matrix assisted laser desorption and ionization MS (MALDI-MS) [139], which confirmed the molecular weight distribution obtained by the GPC method. The three maxima of the molecular weight distributions correspond to oligomers of ca. 42, 28 and 15 3-HB units.

In another experiment, a stirred suspension of P(3-HB) was heated in neat triethylamine at reflux for three weeks. GPC analysis of samples withdrawn at different intervals again produced curves with three maxima (Fig. 30).

In both cases, the chemical degradation reaction (base-induced β-elimination) was governed or actually limited by a characteristic property of P(3-HB). An explanation for the trimodal distribution which is intrinsically connected with the solid state structure of P(3-HB) is given later.

Synthesis of Nearly Monodisperse Oligomers of 3-HB

The degradation of P(3-HB) with lithium amide bases or with triethylamine (heterogeneous reaction conditions) leads to products with a trimodal distribution; hydrolysis, alcoholysis and pyrolysis (homogeneous reaction conditions) lead to monomodal oligomer mixtures where the average chain length can, to some extent, be regulated. However, it has proved impossible to produce entirely monodisperse oligomers by the degradation of P(3-HB).

Oligomers of uniform molecular mass have been of interest in the past for a variety of reasons. These include their use in obtaining more detailed information about the intra- and extracellular degradation mechanism for P(3-HB) [80, 81, 140] and in the synthesis of the corresponding straight-chain oligolide precursors [141, 142]. In all previous syntheses, chain extension was performed by the stepwise addition of monomeric units. Our aim was to study the solid state structures of P(3-HB) and oligo(3-HB) derivatives and the structure and function of the presumed P(3-HB) containing ion channel, already mentioned above, which requires oligomers with a length of 100-150 monomer units. For the synthesis of such large molecules, a stepwise technique is, of course, no longer practical. A possible alternative was the segment condensation strategy in which the two protecting groups on an unsymmetrically protected oligomer are selectively removed. Initially, we chose a benzyl ether protection for the OH terminus and a *t*-butyl ester protection for the COOH terminus [107, 136, 141].

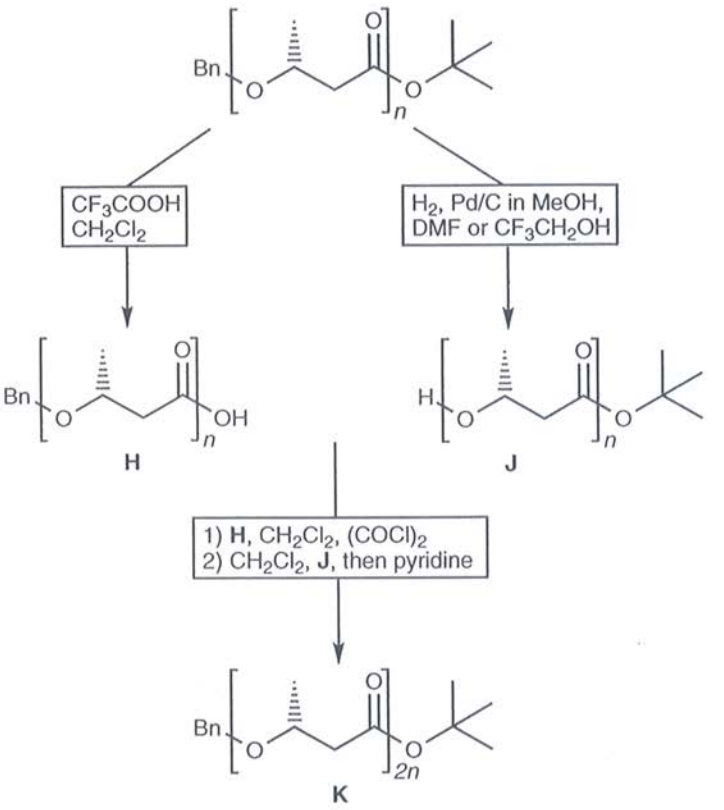

n	Yield [%] after the coupling of the corresponding *n*mer **H** and *n*mer **J**	2*n*mer **K**
2	95	**14** (n = 4)
4	95	**15** (n = 8)
8	90	**16** (n = 16)
16	60	**17** (n = 32)
32	45	**18** (n = 64)
64/32	45	**19** (n = 96)

Fig. 31: Segment condensation algorithm for the synthesis of defined oligomers of (*R*)-3-hydroxybutyric acid. An *n*mer acid **H** is coupled to an *n*mer alcohol **J**, giving rise to a 2*n*mer product **K** of "twice the size". The yield after the acid chloride coupling step decreases with increasing size of the compounds.

The deprotected portions are then coupled after activation of the acid with oxalyl chloride to afford a molecule "twice the size" (see Fig. 31). The dimer **20** used as starting material in Figure 31 was synthesized by the sequence of steps shown in Figure 32.

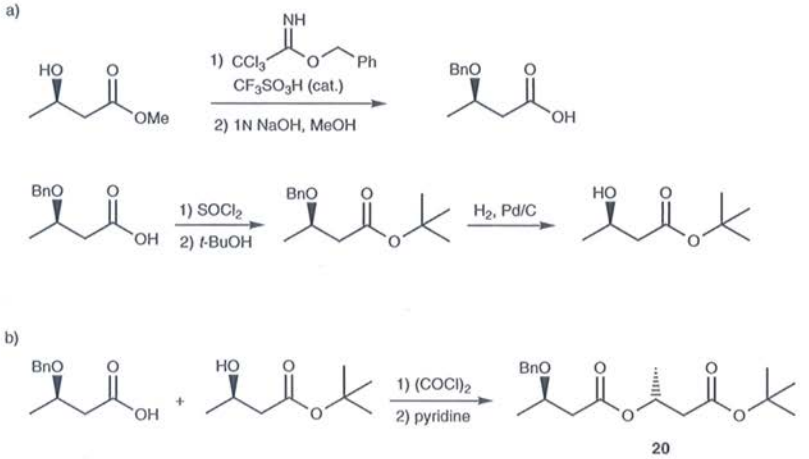

Fig. 32: Preparation of the dimer **20** used as starting material in the synthesis of the oligomers of 3-HB.

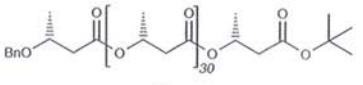

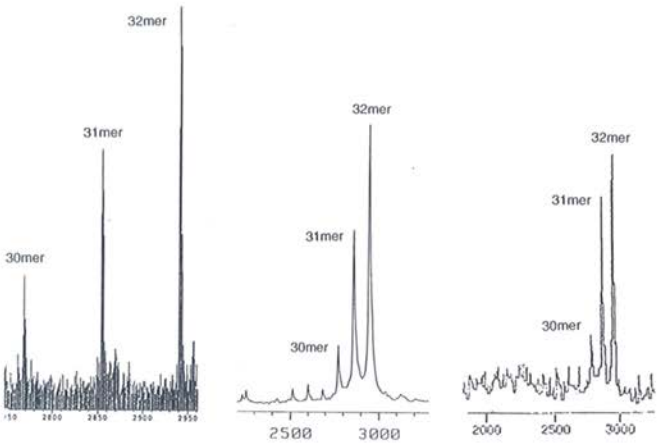

Fig. 33: Liquid secondary ionization (LSI)-MS (in a 3-nitrobenzylalcohol matrix, left), plasma desorption (PDI)-MS (center) and matrix assisted laser desorption and ionization (MALDI)-MS (in a 2,6-dihydroxy benzoic acid matrix, right) of the fully-protected 32mer **17**.

Coupling of the 64mer (COOH terminus unprotected) with the 32mer (OH terminus unprotected) leads to the oligo(3-HB) **19** containing 96 units. At least this was believed to be the case. All compounds were characterized by ^{1}H-NMR, ^{13}C-NMR and IR spectroscopy, specific rotation, melting point, elemental analysis and MS. The last method revealed problems we had not been prepared for: with the 32mer **17** three MS techniques could be applied – liquid secondary ionization MS (LSI-MS), PDI-MS and MALDI-MS. All three showed that single 3-HB units had been lost (see Fig. 33).

The spectra clearly show that this loss is not caused by fragmentation in the mass spectrometer, as the measured masses include the protecting groups on both ends of the chain. Reliable analysis of the high molecular weight oligomers became available to us only after the completion of the first synthesis.

Since none of our purification methods could be used to separate *n*mers from *(n-1)*mers on a preparative scale, it was clear that the oligomers, prepared as outlined above, would consist of mixtures.

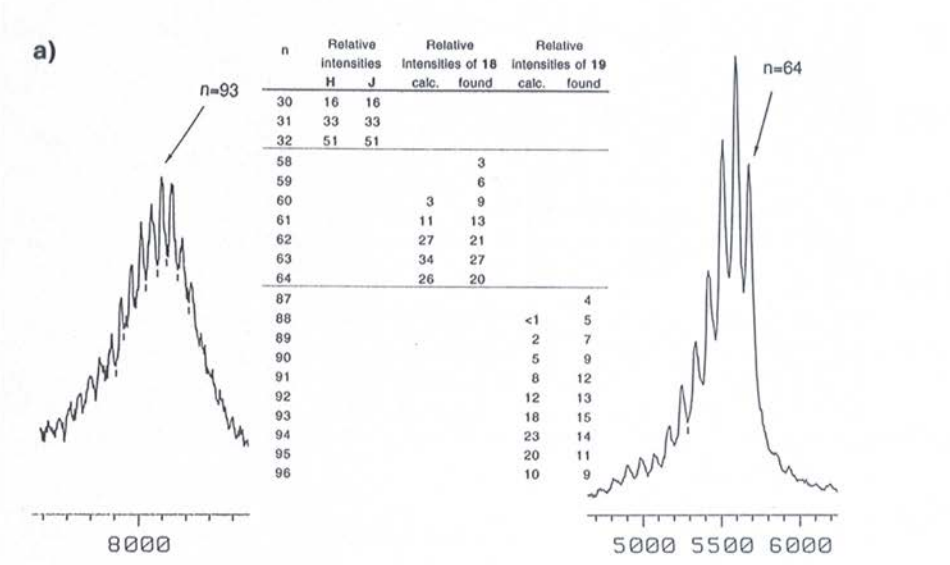

n	Relative intensities H	Relative intensities J	Relative intensities of 18 calc.	Relative intensities of 18 found	Relative intensities of 19 calc.	Relative intensities of 19 found
30	16	16				
31	33	33				
32	51	51				
58				3		
59				6		
60			3	9		
61			11	13		
62			27	21		
63			34	27		
64			26	20		
87						4
88					<1	5
89					2	7
90					5	9
91					8	12
92					12	13
93					18	15
94					23	14
95					20	11
96					10	9

Fig. 34 a: MALDI-MS of the samples synthesized and expected to be the fully protected 64mer and 96mer. As can be seen, the oligomer samples do not consist of uniform molecules but are mixtures containing chains of less than the expected number of 3-HB units. From the distribution of the 32mer used for assembling the 64mer, we have calculated the expected composition: the difference between the calculated and measured distribution might be taken to indicate that there is a further loss of 3-HB units during the coupling step. The distribution of the sample meant to be the 96mer is also given; obviously, we have actually made a 93mer of $M_w/M_n \leq 1.0005$!

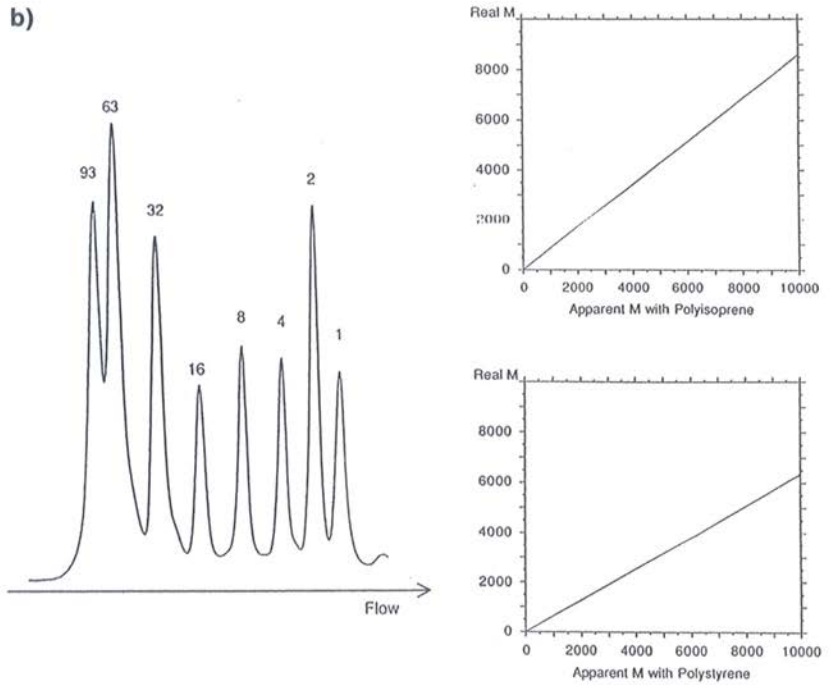

Fig. 34b: Gel permeation chromatogram of the fully protected oligo(3-HB) compounds (left). Comparison with the molecular masses determined after standardization using polystyrene or polyisoprene (right).

A more detailed study of the reaction sequence showed that under the deprotection conditions specified in Figure 31, terminal subunits may be cleaved. A comparison between calculations of the composition of the "64mer" mixture predicted from the compositions of its precursors **H** (n=32) and **J** (n=32) and the resulting mixture of the "64mer" **18** show that there is a loss of subunits during the coupling procedure (see Fig. 34a).

For this reason, the average degree of polymerization of the mixtures obtained was only 63 and 93, respectively, though this was distributed over a narrower range than would have been the case under ideal polymerization conditions: the synthesis of a 93mer with $M_w/M_n \leq 1.0005$ has been achieved.

As a standard for GPC analysis (see Fig. 34b) and for solid-state structure analysis (*vide infra*), the samples of linear oligomers may be considered monodisperse, so that while our effort must be called utterly unsuccessful from the synthetic chemist's point of view, it is a success with respect to polymer chemistry.

Synthesis of Entirely Monodisperse 3-HB Oligomers

To synthesize monodisperse oligomers of 3-HB, the protecting groups and the coupling procedure had to be changed.

It was found that the loss of 3-HB units during the debenzylation is particularly apparent when *N,N*-dimethylformamide (DMF) is used as solvent and elevated temperatures are employed [136]. While this loss can be avoided by the use of trifluoroethanol instead of DMF as solvent, conditions which would prevent the loss of 3-HB units during the cleavage of the *t*-butylester group have not been found. Trifluoroethanol and halogenated hydrocarbons (CH_2Cl_2, $CHCl_3$, $ClCH_2$-CH_2Cl) are the only solvents in which the higher 3-HB oligomers are soluble at room temperature. This fact limits the synthetic methodology applicable for their conversions.

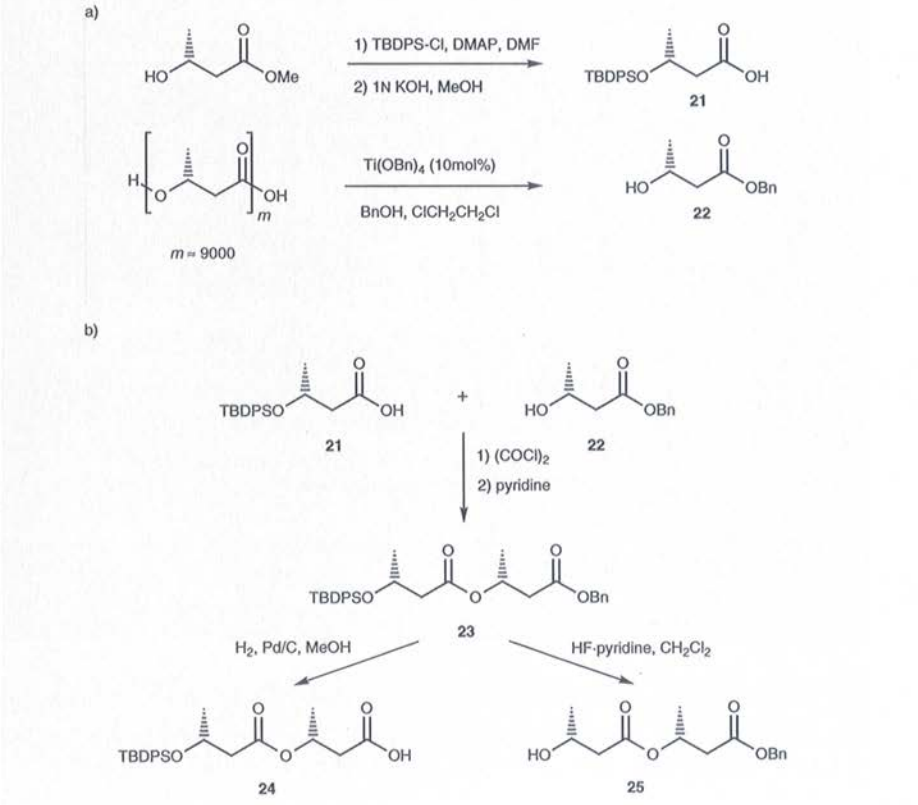

Fig. 35: Synthesis of the monomers **21** and **22** and of the dimers **23, 24** and **25** used as starting materials for the new synthesis of monodisperse oligomers of 3-HB.

Finally, we chose a benzylester protection for the COOH terminus and a *t*-butyldiphenylsilylether (TBDPS ether) protection for the OH terminus. This is the only (commercially available) silyl group stable in the presence of the HCl produced during the conversion of the acid to the acid chloride in preparation for the coupling steps.

The synthesis of the two new monomers **21** and **22** is outlined in Figure 35a and that of the dimer **23** is outlined in Figure 35b. This dimer was now ready for use as the new starting material in the synthesis of monodisperse oligomers.

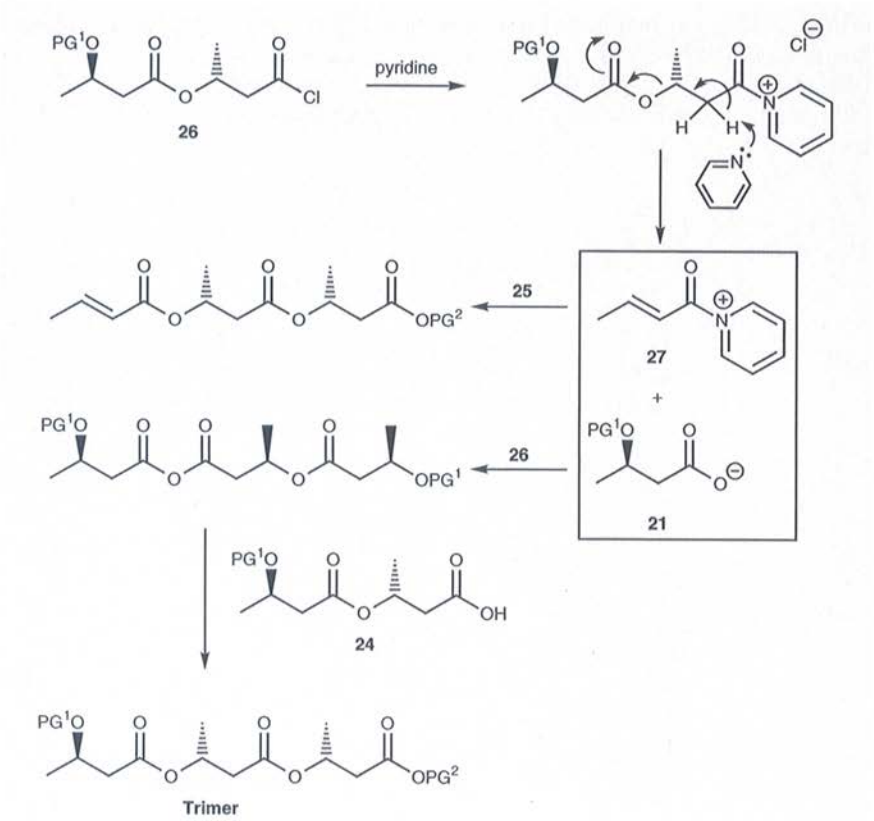

Fig. 36: Cleavage of ester bonds leading to loss of single units during the coupling procedure.

The loss of single 3-HB units during the coupling procedure was studied by ^{1}H-NMR spectroscopy with the dimeric acid **24** as a "model compound".

During the conversion of the acid to the acid chloride **26** with excess oxalyl chloride in dichloromethane at room temperature, there was obviously no loss of

3-HB units. But after the addition of one equivalent of pyridine cleavage occurred: the dimeric acid chloride was cleaved instantaneously by base induced β-elimination to give the carboxylate **21** and the acylpyridinium cation **27** (see Fig. 36).

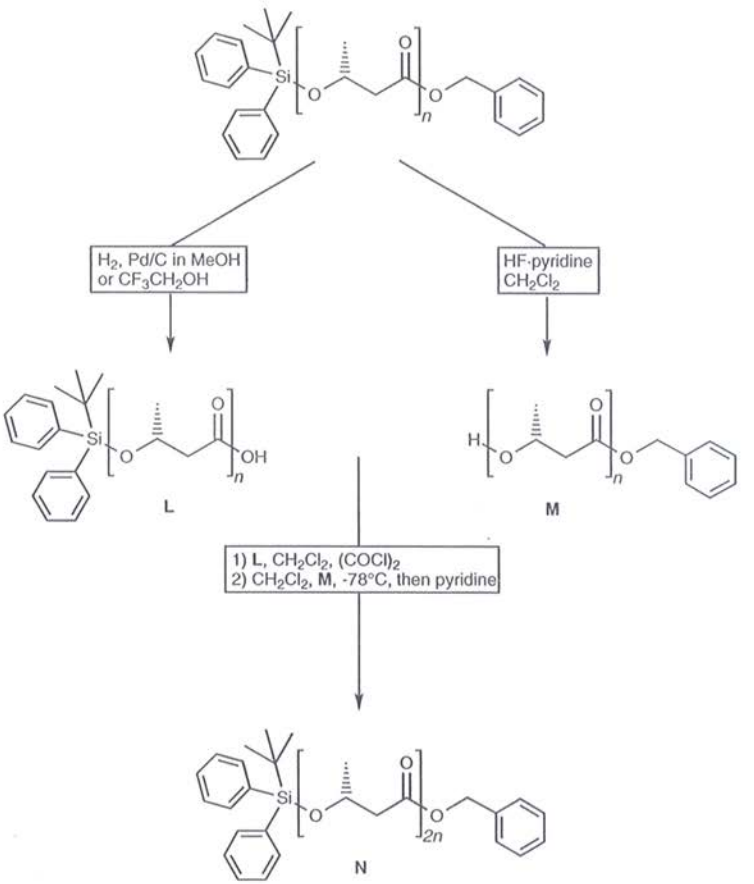

n	Yield [%] after the coupling of the corresponding *n*mer **L** and *n*mer **M**	2*n*mer **N**
2	85	**28** (n = 4)
4	85	**29** (n = 8)
8	90	**30** (n = 16)
16	60	**31** (n = 32)
32	60	**32** (n = 64)

Fig. 37: Segment condensation algorithm for the new synthesis of monodisperse oligomers of (*R*)-3-hydroxybutyric acid **28-32**.

The dimeric acid chloride **26** does not react with the dimeric alcohol **25** without the addition of pyridine. After a reaction time of two days, no product was detectable by ^{1}H-NMR spectroscopy. Fortunately, under pyridine catalysis, the acid chloride reacted with the corresponding alcohol at -78 °C. At this temperature, there was no loss of 3-HB units.

The new synthesis (see Fig. 37) led to oligomers containing 16, 32 and 64 units. All compounds were fully characterized. The LSI-MS of the 16mer **30** and 32mer **31** and the MALDI-MS of the 64mer **32** prove that the synthesized oligomers are monodisperse (Fig. 38).

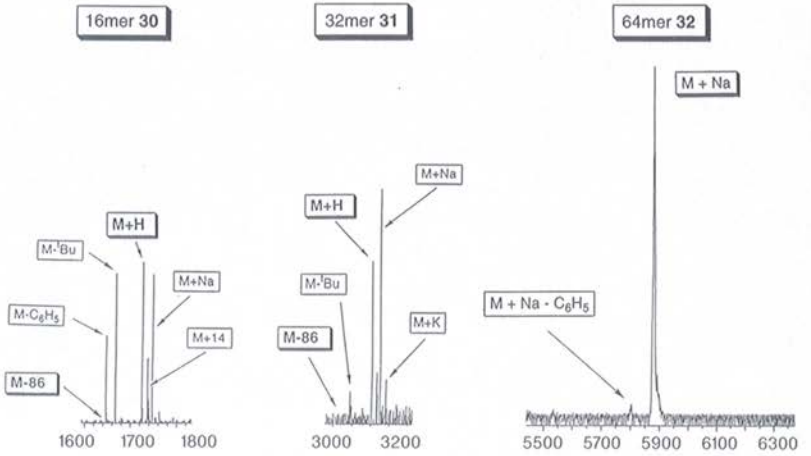

Fig. 38: LSI-MS (in a 3-nitrobenzyl alcohol matrix) of the fully protected 16mer **30** (left) and the fully protected 32mer **31** (center) and MALDI-MS of the fully protected 64mer **32** (right).

Solid State Structures of P(3-HB) and Oligo(3-HB) Derivatives

The crystallites formed when P(3-HB) is precipitated from a dilute solution are, in many ways, typical of polymer crystals. They have a lamellar morphology (i.e. they are thin platelet crystals) with the polymer chains running perpendicular to the lamellar crystal surface (the crystallographic *c*-axis) [143]. The length of the chains is much greater than the crystal thickness, which implies that a given chain must double back on itself and cross the crystal several times (see Figs. 39b and 39c for a schematic representation of the molecular arrangement within polymer lamellae).

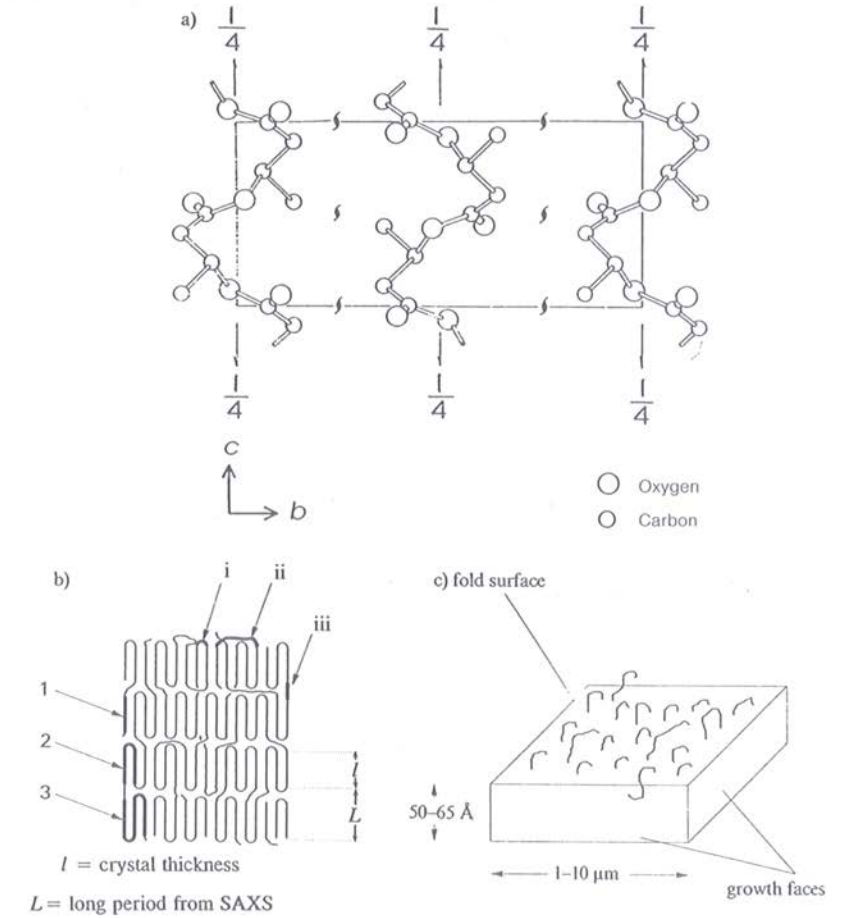

Fig. 39: Structural model for chain folded P(3-HB) crystals. a) Crystal structure on an atomic scale. b) Schematic diagram showing a cross section through a stack of polymer lamellae, some features of chain folding include *i*) tight folds with adjacent re-entry, *ii*) loose folds with random re-entry and *iii*) tie molecules connecting two or more crystals, l = crystallite thickness; L = long period (= l + amorphous part) as determined by SAXS (small angel X-ray scattering), the numbers 1, 2 and 3 indicate chain fragments with lengths in the ratio 1:2:3 that could remain after degradation, assuming that the etching agent can penetrate between the crystal layers, note especially that the repeat period of a stack of crystals is slightly greater than the crystal core thickness since the former includes space for folds and amorphous regions between the crystallite layers. c) View of an isolated lamellar P(3-HB) crystal indicating typical dimensions.

In Figure 40a, a micrograph of isolated crystallites of P(3-HB) grown from dilute solution (0.01 % wt/vol in propylene carbonate at 60 °C) is shown. These crystals were grown slowly and isothermally. In general, faster precipitation leads to multilayered crystallite aggregates.

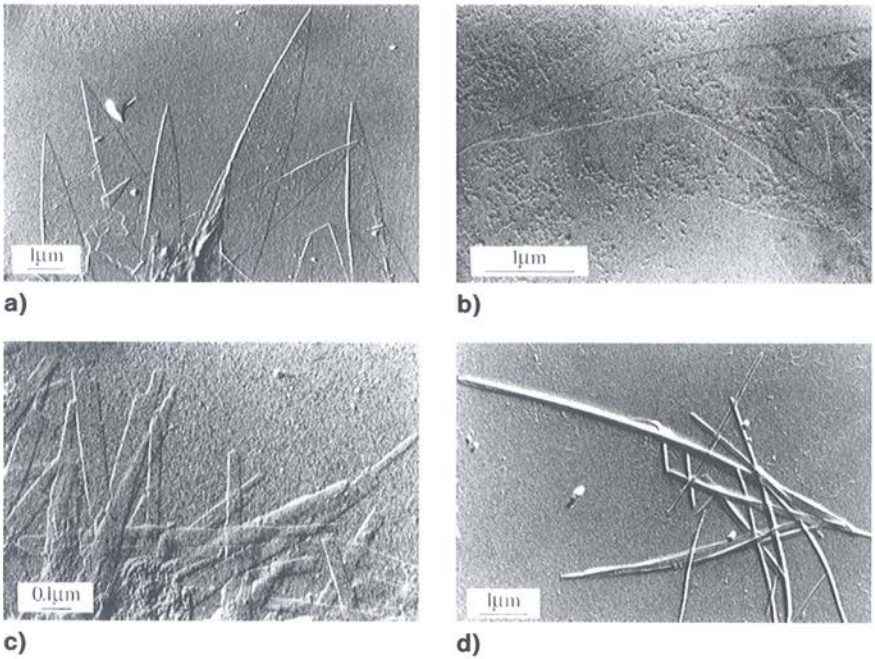

Fig. 40: Transmission electron microscopy of poly- and oligo-(3-HB)derivatives. a) Lamellar crystallites of P(3-HB) grown from solution in propylene carbonate at 60 °C. b) Protected 32mer (**17**). c) Protected 16mer (**16**). d) Unprotected 16mer. Samples for b) – d) were prepared by dissolving the oligomers in propylene carbonate (ca. 1% wt/vol) at 100 °C and subsequently quenched to 0 °C.

Controlled degradation of carefully prepared, isolated polymer single crystals has been used to investigate the structure of the fold surface [144–146]. The etching away of the loosest folds in the surface of the crystallites, using conditions under which the remaining segments are not soluble, has been used to examine the lengths of these segments. If there are tight folds (or "adjacent re-entries"), degradation products with lengths equal to integer multiples of the lamellar thickness may result. In this way, solid P(3-HB) was treated with gaseous methylamine by *Welland et al.* [147] and the analysis of the resulting oligo(3-HB) amides showed a bimodal distribution, just like the distribution obtained by us from the products of the treatment of P(3-HB) with the very aggressive, strong base lithium hexamethyldisilazide (LHMDS). In our degradation, the P(3-HB) had not been carefully crystallized but simply precipitated from a CH_2Cl_2 solution by MeOH/H_2O [138] or obtained by evaporating a $CHCl_3$ solution to dryness (Fig. 29). With the samples from the LHMDS degradation and with the synthetic oligo(3-HB) **15**, **16**, **17** and **18**, we were now in a position to confirm our speculation by the use of transmission electron microscopy (TEM) and wide angle X-ray scattering (WAXS) that we had encountered a similar effect to that observed by *Welland et al.*

Results from Transmission Electron Microscopy, from Small and Wide Angle X-Ray Scattering (WAXS) and from Atomic Force Microscopy

The results of these examinations are shown in Figures 41 and 40b-40d and in Table 6. The X-ray scattering results show that the undegraded P(3-HB) has the

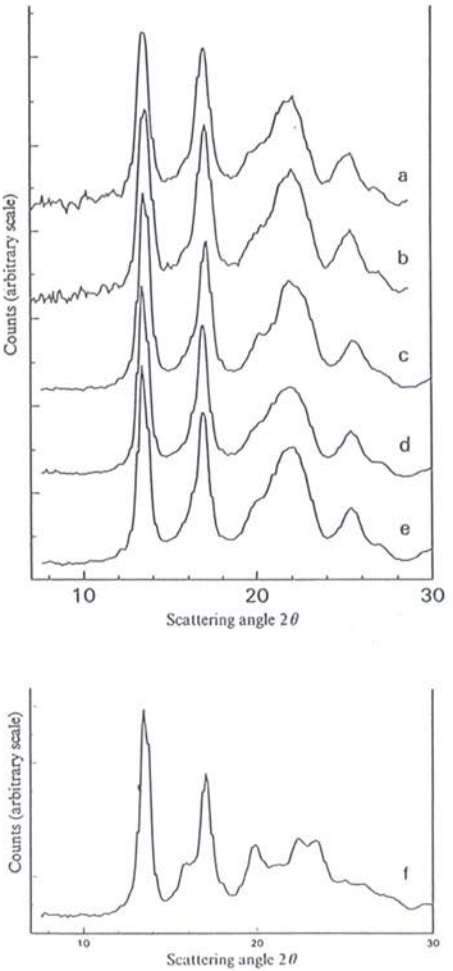

Fig. 41: WAXS profiles of: a) P(3-HB), b) Bacterial P(3-HB) after degradation with Li base, c) The 16mer after removal of the protecting end groups, d) The fully protected 16mer (**16**), e) The fully protected 32mer of 3-HB (**17**). Apart from minor differences caused by changes in crystallinity and crystal perfection, all the patterns are the same. f) Distinctly different WAXS profile of the unprotected 8mer.

normal crystal structure and thickness. It was the observation that the long period (with allowance made for the uncertainty in the amount of amorphous material between the crystallites) gave a thickness of about 58 Å, which was similar to the length of the smallest oligomers seen after degradation (about 45 Å, measured by GPC), which first suggested to us the idea that the oligomers were stable for physical rather than chemical reasons. After degradation, the crystal structure, as shown by WAXS (Fig. 41), was unchanged and the crystal thickness, as shown by SAXS, Table 6, dropped from 58 Å to 47 Å. These results indicate that the crystal cores had been relatively unaffected by the degradation.

Sample	Crystallite thickness [Å]	Number of monomers
Free 8mer	26	9
Protected 16mer **16**	52	17
Free 16mer	49	16
Protected 32mer **17**	53	18
Polymer	65-50[a])	22-17
Degraded Polymer **G1**[b])	54-40[a])	18-13

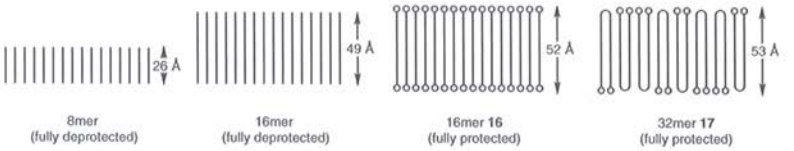

[a]) This represents the range between two extreme assumptions for interpreting the SAXS reflection: *i*) that the periodicity seen is the crystal thickness, *i.e.* that there is no amorphous material between the lamellae; *ii*) that the volume fraction of crystal in the sample is 75 % and the amorphous material alternates with crystalline lamellae.

[b]) P(3-HB) was degraded following the procedure outlined in *Figure 29*, omitting the extraction with $CHCl_3$ to preserve the lamellar structures.

Table 6: The results of small angle X-ray scattering. The uncertainty of the crystallite thickness is ± 2 Å. The number of monomers was calculated from the crystallite thickness with a helical pitch of 5.96 Å for P(3-HB). Below the Table, an idealized presentation of the arrangements of the chains in the linear oligomers **15, 16** and **17** studied by SAXS is shown. The unprotected 16mer forms crystallites which are slightly thinner than those of the *O*-benzylated *t*-butyl ester **16**. The 32mer **17**, having approximately the same lamellar thickness as the fully protected 16mer **16**, must be present in a hair-pin arrangement, the turn of which can not contain more than one or two HB units; otherwise, a smaller lamellar thickness should have been found. It remains uncertain whether the chains in **16, 17** and the fully unprotected 16mer are arranged in an antiparallel fashion, known from P(3-HB) itself, or whether they are packed parallel with all the acid or ester groups on one face and the alcohol or benzylether moieties on the opposite face of the lamella.

The WAXS results show that the monodisperse synthetic oligomers have the same crystalline structures as the high molecular weight polymer. The presence or absence of protecting groups on the termini of the 16mer makes no difference to the crystal structure, although it does seem to affect the way in which the crystals aggregate. The TEM shows that all the samples form lamellar crystals, with the 32mers being very similar to high molecular weight P(3-HB). It was especially interesting for us to see from the SAXS data (Table 6) that the crystal thickness of the 32mer **17** (53 Å) was almost exactly equal to that of the 16mer **16** (52 Å), which in turn corresponded closely to the length of 16 3-HB units in the 2_1-helical P(3-HB) lattice (48 Å). This implies that the 32mer is chain folded forming "hair pins" and, furthermore, that there is only a very short length of chain in the fold. Thus we conclude that the P(3-HB) chain is capable of folding tightly with adjacent re-entry.

For our present purposes, we use our results on the oligomers to show that removal of the fold surface need not render P(3-HB) crystals unstable or change the crystal structure. The observation of an unchanged crystal core after Li base treatment is therefore consistent with the removal of amorphous chains which form the loose folds and interlamellar ties. The molecular trajectories, which are most stable to degradation, are tight folds and tight tie molecules. Inspection of Figure 39b shows that this physical constraint naturally leads to chain fragments which have lengths in the ratio 1:2:3, where the unit is the lamellar thickness.

Figure 42 shows an atomic force microscopy (AFM) image of a crystal of the 32mer **17**, rather similar to crystals seen in TEM studies of these sample (see Fig. 12b). AFM has the advantage over TEM of giving direct information about the height of the crystal. Typical measurements of the thickness of the crystal yielded values of 55 Å (see Fig. 42). These data compare well with the long period obtained from SAXS, 52 Å [148].

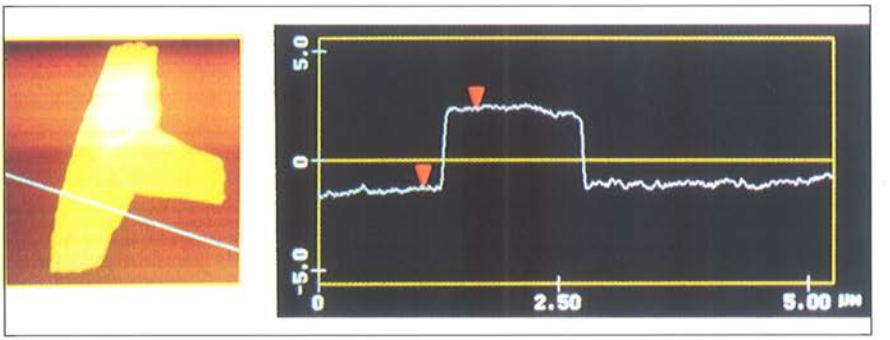

Fig. 42: Low-magnification AFM image of a lamellar crystallite of the 32mer **17** (left) and the corresponding line profile data (right).

Preparation of Cyclic Oligomers from (*R*)-3-Hydroxybutyric, -valeric and -octanoic Acid

As crystallization attempts of open chain oligomers of (*R*)-3-hydroxybutyric acid did not lead to single crystals suitable for X-ray analysis, we decided to concentrate our interest towards the synthesis of cyclic oligomers of 3-HB, so-called oligolides, of type **O**. In order to obtain information relevant to the role of biological P(3-HB) complexes, we set out to study the oligolide structures, their complexes with ions and their physical properties. The "higher" oligolides, those with five or more monomeric units, we hoped, could be model compounds for the low molecular weight *c*-P(3-HB) extracted from genetically transformable *E. coli*.

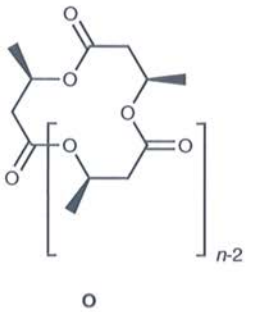

O

1 $n = 3$ (triolide)
33 $n = 4$ (tetrolide)
34 $n = 5$ (pentolide)
35 $n = 6$ (hexolide)
36 $n = 7$ (heptolide)
37 $n = 8$ (octolide)
38 $n = 9$ (nonolide)
39 $n = 10$ (decolide)

Fig. 43: Macrolides of type **O** and their nomenclature.

The preparation of these compounds can be achieved by two different strategies. In principle, the open chain precursor of each oligolide is accessible by the segment coupling method [142] outlined above and can be cyclized by the use of well established macrolactonization reactions under high dilution conditions. Several experiments have been successfully performed in our laboratories [141]. The advantage of this method is the simple isolation of the desired oligolide. On the other hand, mixtures of the different oligolides should be formed in a *single* reaction, starting from (*R*)-3-hydroxybutyric acid itself. The crucial problem then will be the separation of the product mixture. We decided to follow mainly the second strategy, because during our work we have developed suitable separation and analytical techniques [22]. Particularly, ^{13}C-NMR spectroscopy has been found to be an excellent tool for the determination of the composition of the crude oligolide mixtures. The resonance signals of the carbonyl carbons appear as sharp *singlets* for each oligolide (average C_n symmetry in solution). Under special measurement conditions (inverse gated experiment), a quantitative analysis is possible. In the following, different methods and conditions for preparing oligolides from (*R*)-3-hydroxybutyric, (*R*)-3-hydroxyvaleric and (*R*)-3-hydroxyoctanoic acid are described.

Macrolides of type **O** (Fig. 43) can be either obtained directly from P(3-HB) by acid-catalyzed transesterification [106] or from the monomeric building blocks shown in Figure 44, by macrolactonization with dicyclohexylcarbodiimide (DCC) [149], the methods of *Yamaguchi* and *Shanzer* or again by acid catalysis [141].

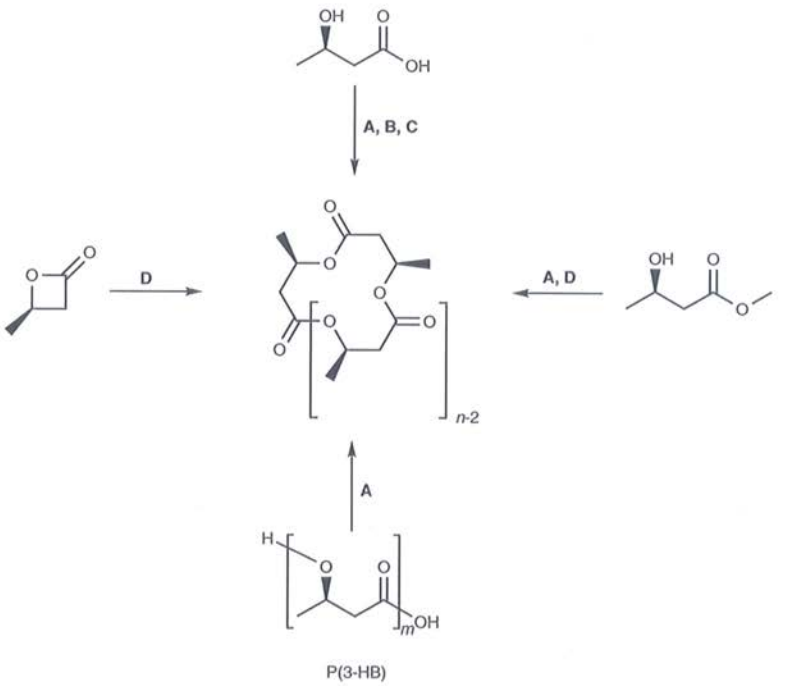

A: *Acid catalysis* - TosOH·H_2O, C_6H_6, reflux with azeotropic removal of H_2O

B: *Yamaguchi's method* - 1) 2,6-$Cl_2C_6H_3COCl$, pyridine; 2) DMAP/MeC_6H_5, high dilution

C: *DCC-activation* - N,N'-Dicyclohexylcarbodiimid/solvent, cat. DMAP or 4-pyrrolidino-C_5H_4N

D: *Shanzer's method* - Sn-catalyst, C_6H_6, reflux

Fig. 44: Preferred macrolactonization methods investigated in our laboratories.

Depending on the reaction conditions, the oligolides are obtained in various proportions and can be separated from each other up to the decolide **39** (40 ring atoms!) by careful chromatography. Under thermodynamic control, the triolide **1** predominates (Fig. 45a). Hence, acid-catalyzed transesterification or esterification of P(3-HB), 3-HB, or its methyl ester with *p*-toluenesulfonic acid monohydrate (TosOH·H_2O) affords this molecule in ca. 50% yield by simple dis-

tillation of the crude product mixture. The DCC-induced lactonization of 3-HB was found to be dependent upon the type of carbodiimide, the catalyst, the concentration of the hydroxy acid, the reaction temperature and significantly, upon the kind of solvent used. In all investigated cases, oligolides with five or more monomeric units are formed as main products (Fig. 45b). *Yamaguchi's* macrolactonization by means of the mixed anhydride consists of two steps: the formation of the mixed anhydride with 2,6-dichlorobenzoyl chloride and the alcoholysis of the anhydride under high dilution conditions with 4-(dimethylamino)-pyridine [150]. As can be seen from Figure 45c, this reaction leads again to the formation of "higher" oligolides ($n \geq 5$). *Shanzer's* so-called template mediated macrolactonization with the tin catalyst [151] gave oligolides containing four and more hydroxy acid units as main products (Fig. 45d).

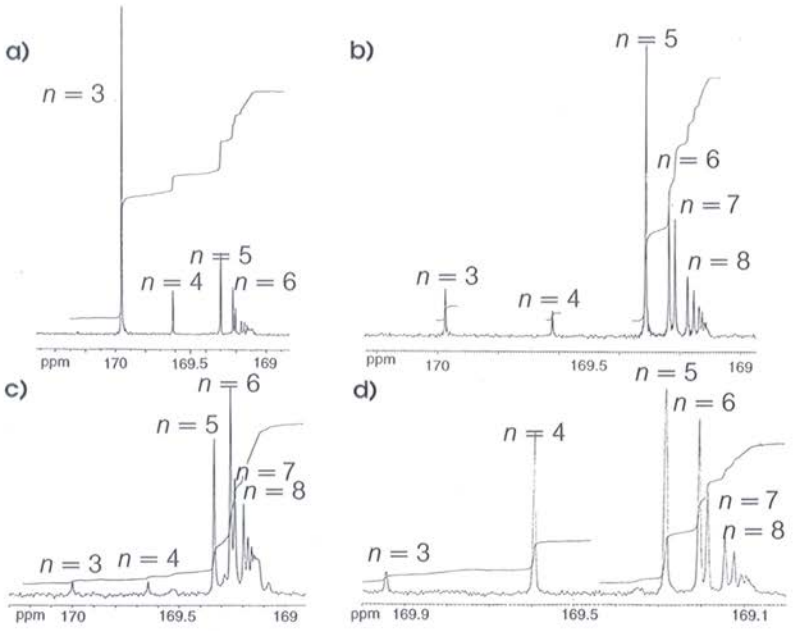

Fig. 45: Quantitative ^{13}C-NMR spectra of the carbonyl region of oligolide mixtures obtained from (*R*)-3-hydroxybutyric acid by a) Acid catalysis with TosOH·H_2O, b) DCC-activated lactonization, c) *Yamaguchi's* method and d) *Shanzer's* procedure.

The oligolide distributions obtained by *Yamaguchi's* lactonization method as well as *Shanzer's* procedure at low temperatures changed clearly, when the reaction times and temperatures were drastically increased. Thus, both reactions gave larger amounts of triolide **1** under these conditions.

In some extractions of *c*-P(3-HB) from genetically transformable *E. coli* performed in our laboratories [133], we found P(3-HB) containing small amounts of 3-HV (ca. 14% by ^{1}H-NMR spectroscopy and gas chromatography of the degradation products, see Figs. 25 and 26). This discovery of 3-HV units in *c*-P(3-HB), as well as the quite different properties of BIOPOL as compared to pure P(3-HB), led us to prepare analogous macrocycles with (*R*)-3-hydroxyvaleric acid (**40**) as monomeric unit. This chiral acid can be obtained by transesterification of the copolymer BIOPOL with methanol under acid catalysis to yield a mixture of the corresponding monomeric methyl esters, which are separable by careful distillation using a *Spaltrohrkolonne.* Finally, the methyl ester of 3-HV is saponified, yielding pure (*R*)-3-hydroxyvaleric acid (**40**).

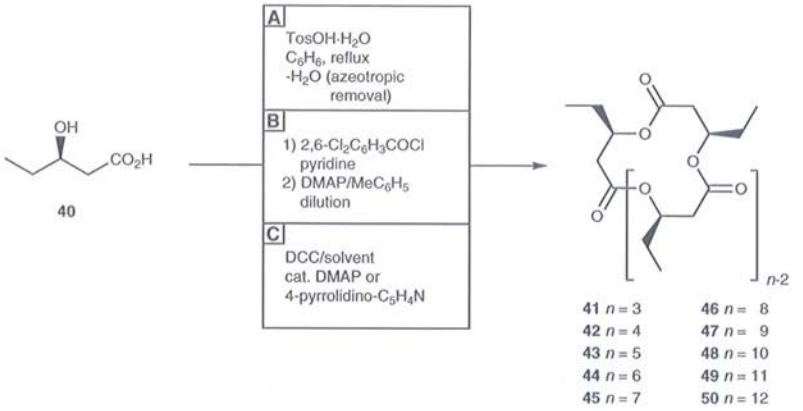

Fig. 46: Preparation of macrocyclic oligomers **41-50** starting from (*R*)-3-hydroxyvaleric acid (**40**) according to the acid-catalyzed macrolactonization procedure (A), *Yamaguchi's* method (B) and to the DCC-mediated macrolactonization procedure (C).

Once again, the well established methods for macrolactonization shown in Figure 46 were used. The product ratios obtained in these experiments are comparable to our results with 3-HB as starting material. Oligolides with three to twelve monomeric units (**41-50**) have been isolated and fully characterized [149].

To increase the lipophilic character of our model compounds, the same macrolactonization methods were applied with (*R*)-3-hydroxyoctanoic acid (**51**) as starting material (Fig. 47). The chiral acid **51** can be obtained from a copolymer (produced by fermentation with *P. oleovorans;* containing (*R*)-3-hydroxyhexanoate and (*R*)-3-hydroxyoctanoate [152]) by a similar method as described above for the isolation of 3-HV from BIOPOL.

Again, the resulting product ratios of oligolide mixtures in these runs are comparable to our results with 3-HB as well as with 3-HV as starting materials. Here, the resulting macrocycles, with three to five monomeric units (**52-54**), have been isolated and fully characterized.

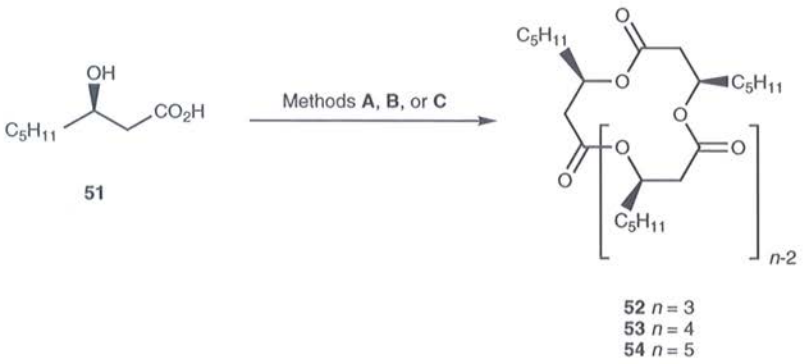

51

52 $n = 3$
53 $n = 4$
54 $n = 5$

Fig. 47: Preparation of macrocyclic oligomers **52-54** starting from (*R*)-3-hydroxyoctanoic acid (**51**) by acid-catalyzed macrolactonization (A), *Yamaguchi's* method (B) and DCC-mediated macrolactonization (C). For preparative details see Figure 46.

Structural Studies – the Cyclic Oligomers as Model Compounds for the Polymer

Important structural information was obtained from the X-ray diffraction on the polymer fibre and from the investigation of the lamellar crystallites of P(3-HB). However, it had been hoped that a more precise knowledge of the biological significance of P(3-HB) could be deduced from the X-ray analysis of single crystals of the 3-HB oligomers, but unfortunately none of the linear 3-HB derivatives gave suitable crystals. Therefore, our efforts were concentrated on the macrocyclic compounds. With all the oligolides mentioned so far, we have model compounds in hand, which allow the study of their solid state structures, their interactions with ions and their physical properties, which should be representative of the corresponding polymeric materials. The advantage of these compounds is evident: they have a defined molecular weight and show a rather high tendency to crystallize. Single crystals of the oligolides **1, 33–37** (see Fig. 43) were grown and their structures were determined (Fig. 48). For both, hexolide **35** and octolide **37**, two crystal forms containing different conformers were isolated and identified. In addition, the solid-state structure of the racemic (*R,R,S*) triolide **55** was determined [141].

The structures are remarkably similar (Fig. 49). Comparison of the two C_2 symmetric conformations of the tetrolide **33** and the C_2-symmetrical conformation of

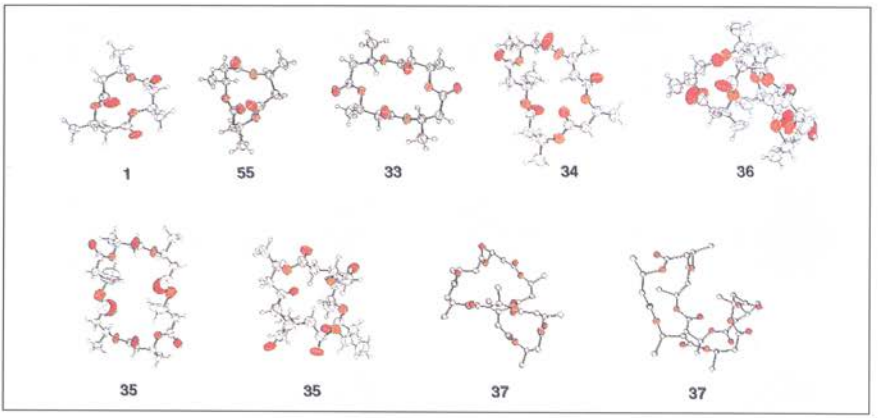

Fig. 48: Structures of the oligolides **1, 33–37** and **55**. The hexolide **35** can adopt a flat or a folded conformation. The octolide **37** has two different folded conformations.

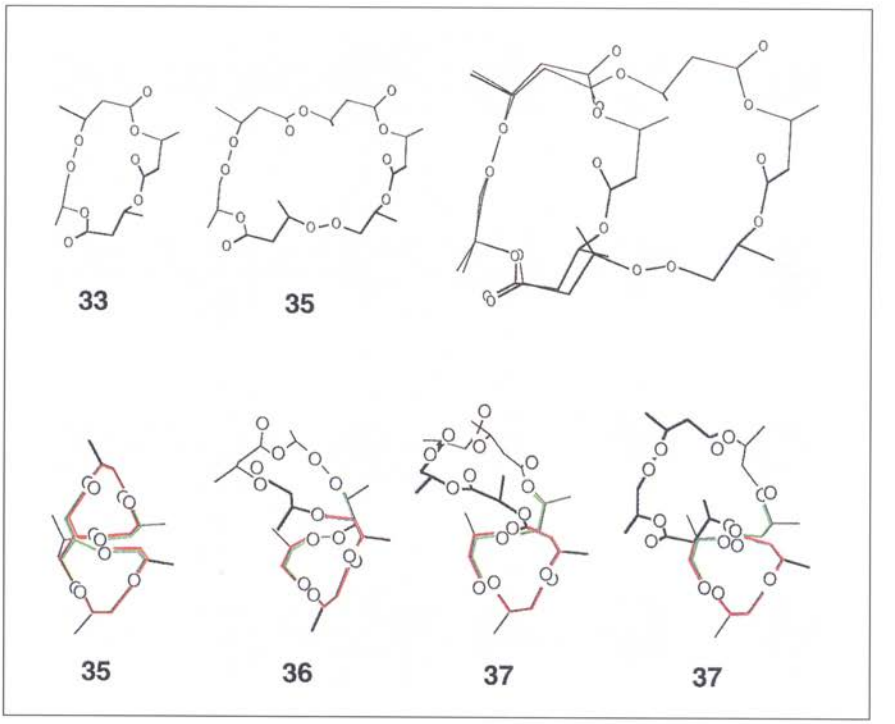

Fig. 49: Structural similarities between the macrolides. MacMoMo views of **33** and the C_2-symmetrical conformation of **35** and their superposition. The higher macrolides all contain, as common structural fragments, a Δ-shaped portion (red) and an S-shaped moiety (green).

the hexolide **35** show that the latter can be constructed from **33** by halving and introducing two further hydroxybutyric acid units. The larger macrolide structures **35–37** are all constructed of folded rings and contain, as common structural elements, an S-shaped and a Δ-shaped region (Fig. 49) [141]. Compared to the results of the 3-HB derivatives, the oligolides of 3-HV show a distinctly poorer crystallization tendency. For this reason, only four 3-HV oligolide structures have been determined by X-ray crystal structure analysis (Fig. 50) [149].

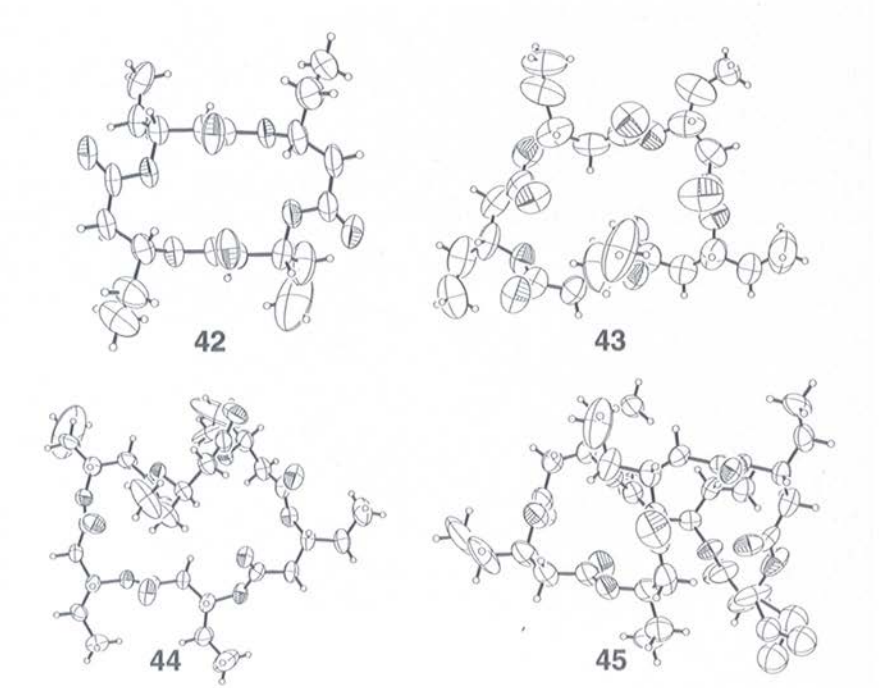

Fig. 50: ORTEP plots of the crystal structures of **42, 43, 44** and **45**.

The difficulties in obtaining single crystals of 3-HV derivatives, compared to those of 3-HB, may be explained by the additional degree of freedom provided by the rotation of the ethyl groups, which also causes the disorder phenomena observed in the pentolide **43** and heptolide **45** structures. The overall similarity with the 3-HB oligolides is striking and can be clearly recognized by inspection of Figure 51 in which best fits of the oligolide backbones (3-HB in black, 3-HV in red) have been superimposed.

For the tetrolides, pentolides and heptolides, the agreement decreases slightly with increasing ring size. Only the 3-HV hexolide structure deviates considerably

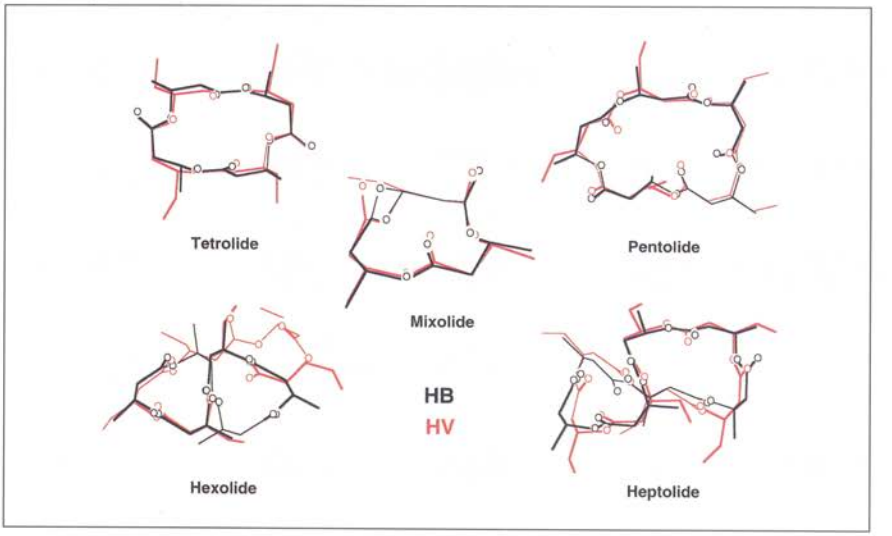

Fig. 51: Superposition of the 3-HV oligolides **42–45** and of the mixolide (with 27 % 3-HV content) with their 3-HB analogs. The 3-HV oligolides are indicated in red, the 3-HB derivatives in black.

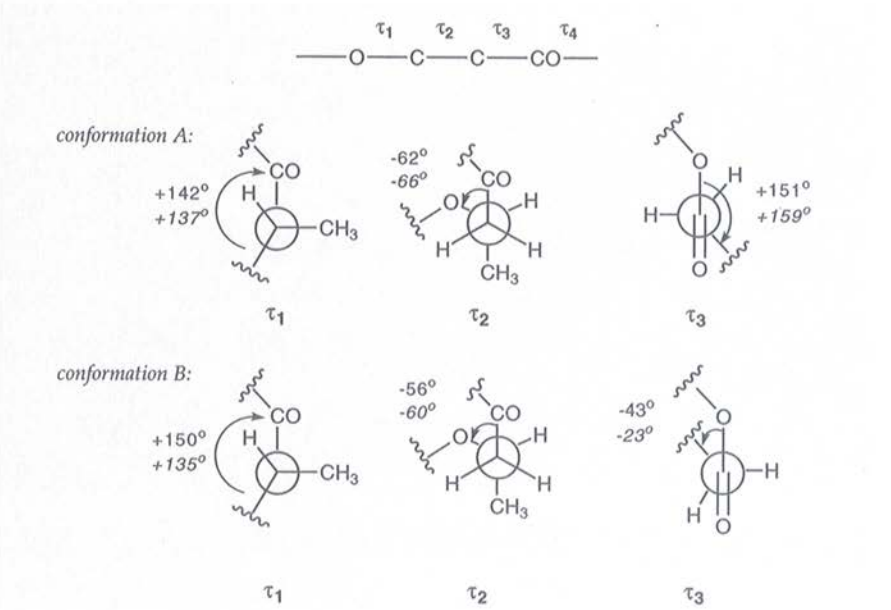

Fig. 52: Mean torsion angles $\tau_1 - \tau_3$ and Newman projection of the bonds of the (*R*)-3-hydroxy acid units in conformation A (Δ-shaped building block) and conformation B (S-shaped fragment) of the higher 3-HB and 3-HV oligolides (the values for the 3-HV derivatives are given in *italics*).

from the structures of **35** but the structural element of the Δ-fragment can still easily be recognized. A study of the interdependence of the torsion angles τ_1, τ_2 and τ_3 reveals two preferred configurations of the hydroxy acid units in these cycles, which differ slightly for 3-HB and 3-HV derivatives (Fig. 52).

There appear to be two conformational minima for τ_3, the dihedral angle for the α-carbonyl C-C bond. The larger one, which forms the Δ-shaped structural element occurs about three times more frequently than the smaller, which forms part of the S-shaped fragment. Using the average torsion angles of the S-fragments, two 2_1 helices for P(3-HB) and P(3-HV) can be constructed and these are shown in Figure 53 [141, 149]. As can be seen, the pitch of the two helices is quite different (6.1 for HB *vs.* 5.6 Å for HV) and both agree excellently with the structures derived from stretch-fibre X-ray diffraction measurements (6.0 for HB *vs.* 5.6 Å for HV) [153, 154]. A helix with almost perfect 3_1 symmetry can be modelled with the average angles τ_1, τ_2, τ_4 and the larger τ_3 value. Both 3_1 helices are compared in Figure 54. The 3-HV deviates more than the 3-HB helix from the ideal 3_1 geometry. The somewhat different torsion angles in the 3-HB and 3-HV units lead again to different pitches of the corresponding "3_1" helices. In this case, the 3-HV helix is steeper than that derived from 3-HB (6.0 for HB *vs.* 6.7 Å for HV). However, it must be stressed that the 3_1 helix has not been found experimentally in the polymer and that it may be an artefact of the ring closure.

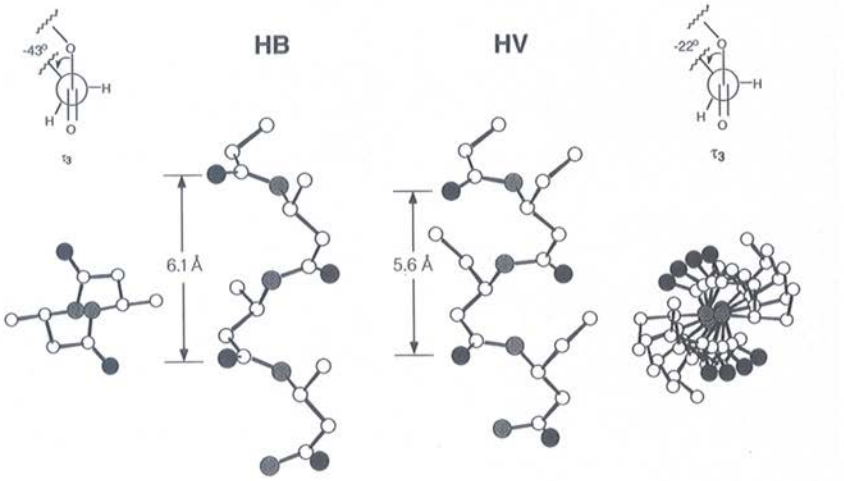

Fig. 53: Left-handed 2_1 helix, constructed with the averaged torsion angles of the S-fragment.

Since a remarkably simple method of preparing the triolide **1** directly from P(3-HB) on a 40 g scale had been found, the cheaper copolymer BIOPOL (73 %

3-HB/27 % 3-HV) was treated under the same conditions (Fig. 55). After simple work-up and distillation of the residue, a mixture of four differently substituted triolides ("mixolide") was obtained in 25 % to 35 % yield. To our surprise, this mixture was a material of extremly high crystallinity and crystallized in the receiver flask of a vacuum destillation apparatus (an impurity usually causes melting point depression!).

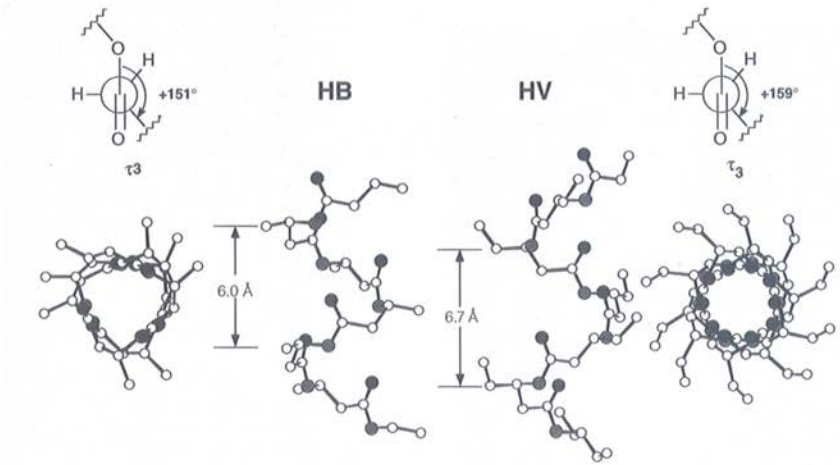

Fig. 54: Right-handed 3_1 helix, constructed with the averaged torsion angles of the Δ-fragment.

After recrystallization, the crystals include half a solvent molecule per triolide which could be identified as diethylether by ^{1}H-NMR spectroscopy. The oxygen atom of the ether molecule is situated on a screw axis in the crystal lattice. The triolide molecules are arranged around this axis and form channels through the crystal, which accommodate the solvent (Fig. 56).

These channels allow for fast diffusion of the solvent molecules out of the crystal: the crystals are unstable outside a solvent-saturated atmosphere. Crystals damaged by loss of solvent can be restored by short washing with mother liquor. This means that the triolide lattice has more or less survived the loss of solvent molecules and that the diffusion of these molecules is reversible – a phenomenon reminiscent of the behavior of zeolites. The channel housing of the solvent molecules must be chiral (it is formed with only (*R,R,R*)-triolides) and, therefore, chiral molecules may be selectively included. We also prepared a *mixolide* from a mixture of 33.3 % 3-HB and 66.7 % 3-HV units and obtained a mixture containing **1** (2 %), **56** (20 %), **57** (46 %) and **41** (32 %). Again, crystals could be prepared which were suitable for an X-ray analysis. Also, the arrangement of the molecules within the lattice is almost identical, with one methyl group being replaced (statistically speaking) by an ethyl group. This additional ethyl group points into the channel region which is

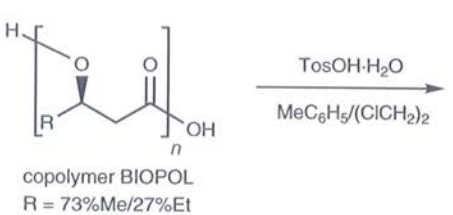

R = Me, Me, Me: 39% **1**
R = Me, Me, Et: 43% **56**
R = Me, Et, Et: 16% **57**
R = Et, Et, Et: 2% **41**

Fig. 55: Acid-catalyzed transesterification of BIOPOL gives a mixture of four differently substituted triolides. The photograph shows crystals of this four component mixture.

occupied by solvent molecules and consequently, there are less ether molecules present per triolide (1:4) than in the other structure (1:2).

As can be seen in Figure 48, the three carbonyl groups of the triolide point in the same direction. This conformation is also present in solution, as deduced from a detailed analysis of the NMR spectra and from the large dipole moment of **1** (4.6 Debye in CCl_4 [141]; 1.72 Debye for CH_3COOCH_3 [155]). Since linear oligo(3-HB) containing between 100 and 200 3-HB units has been postulated to be involved in complexing calcium polyphosphate as part of an ion channel through the cell membrane (see Fig. 21), we thought that the triolide **1** with its three unidirectional carbonyl groups could serve as a model for the complexation of ions by oligo(3-HB) derivatives. In fact, ion transport experiments proved that the (*R,R,R*)-triolide **1** is a more efficient ionophore than its (*R,R,S*)-isomer **55** (with only two unidirectional C=O groups) (*vide infra*). From a solution of NaSCN in MeCN containing a stoichiometric amount or a slight excess of triolide **1**, crystals suitable for X-ray diffraction were obtained. The composition was (3 NaSCN · 4 **1**). A look at a larger section of this structure (Fig. 57) is reminiscent of the chaos in solution!

Closer inspection reveals that there are four types of triolide molecules in this structure: (i) those making no contact at all with Na^+; (ii) those using a C=O

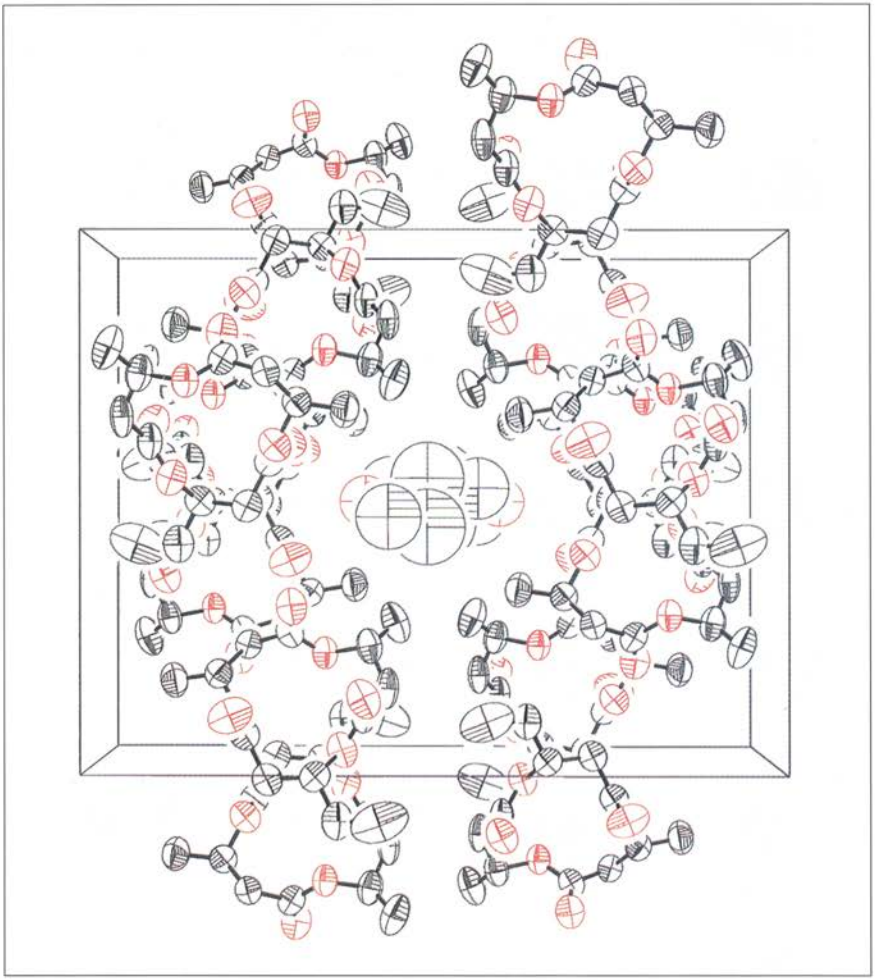

Fig. 56: Packing plot of the mixolide 27% 3-HV crystal structure, containing 0.5 equiv. of Et_2O.

oxygen for a single contact with Na^+ and another one for a bridging $C{=}O(Na^+)_2$ between two sodium ions; (iii) those forming a chelate $C{=}O\text{-}Na^+\text{-}O{=}C$ and at the same time bridges between sodium ions with their other carbonyl oxygens; (iv) finally, there are triolides forming the crown ester complex, using all three of their C=O oxygens for contact with the same Na^+ (Fig. 58), and simultaneously two of their C=O oxygens act as bridging elements. While there are numerous crystal structures of crown ether complexes with ions, as well as complexes containing ester carbonyl *and* ether oxygen ligands, or amide oxygens around the metal [156, 157], the ester crown seen in the present structure is unique.

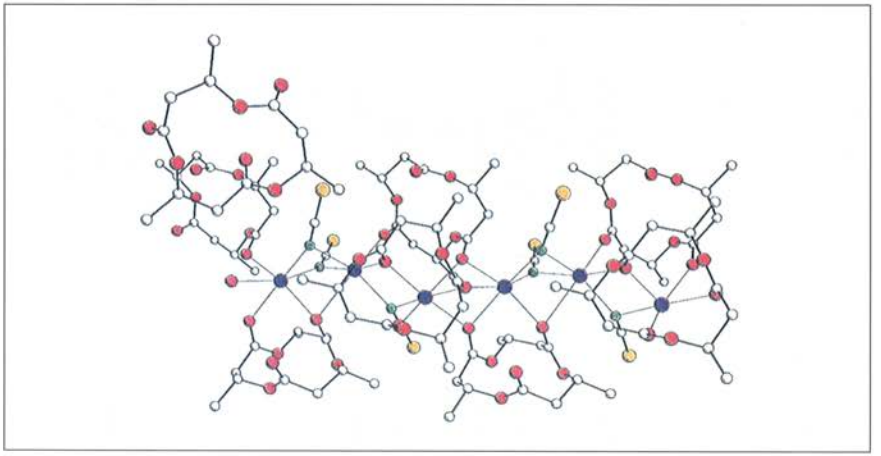

Fig. 57: A representative section of the structure of (3 NaSCN · 4 **1**) containing the four different types of triolides making zero, one, two (chelate) and three (crown) contacts with Na^+ ions.

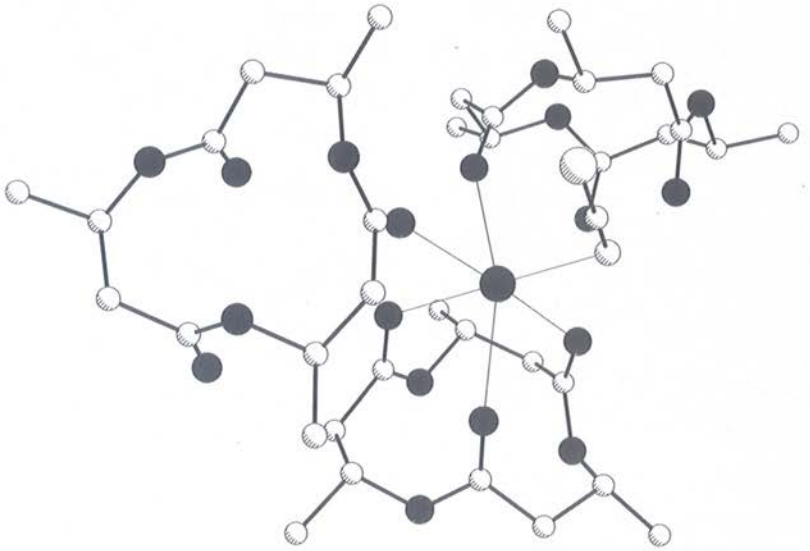

Fig. 58: Section of the Na^+ complex structure (3 NaSCN · 4 **1**) containing the ester crown.

In a similar complex from a crystallization experiment with KSCN there was no crown ester substructure but again chelates between a triolide **1** molecule and

K^+, and four-membered rings containing O-K-O-K (Fig. 59). The only alkaline earth ion complex we have been able to isolate as suitable crystals contains $Ba(SCN)_2$, the triolide **1**, H_2O and THF molecules (ratio 2:2:2:1) (Fig. 60). Salts of the biologically relevant ions Mg^{2+} and Ca^{2+} have so far, in our hands, not formed single crystals containing **1**.

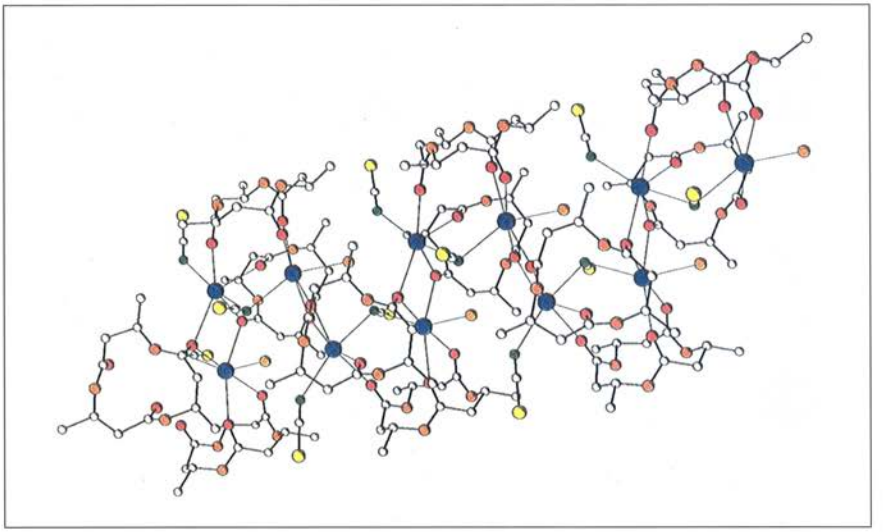

Fig. 59: Section of the K^+ triolide complex (2 KSCN·2 **1**·H_2O) showing all varieties of complexation between the cations and triolides or thiocyanate anions.

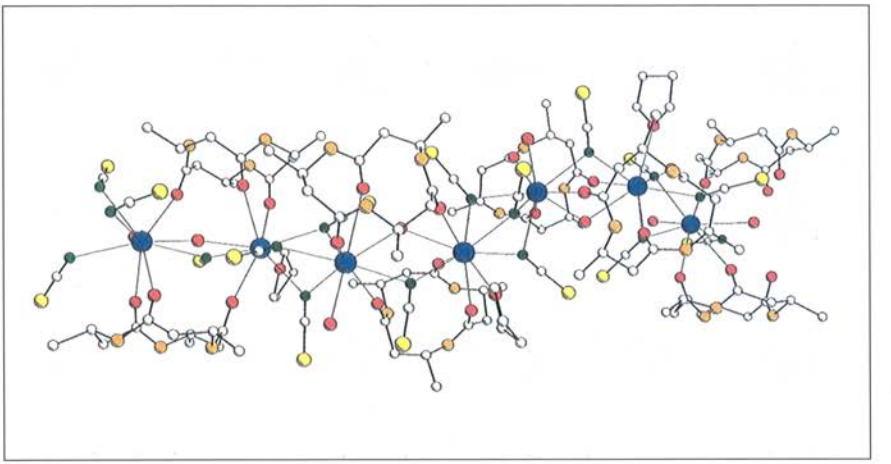

Fig. 60: Section of the polymeric structure of the Ba-triolide complex (2 $Ba(SCN)_2$·2 **1**·2 H_2O·THF). The coordination sphere of Ba is occupied by 9 ligands, containing triolide C=O, THF and water O-atoms, as well as N-atoms of SCN^-.

The geometry of the triolides with the three approximately parallel C=O groups is preserved in the complexes, superposition of the free triolide **1** and the triolides complexed to the ions reveals, however, that the C=O O-atoms can move somewhat closer to improve chelation (see Fig. 61).

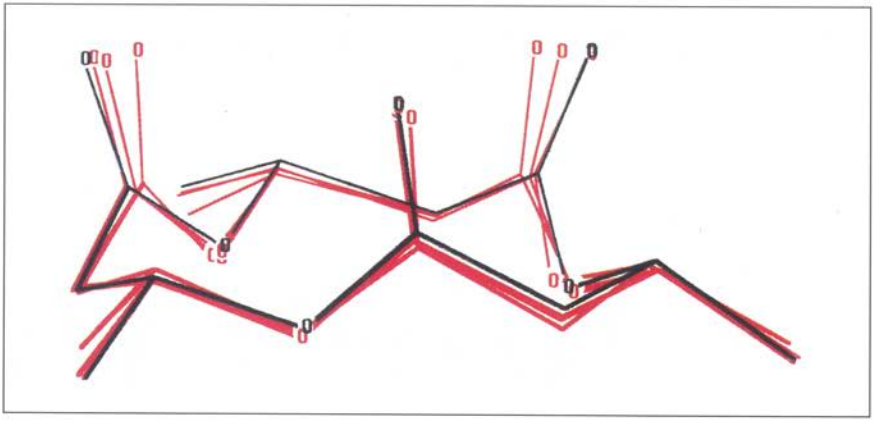

Fig. 61: Superposition of the triolide molecules in the crystal structure of ligand **1** (red) and in the three different complexing modes of the triolides in the NaSCN complex of the 3-HB triolide (black). The structures of the triolide molecules in the other complexes of **1** are very similar.

As already mentioned above, crystals of the triethyl triolide **41** have not yet been obtained. So it is most remarkable that structural information about this elusive triolide **41** was gathered in an indirect way. In the crystal structure of its NaSCN complex (**41** · NaSCN · 2 H_2O · 0.5 MeCN) [149] both Na^+ ions are hexacoordinate: they are bridged by two H_2O molecules and by one triolide **41**. The octahedral coordination spheres are completed by two more H_2O molecules bridging the symmetrically equivalent sodium ions. This bridging leads to a one-

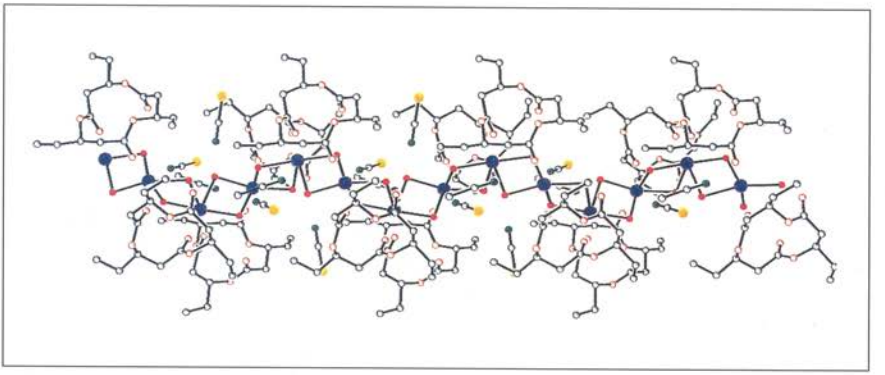

Fig. 62a

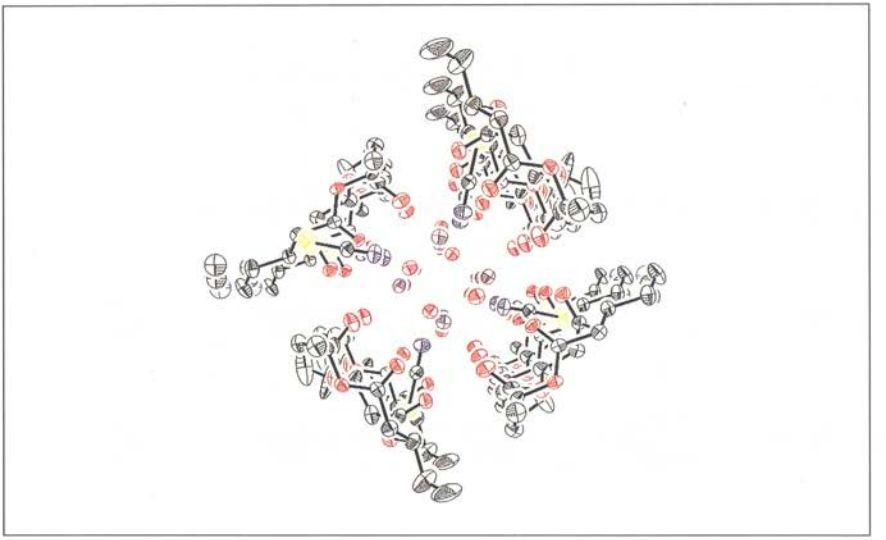

Fig. 62b

Fig. 62 a, b: Representation of the polymeric structure in the Na^+ complex (**41** · NaSCN · 2 H_2O · 0.5 MeCN). a) View perpendicular to the *a*-axis. b) Projection along the *a*-axis, to show the channel formed by the triolides **41** around the coordinated Na^+ ions and H_2O molecules.

dimensional polymeric structure (Fig. 62a). Only two of the three carbonyl oxygens of each triolide **41** are coordinated to sodium in such a way that pairs of Na^+ ions are connected via a triolide **41**; the third carbonyl oxygen forms a hydrogen bond with a bridging H_2O molecule.

The type of complexation seen between the Na^+ ions and the triolide molecules **1** in the 3-HB triolide **1** NaSCN complex (4 **1** · 3 NaSCN) [106, 158] and that seen in the complex (2 **41** · 2 NaSCN · 4 H_2O · CH_3CN) differs remarkably: there is no ester crown, no chelated 8-membered ring and no double coordination of two sodium ions to the same carbonyl oxygen in the complex of **41**. This difference between the two complexes is probably due to the presence of water molecules in the complex of **41**. The need for inclusion of water might be due to the fact that the more bulky ethyl substituted triolide molecules **41** can not move close enough together in order to completely fill the Na^+ ion coordination sphere.

As can be seen from the projection along the *a*-axis shown in Figure 62b, the crystal structure of the NaSCN complex of **41** contains a kind of channel formed by triolide molecules **41**. The inner surface of this channel is covered by carbonyl oxygens and the channel is filled with water molecules and Na^+ ions. The outer surface of the channel is nonpolar. The counter ions SCN^- are sticking in the wall of the channel like needles, with nitrogen ends pointing inside. Thus, this struc-

ture, like those of the previously described complexes, may be considered as a model for the proposed cellular ion channel formed from *c*-P(3-HB) and Ca·PP_i [120, 121, 126, 136]. A conceptually new aspect in connection with ion channel formation involving 3-HB oligomers is the presence of water molecules as "cement" holding the components together. Inclusion of water in such a channel structure will increase the number of donor ligands available for complexation of cations – so far only the counter ions and the carbonyl oxygens have been assumed to be present. Thus, missing oxygen donor atoms for providing eight ligands to each Ca^{2+} in the channel structure for *c*-P(3-HB)/Ca·PP_i proposed by *Reusch* could be provided by water molecules, rather than by energetically unfavorable distortions of the P(3-HB) backbone.

Cation Transport across Bulk Liquid Organic Membranes

In the previous chapter, the X-ray crystal structures of several cyclic oligomers of 3-HB and 3-HV have been described. Moreover, the formation of single crystals of the triolide (of 3-HB as well as of 3-HV) in the presence of alkali and alkaline earth metal salts was demonstrated. Encouraged by these results, an investigation of possible ionophoric activity of P(3-HB) and its derivatives was undertaken. Therefore, the ion transport rates for alkali and alkaline earth metal ions

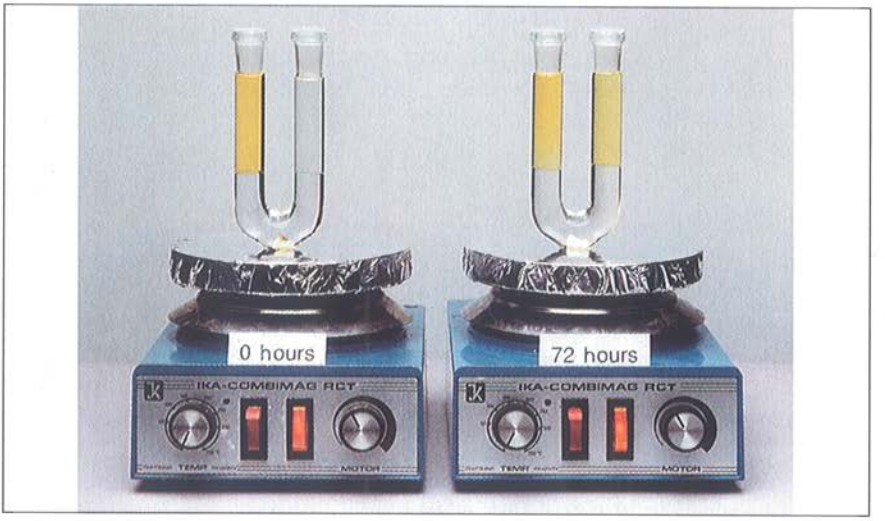

Fig. 63: Apparatus for performing transport experiments through a bulk liquid organic membrane. The ions are transported out of a TRIS-buffered solution initially 1 mM in alkali or alkaline earth metal picrate and 100 mM in alkali or alkaline earth metal chloride (left side of the U-tube), through a CH_2Cl_2 ionophore solution into the other arm of the U-tube, where the water phase becomes progressively more yellow as the experiment proceeds. The picrate concentration changes are monitored by UV spectroscopy at $\lambda_{max} = 356$ nm.

mediated by cyclic and open chain 3-HB derivatives across bulk liquid membranes have been examined [159]. Additionally, to investigate the effect of the lipophilic side chain, several experiments with oligolides of 3-HV have also been performed. To the best of our knowledge, this is the first example of ion transport through bulk liquid membranes by ionophores that carry exclusively ester carbonyl oxygen atoms as complexing sites for the cations. We made sure that, for instance, butyl acetate did not show the effects to be described.

A simple device to test compounds for ionophoric activity is a U-shaped tube in which a more dense organic phase containing the carrier is covered with aqueous solutions in the two legs. The metal ion solution is placed in one leg (donor solution) and an aqueous receiver solution placed in the other (Fig. 63). As this apparatus allows for stirring of the organic phase, diffusion processes across the liquid membrane are minimized and the overall transport rate is determined mainly by the rates of complex formation or dissociation and diffusion in the unstirred layers at the phase boundaries [160].

To avoid the formation of a pH gradient, we used a set-up similar to that used by *Okada et al.* for transport experiments with nonactin [161]: buffered aqueous donor or receiver solutions were employed and CH_2Cl_2 was the bulk liquid membrane. In addition to a metal ion picrate, the donor solutions contained a hundred fold excess of the corresponding metal chloride. This increases the chemical potential of the cation and leads to the desired linear correlation of % transport with time. The choice of the counter ion is important because it has to accompany the cation on its migration through the organic phase. The picrate anion was chosen for two reasons: picrates show higher transport rates than salts of other anions with crown ethers [162] and the progress of the transport is easily monitored by UV spectrophotometry.

Using the set-up described above, the transport of potassium picrate with several cyclic (*R*)-3-hydroxybutyric acid derivatives was first compared to the corresponding cyclic oligomers of (*R*)-3-hydroxyvaleric acid, the cyclic trimer of (*R*)-3-hydroxyoctanoic acid and several open chain oligomers of (*R*)-3-hydroxybutyric acid having variable chain lengths. For the sake of comparison, the molar equivalents of carbonyl groups per ml CH_2Cl_2 were maintained at a constant value in all experiments. Figure 64 shows the potassium ion transport with cyclic 3-HB oligomers of increasing ring size.

From its crystal structure, the triolide **1** was expected to be the most efficient ionophore because of its three unidirectional C=O groups. Indeed, it does have a high transport activity. But it was surprising to see that the tetrolide **33** is a better carrier than the triolide **1**, as its conformation in the crystal does not look as "attractive" for simultaneous multiple complexation of an ion when compared to

the "tripole" of the triolide **1**. It must be concluded that the conformation of the tetrolide **33** in solution is quite flexible like that of all the higher cyclic oligo (3-HB) derivatives. On the other hand, the pentolide **34**, which has an average C_5 symmetry in solution and a conformation in the crystal which does not look favorable for complexation, transports potassium ions less efficiently than the triolide **1**. Astonishingly, the hexolide **35** showed the lowest transport activity of all investigated oligolides.

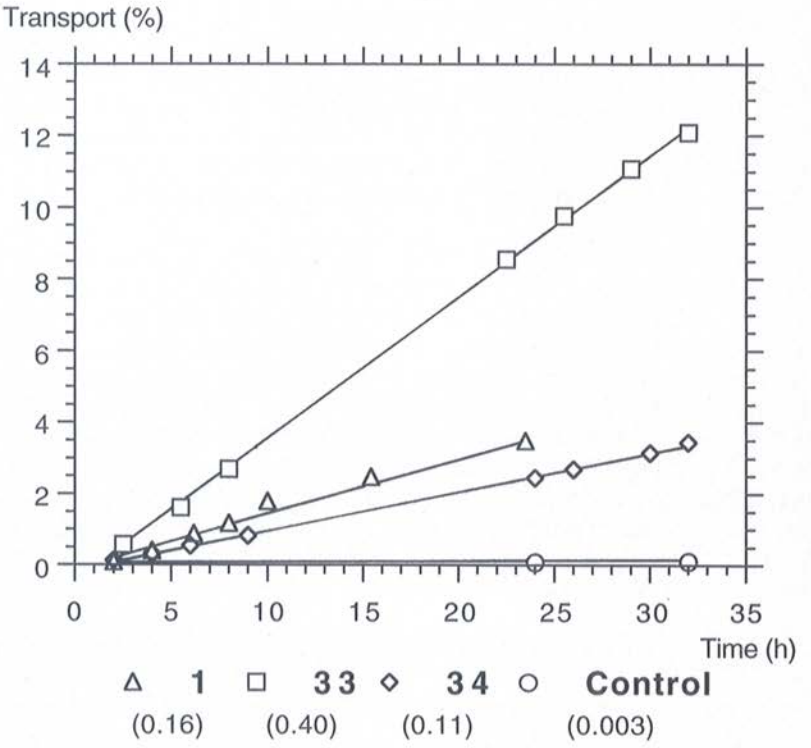

Fig. 64: Comparison of the potassium ion transport with the triolide **1**, tetrolide **33** and pentolide **34** of (*R*)-3-hydroxybutyric acid. The values on the y-axis correspond to the percentage of the initial amount of picrate from the donor phase. The numbers given in brackets underneath the codes denote % picrate migrating per hour. In the control experiment, no ionophore was added.

In subsequent experiments, the transport of potassium picrate mediated by the corresponding 3-HV oligolides **41-44** was investigated. For all these compounds, an enhancement of the transport rate compared to their homologous 3-HB macrocycles was found. This effect can be rationalized as the solubility of

the more lipophilic 3-HV derivatives (Et *vs.* Me groups) in water is much lower than that of the 3-HB compounds. An increase in the transport rate is known to occur when the hydrophobic nature of a ligand is increased without altering its complexation behavior [162]. With the cyclic trimer **52** of (*R*)-3-hydroxyoctanoic acid, a decrease in the transport of potassium picrate compared to its 3-HV derivative **41** was found. However, the transport was better than that seen for the 3-HB triolide **1**. This appears to indicate that the pentyl substituents hinder the complexation of metal ions at the phase boundary by the ligand **52**.

Encouraged by the strong transport effect of the oligolides mentioned above, experiments have been performed with the open chain oligomers of 3-HB of type **J**, **K** and **N**. Here, the observed transport rates were within the range of those found with the 3-HB pentolide **34**. In particular, the TBDPS protected compounds **N** showed a rather low transport activity, probably because of the bulky, hydrophobic protecting group. The deprotected compounds **J**, however, showed a somewhat higher transport activity. But two open chain oligomers, the degradation product mixture of P(3-HB) with ca. **28** units **58** and the 16mer **16** (shown in Fig. 65), have been found to be excellent ionophores in our experimental set-up.

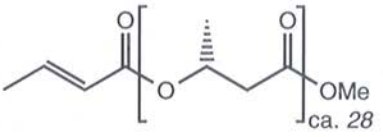

58

0.32 % picrate/h

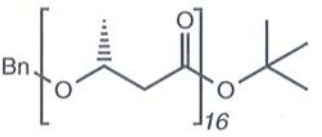

16

0.17 % picrate/h

Fig. 65: Two open chain oligomers, which are excellent ionophores for alkali and alkaline earth metal cation transport. The value of the transport rate for potassium picrate is given for both compounds. No correction was made for the migration rate due to the different viscosities of these oligo(3-HB) solutions.

The high transport activities (in the range of the 3-HB and the 3-HV triolides **1** and **41**) of these open chain 3-HB derivatives are somewhat surprising to us, as these ligands are not expected to possess a preformed geometry which is suitable for complexation. However, the flexible nature of the chain may allow it to adopt the conformation required for complexation of cations. It is also worthwhile to note that the addition of $Ba(SCN)_2 \cdot 3H_2O$ to a solution of microbial high molecular weight P(3-HB) in CF_3CH_2OH / H_2O causes a change in its specific rotation. This may indicate that a conformational change of the polymer structure has taken place and that conformers capable of varying cavity dimensions to adjust to the size of the different cations can be formed [163].

Under conditions similar to those outlined above, the transport ability of the triolide **1** was examined with all alkali metal cations from lithium to cesium and with all alkaline earth metal cations from magnesium to barium. The transport rates ($Li < Na < K < Rb < Cs$ and $Mg \approx Ca < Sr < Ba$) increase in the lyotrophic order [164], i.e. in both series, the transport efficiency becomes greater with increasing ionic diameter and decreasing heat of hydration. There is no detectable, exceptional selectivity for one of the ions.

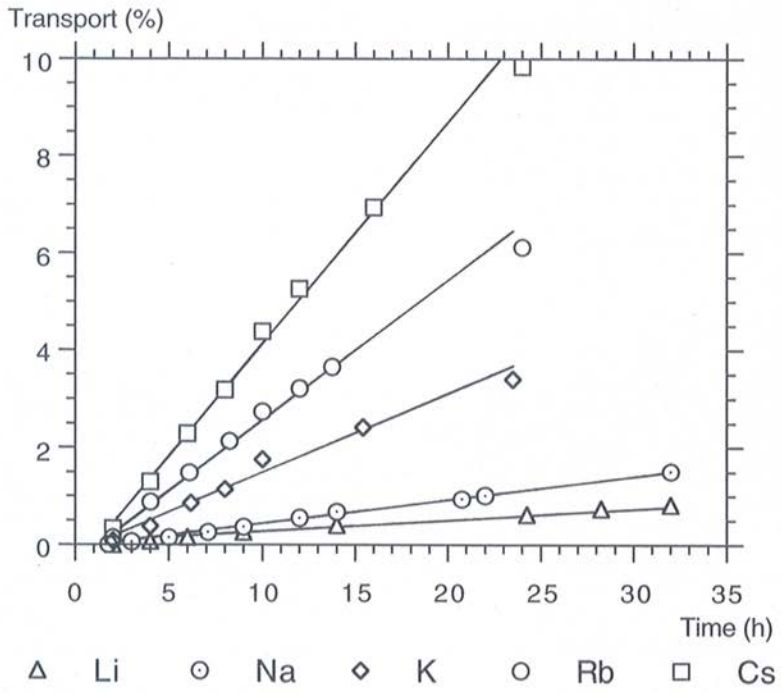

Fig. 66: Relative rate of transport of the alkali ions from lithium to cesium through a CH_2Cl_2 bulk liquid membrane mediated by the 3-HB triolide **1**.

The same experiments have been performed with the corresponding triolide **41** of 3-HV. For all cations, the transport activity was higher. Again, this is an effect of the lower solubility of these compounds in water compared to the 3-HB macrocycles. As before, the transport rates increase in the lyotrophic order.

With the two open chain oligomers shown in Figure 65, the transport ability with all alkali and alkaline earth metal cations has been investigated. No cation selectivity has been found; the lyotrophic order resulted again.

All these experiments demonstrate that several oligomers of 3-HB and 3-HV are well suited for the ion transport across bulk liquid CH_2Cl_2 membranes. Probably the most surprising finding is the high transport ability of the two open chain oligomers, which – *a priori* – do not possess a geometry suitable for complexation. This result is in support of the proposed function of linear oligo(3-HB) with 100 to 150 3-HB units as a component of an ion channel complex in cell membranes. It must be stressed, however, that there is no cation selectivity with our model compounds under the conditions described above.

Electrophysiological Investigations on the Native P(3-HB)/Ca·PP_i Complex from Competent *E. coli*

Independently from our studies on the complexing and transporting properties of synthetic P(3-HB) derivatives, *Reusch* began to characterize the complex extracted from competent *E. coli* by electrophysiological methods.

Because of their great physiological importance, transmembrane ion channels have been the subject of intensive research since the thirties. It has been observed that membranes of the nervous system are permeable for ions when a certain voltage is applied [165–167]. Since then, technology allowing the detection and characterization of all the different ion channels has been developed to an outstanding level. It is now possible to perform studies on living cells at single isolated channels. The importance of this field of research was demonstrated by the presentation of the Nobel Prize for medicine to *Neher* and *Sakmann* in 1991.

Once a membrane protein has been identified and purified, it can be transferred to an artificial bilayer where it can be studied without interference by the complicated cellular environment. Developed in the 1960s, ion channel reconstitution in planar bilayers has become a standard technique for the characterization of excitable membrane proteins [168].

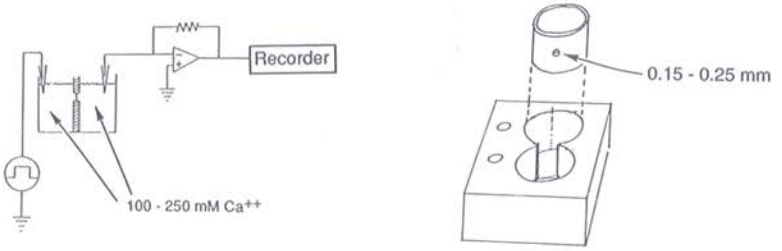

Fig. 67: Left: Schematic plan of a planar bilayer experiment. Right: Membrane chamber [168,169].

The experimental set-up is quite simple. It consists of a block with two intersecting holes; a cup, which is perforated on one side, can be fitted into one of these holes. The two chambers can now be filled with the appropriate salt solution. A typical experimental set-up is shown in Figure 67.

Membranes are formed by placing a small amount of lipid dissolved in hydrocarbons on the small hole that separates the two aqueous solutions. By draining, the lipid solution forms a film on the hole. This film gets thinner and thinner and finally becomes a bilayer. Membrane proteins are inserted into the planar bilayer either by direct incorporation or fusion [169]. In the direct incorporation technique, a small volume of a detergent solution containing the protein of interest is added to the aqueous solution with the hope that the channel will insert spontaneously into the bilayer. In the fusion technique, native membrane vesicles or liposomes containing the purified channel protein are added to the aqueous solution and are induced to fuse with the planar bilayer by applying osmotic conditions, which lead to the swelling of the membrane vesicles.

Electrodes are dipped into the aqueous solutions, which are now separated by the planar bilayer and a voltage can be applied. If only a lipid bilayer covers the separating hole, resistance in the giga-Ohm region is observed [170]. If a single channel protein is incorporated into the bilayer, the ion flux through this single protein can be detected by amplifying the measured current using the proper electrical set-up. A wide range of ion channels have been studied in model membranes using this technique, including nicotinic acetylcholine receptor channels, voltage dependent Na^+ and Ca^{2+} channels, Ca^{2+}-activated K^+ channels, Cl^- channels and a wide variety of porins from the outer membranes of bacteria and mitochondria [169].

Although it had been shown that Ca^{2+} channels are practically ubiquitous in eukaryotic systems, not much is known about Ca^{2+} transporting systems in prokaryotic cell membranes. As in the eukaryots, Ca^{2+} plays an important role in the metabolism of prokaryotes [171]. Here again, the extracellular concentration of Ca^{2+} is higher than the concentration in the cytosol. Some Ca^{2+}-uniporters have been described, but it has not been proved that these systems are specific for Ca^{2+} or if the Ca^{2+} is taken up by universal ion transporters. As yet, no transporting system has been purified to homogeneity. For *E. coli,* a phosphate-dependent [172] as well as a phosphate-independent [173] Ca^{2+}-uptake system have been reported. Both systems work only if a membrane potential or a pH-gradient builds up.

However, no prokaryotic Ca^{2+}-selective ion channel has yet been isolated and purified to a quality sufficient for reconstitution in planar bilayers.

About two years ago, *Reusch* started to investigate the electrophysiological properties of the proposed P(3-HB)/Ca·PP_i complex using the planar bilayer

technique outlined above. Freshly prepared competent *E. coli* were dried and extracted with $CHCl_3$ and this extract was mixed together with synthetic phospholipids in $CHCl_3$. Decane was added to this mixture and after evaporation of the $CHCl_3$, a planar bilayer was prepared using the resulting decane solution. When holding potentials greater than 60 mV were maintained across the bilayer, stepwise current fluctuations were observed, these being characteristic for voltage dependent ion channels. A representative electrogram obtained with the *E. coli* extract is shown in Figure 68.

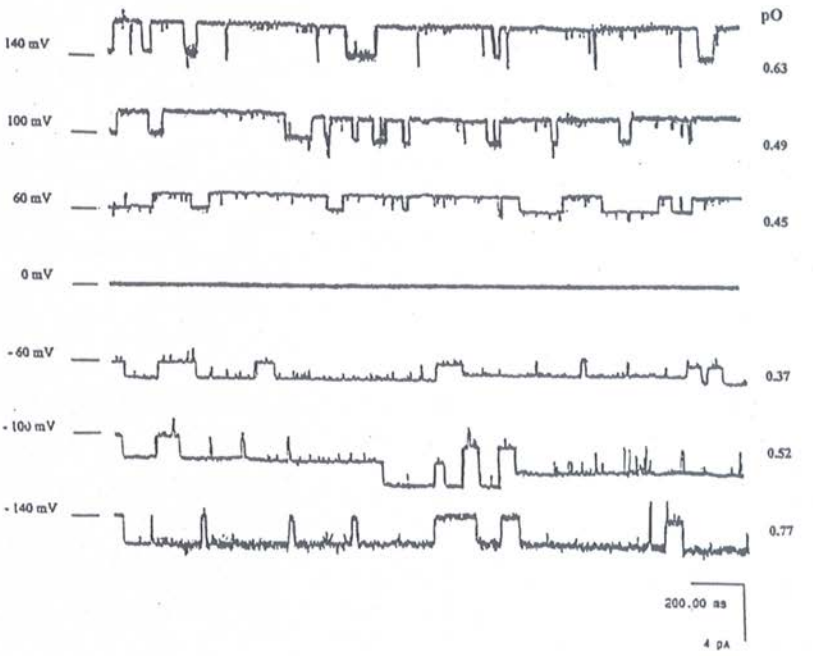

Fig. 68: Representative single channel current fluctuations as a function of voltage obtained with the P(3-HB)/Ca·PP_i complex extracted from *E. coli* [174].

The channel isolated and observed by *Reusch* shows all the characteristics of eukaryotic Ca^{2+}-selective channels described in the literature [175, 176] : it is impermeable to Mg^{2+}, it is selective for divalent over monovalent cations and it is blocked by the addition of various transition metals such as La^{3+}, Cd^{2+} or Co^{2+}. It was also possible to purify the extracted complex by GPC. No channel activity could be observed, if the extracted complex solution was treated with water to remove the Ca·PP_i from the complex [174]. The P(3-HB)/Ca·PP_i complex seems to be extremely sensitive to humidity when stored in $CHCl_3$ with no phospholipids added.

Patch Clamp Experiments on Planar Bilayers with the Synthetic Oligomers of 3-HB

With the (3-HB) oligomers of the appropriate chain lengths in hand, a collaboration with *Reusch* was begun with the aim of incorporating a completely synthetic P(3-HB)/Ca·PP_i complex into a planar lipid bilayer. However, mixing of various (3-HB) oligomers with commercially available Ca·PP_i using ultrasonication gave no products that showed single channel behavior when incorporated into planar lipid bilayers. When the concentration of P(3-HB) in the lipids was raised from the initially used sub-ppm region to a concentration of 0.1–1 %, we were, however, able to detect single channel-like behavior with selected P(3-HB) oligomers and Rb^+ or Ba^{2+} ions. For this kind of channel activity, it was not necessary to mix the P(3-HB) with Ca·PP_i. A selection of single channel recordings with synthetic P(3-HB) oligomers is given in Figure 69.

The experiments were carried out in the following way: 1 to 10 µg of the 3-HB oligomers in $CHCl_3$ were mixed with 1 mg phospholipids in $CHCl_3$, 25 µl decane were added and the $CHCl_3$ evaporated. With this lipid mixture, planar bilayers were painted and after thinning, a voltage of 60 to 120 mV was applied. After periods of between several seconds and several minutes, stepwise current fluctuations could be observed that were stable for a short time, varying from seconds to minutes. We tested a wide range of our synthetic linear oligomers, with and without protecting groups at the carboxylate and alcohol termini. Interestingly, it was only possible to obtain square openings when the oligomer was constructed of at least 16 (3-HB) units and the end groups were not protected. High molecular weight *s*-P(3-HB) was also inactive. It seems that the oligomers used do not need to be strictly monodisperse. This was proved in an experiment with thermally degraded P(3-HB) with an average chain length of 60 monomeric units. Here again, square openings could be obtained as long as the alcohol and the carboxylate termini were unprotected. The general requirements for 3-HB oligomers, in order to show single channel behavior when incorporated into a planar bilayer, are shown in Figure 70.

Single channel recordings, as shown in Figure 69, have been obtained with the appropriate oligomers at different voltages and were reproduced several times. Nevertheless, the channel activity thus obtained was too unstable for a more precise characterization such as a current-voltage relationship or selectivity experiments. Altogether the single channel records obtained with the selected 3-HB oligomers are quite similar to channels obtained from nonionic detergents like Triton X-100 mixed with phospholipids [177, 178]. This single channel-like behavior of amphiphilic molecules is well known, among experts in electrophysiology, under the term "detergent effect". The appearance of similar single ion channels was also reported in unmodified lipid bilayer membranes at the phase transition temperature [179].

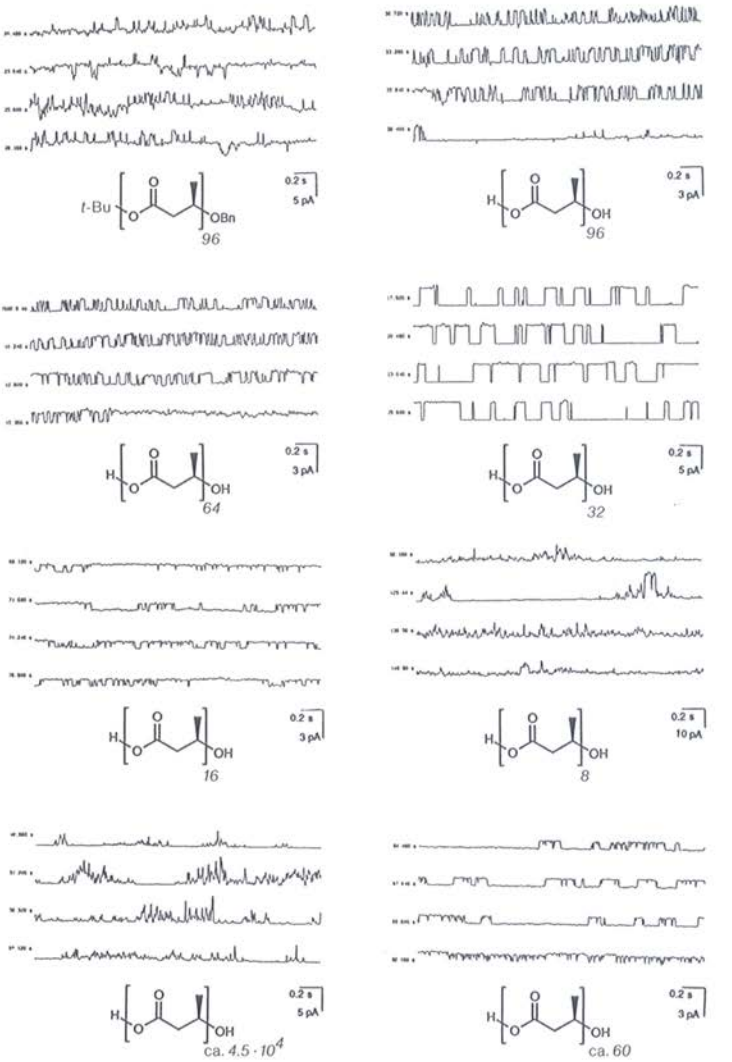

Fig. 69: Electrograms obtained with different synthetic P(3-HB) samples. All experiments were carried out in 60 mM RbCl at voltages ranging from 40 to 140 mV.

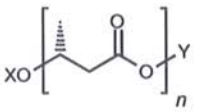

Single channel behavior for $n \geq 16$, X = H, Y = H

No single channel behavior for $n \leq 8$, X and Y variable, or for n variable, X = Bn, Y = *t*-Bu, or for high molecular-weight *s*-P(3-HB).

Fig. 70: General formula for 3-HB oligomers showing single channel behavior in planar bilayer experiments.

Artificial nonpeptide single ion channels have also been reported by *Kobuke et al.* [180], where glycolate ethers complexed with dioctadecyldimethylammonium cations as ionophores were incorporated into planar bilayers.

The occurrence of single channel behavior for amphiphilic nonpeptide compounds is thus well established. To our knowledge, P(3-HB) is the first polyester that shows the ability to make bilayers permeable to ions; almost all of the reported synthetic "pore-builders" are polyether derivatives. It is also striking that only the oligomers showing a similar molecular weight range as the *c*-P(3-HB) isolated from competent *E. coli* are able to induce single channel-like activities in synthetic planar bilayers and that the effect is only observed when the end groups are unprotected.

Considering the high concentration of P(3-HB) needed (0.1–1 %) for the detection of stepwise current fluctuations, it is unlikely that single P(3-HB) molecules can cause pores in the planar bilayer responsible for the ion flux; the P(3-HB) content in the membrane has to pass a certain critical value in order to make it permeable for ions. This is reminiscent of the observation in *E. coli,* where freeze-fracture micrograms revealed an alteration in the membrane structure with increasing P(3-HB) content (see Fig. 19) [116]. Nevertheless, *Reusch* was able to obtain single channel recordings with *E. coli* extracts where the P(3-HB) content was clearly below 0.1 % in the final phospholipid preparation used. The structure of the naturally occurring Ca^{2+} selective ion channel described by *Reusch* remains to be resolved.

An Alternative Model for the P(3-HB) Ion Channel

Reusch has proposed that *P*-helical Ca·PP_i wrapped in a *P*-helix of *c*-P(3-HB) could act as an ion channel through a cell membrane or other hydrophobic barrier [120, 121]. In the suggested structure, the P(3-HB) contains unfavorable dihedral angles [141] along the oligo(3-HB) backbone (Fig. 21). So far we have not been able to find an alternative conformation of the polyester backbone fulfilling the following necessary conditions: (a) forming a helix wide enough to incorporate Ca·PP_i; (b) having the carbonyl groups inside for Ca^{2+} complexation; (c) pointing the methyl groups to the outside for exolipophilicity; and (d) containing the favorable dihedral angles determined by X-ray crystal structure analysis of various oligolides from 3-HB.

We can, however, model [141] the P(3-HB) 2_1 helix of *M*-helicity and a pitch of ca. 6 Å, as derived independently by three groups [42, 153, 181] from fibre X-ray scattering measurements (see Fig. 53). Since P(3-HB) has repeatedly been found to form a helix of pitch 6 Å, it is unlikely that a helix of pitch 20 Å could also exist as a low energy structure. Thus, we believe that, whatever structure the Ca^{2+}

ion channel involving oligo(3-HB) has, it *must* contain a polyester chain with the stable dihedral angles discussed [141]. The fact that oligo- and poly(3-HB) form crystallites of ca. 50 Å thickness, when crystallizing at temperatures below 40 °C, is intriguing when one considers that the sum of the lengths of two lipidic side chains of a phospholipid is also ca. 50 Å. Thus, a chain of ca. 140 3-HB units in a 6 Å-pitch 2_1-helical conformation folded as in the lamellar crystallites could form 8 folds of the kind shown in Figure 39 assuming tight folds of two 3-HB

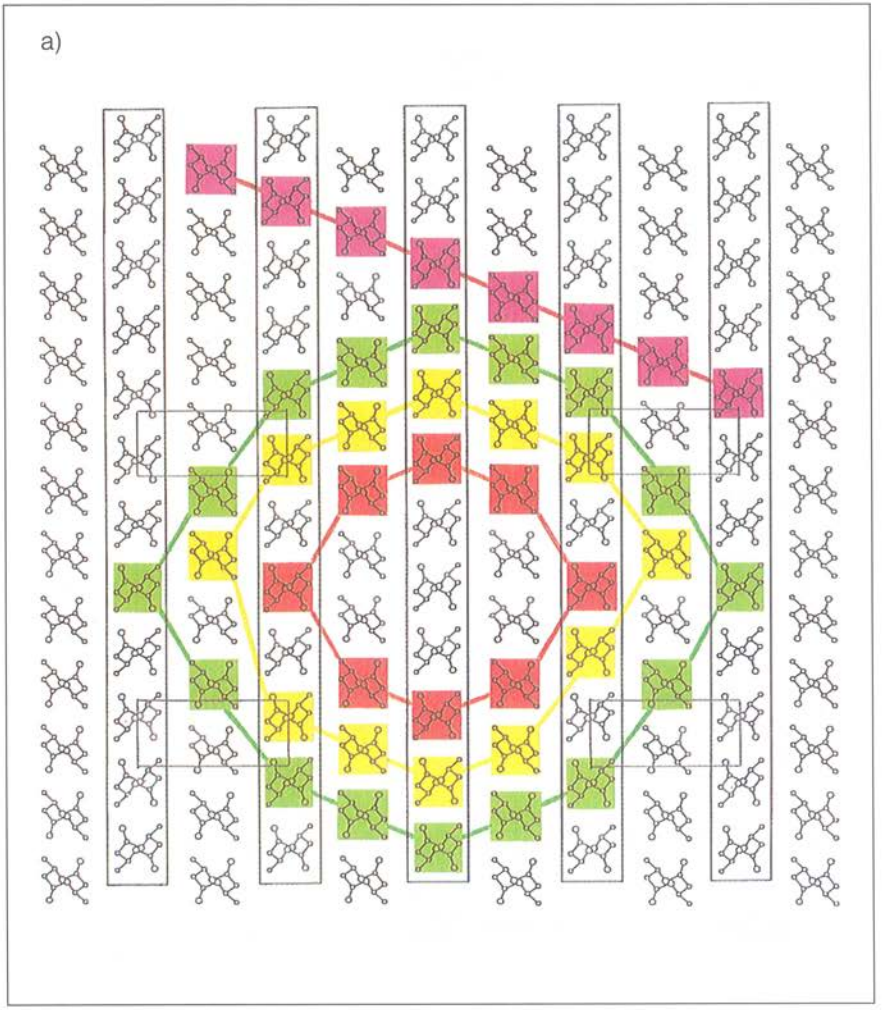

Fig. 71 a: Presentation of the structure of P(3-HB) as derived from fibre X-ray scattering [153]; layers containing neighboring parallel and antiparallel 2_1 helices (framed and not framed); a sheet and three tubules consisting of neighboring helices running alternatively up and down the lattice.

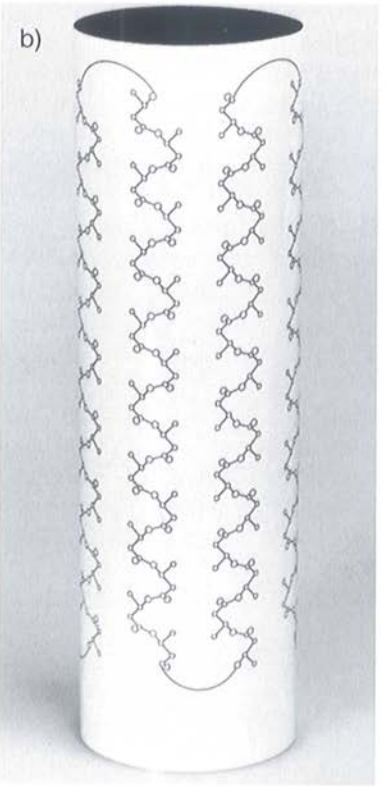

Fig. 71 b

Fig. 71 b: Model for the tube-like arrangement of the 2_1 helices.

units. The resulting structure would be a square-shaped sheet (ca. 50 x 50 x 7 Å) which can be viewed as a section cut out of the stretch fibre P(3-HB) arrangement and, by the same token, out of a lamellar crystallite. In Figure 71a we show a parallel projection of the P(3-HB) structure from published data [153]. Neighboring helices running up and down and parallel to the projection axis are shown outside or inside the frames. A stretch of eight antiparallel helices (the 50 x 50 Å sheet) is shown in red in Figure 71a. As can be seen, there are also eight consecutive antiparallel helices forming a slightly ellipsoid arrangement (orange in Fig. 71a). The mean of the long and short axes of this ellipse is ca. 20 Å. Thus, a 50 Å long cylinder of 20 Å diameter would result. This would be wide enough to house a $Ca{\cdot}PP_i$ helix, thus agreeing with the experimental findings of *Reusch* [120, 121]. On the other hand, a different set of oligo(3-HB) helices could easily be found (yellow and green in Fig. 71a) which would provide a wider cylinder of 30 Å and 40 Å diameter, respectively. These could house polyphosphates with larger dia-

meters such as DNA. It should, however, be made clear that since the P(3-HB) chains would not be surrounded by a complete P(3-HB) crystal but by lipid chains, the P(3-HB) chains would no longer be confined to the P(3-HB) lattice positions. Instead, the P(3-HB) chains would be free to adopt various positions within the lipid lattice, depending on the effect of the lipid chains and should be able to form cylinders of varying diameter. Even stronger effects on the arrangement of the helices would be expected by the interaction with complexed ions. The suggestions in Figure 71 are just some of the possibilities.

The problem with this alternative proposal is that a) the resulting oligo(3-HB) Ca·PP_i complex is not *exo*-lipophilic/*endo*-polarophilic to suit a lipidic membrane bilayer environment and b) to few carbonyl oxygens may be available on the inside of the tube to satisfy the Ca^{2+} ions' need for coordination, which could be achieved instead by the incorporation of water molecules (cf. Fig. 62, the structure of the NaSCN · H_2O complex of the 3-HV triolide **41**).

Degradation Studies with 3-HB Oligolides and with Linear 3-HB Octamers Bearing Various End Groups

For statistical reasons, the first enzymatic degradation step of P(3-HB) should be an attack of the enzyme in the midst of a polymer chain. "Hairpin loops" occur on the surface of crystalline regions of the polymer especially when crystals are in a lamellar configuration (Fig. 39) [182]. Cyclic oligomers of 3-HB should therefore provide a model system for these loops and the initial point of attack for the enzymatic degra-

Oligolide	Degraded by *A. delafieldii*	Degraded by cell free enzymatic degradation system
all-(*R*)-triolide **1**	-	-
all-(*R*)-tetrolide **33**	+	+
all-(*S*)-tetrolide *ent*-**33**	-	-
all-(*R*)-pentolide **34**	+	+
all-(*S*)-pentolide *ent*-**34**	-	-
all-(*R*)-hexolide **35**	+	+
all-(*R*)-heptolide **36**	+	+

+: degraded, -: not degraded

Table 7: Degradation of 3-HB oligolides by *A. delafieldii* or the extracellular enzymatic degradation system.

dation of P(3-HB) respectively. We investigated the degradation properties of a set of 3-HB oligolides (Table 7) with a modified clear zone test [183] (Fig. 72).

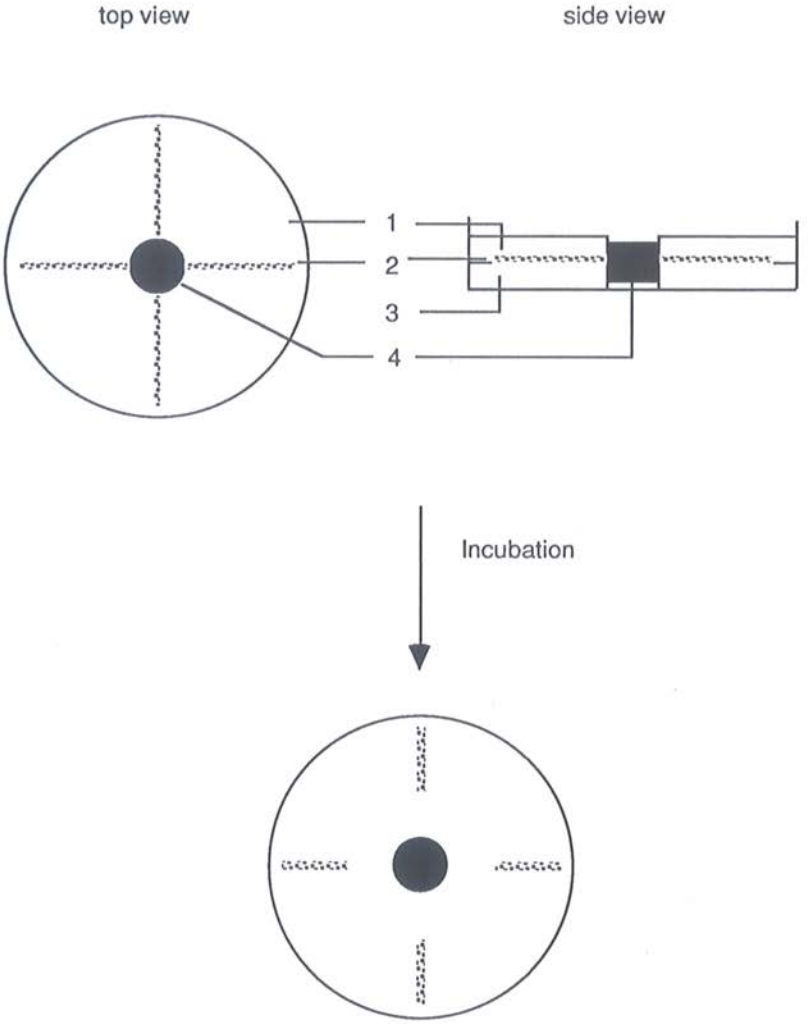

Fig. 72: Modified "clear zone test" to study biodegradation of powdered polymeric material. The material was strewn through a cross-shaped template onto agar plates. Biodegradation was determined by the visual appearance of a clear zone around the well in the center of the plates. 1: Top agar layer. 2: Polymeric material. 3: Bottom agar layer. 4: Degrading system such as pure culture of *A. delafieldii* or as crude extract of extracellular depolymerase of this organism. Plates were incubated for five days at 30 °C.

Of the all-(*R*)-oligolides (**1, 33-36**) tested, all but the triolide **1** were degraded. This result shows that degradation can be microbially-catalyzed even if a free hydroxy terminus is not available. Triolide **1** is not degraded suggesting that enzymatic attack is prevented due to the steric restrictions in the ring system. None of the all-(*S*)-oligolides (*ent*-**33**, *ent*-**34**)was biodegradable, which is in accordance with the stereoselective enzymatic degradation mechanism of the depolymerase [18].

In order to investigate the mechanism of the extracellular enzymatic P(3-HB) degradation, octamers with a variety of end groups on both the hydroxy and the carboxyl termini were synthesized. Degradation experiments with the clear zone test [183] showed that neither a free hydroxy nor a free carboxyl end group is required for an enzymatic degradation (Table 8). Moreover, only an FMOC group at the hydroxy terminus prevents the degradation of these octamers. All other protecting groups did not influence the degradation process by a crude enzyme extract from *Acidovorax delafieldii*. These results support the theory that the depolymerase attacks the second or third ester bond in preference to the first and that degradation occurs by enzymatic chain scission starting from the hydroxy terminal group.

R_1 (hydroxy terminus)	R_2 (carboxy terminus)	Degraded by *A. delafieldii*	Degraded by a cell free enzymatic degradation system
H	H	+	+
benzyl	H	+	+
H	*tert*-butyl	+	+
benzyl	*tert*-butyl	+	+
benzyl	methyl	+	n.d.
CF_3CO	*tert*-butyl	+	n.d.
FMOC	*tert*-butyl	-	-
crotyl	*tert*-butyl	+	+
(*S*)-hydroxybutyryl	*tert*-butyl	+	n.d.

+: degraded; -: not degraded; n.d.: not determined

Table 8: Degradation of linear substituted octamers of 3-HB by *A. delafieldii* or the extracellular enzymatic degradation system.

Degradation Studies on Linear 3-HB Octamers with a Specific Sequence of (*R*)- and (*S*)-Configurations

The fact that even an octamer with a 3-HB unit of (*S*)-configuration at the carboxyl terminus was degraded readily by extracellular enzymes (Table 8) implies that P(3-HB) with a certain number of terminal units of (*S*)-configuration is still biodegradable. At the same time, it is known that synthetically produced all-(*S*)-P(3-HB) is not biodegradable, neither is a block-P(3-HB) built up of (*R*)- and (*S*)-residues [18]. A "library" of octamers with a specific sequence of (*R*)- and (*S*)-configurations was therefore synthesized by means of the segment coupling strategy outlined earlier (Fig. 73). It is now our intention to conduct further degradation experiments with these "mixed" octamers and a purified extracellular depolymerase and dimer hydrolase. By the means of new, more sophisticated analyti-

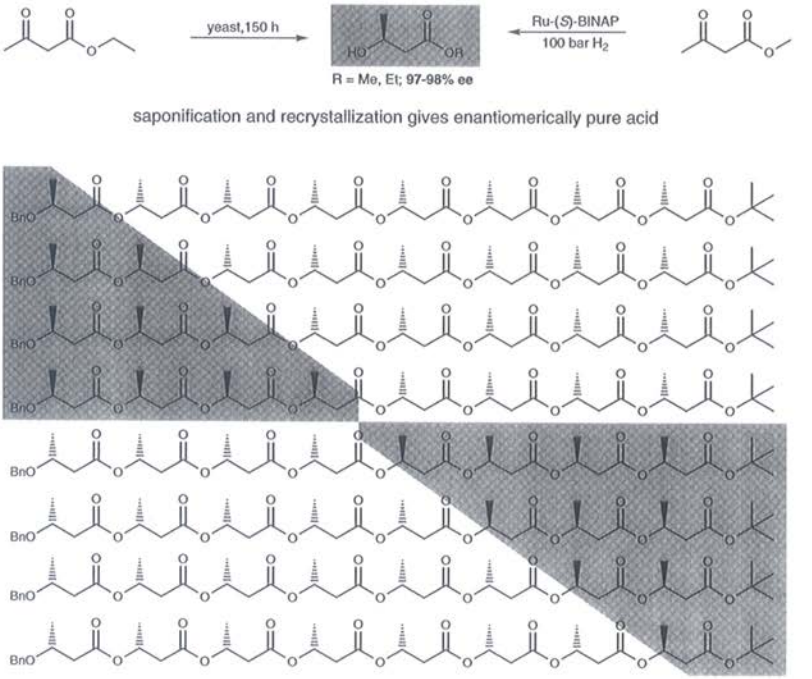

Fig. 73: Top: Synthesis of enantiomerically pure (*S*)-3-HB esters. Bottom: 3-HB octamers with a specific sequence of (*R*)- and (*S*)-configurations as substrates for the projected studies on degradation by a purified extracellular depolymerase and oligomer hydrolase.

cal methods, our aim is to determine the number of units of (*S*)-configuration, on both the hydroxy and the carboxyl end of an oligomer, which still allows the degradation process to occur. The results of these studies will hopefully provide us with new insights into the mechanistic principles of the enzymatic P(3-HB) degradation.

Conclusions and Outlook – PHAs, a Fifth Class of Physiologically Important Biopolymers

The world-wide efforts in research and development with high molecular weight storage polyhydroxyalkanoates (*s*-PHAs) are being focused on the cloning of PHA producing enzymes into cultural plants. The production of PHAs in plants and their isolation (harvesting) will circumvent the production of sugar or starch and the subsequent fermentation used now. Governmental regulations will make biodegradable polymers mandatory, especially for packaging and disposal purposes. The PHAs have favorable material and biocompatibility properties for large-scale applications [48].

Another focus will be on the mechanism of degradation of both, the native amorphous PHAs as deposited in the microbial granula, and the highly crystalline material formed in the isolation and manufacturing procedures.

The occurrence of short chain P(3-HB), *c*-P(3-HB), in genetically competent microorganisms and in all eukaryotic organisms looked at so far [133], suggests that the oligomers of (*R*)-3-hydroxybutyric acid play an important role in the

Monomers	Oligomers	Polymers
Metabolism	Regulation, recognition, signalling	Catalysis, storage, transport, structure, information
Aminoacids	Oligopeptides (endorphines)	Polypeptides (enzymes, silk)
Carbohydrates	Oligosaccharides (blood-group determinants)	Polysaccharides (cellulose)
Acetic acid, Isoprene derivatives	Isoprenoids (steroids)	Polyisoprenoids (rubber)
Nucleotides	Oligonucleotides (tRNA)	Polynucleotides (DNA)
Hydroxy-alkanoic acids	*c*-P(3-HB) (channel component)	*s*-P(3-HB) (storage)

Table 9: Comparison of monomers, oligomers and polymers in chemistry and biochemistry of natural products.

chemistry of life. The results of all our chemical investigations are compatible with an involvement of P(3-HB) in ion transport processes through phospholipid bilayers, as first suggested by *Rosetta Reusch*. While models have been proposed, the actual structures of ion channels containing P(3-HB) are unknown. Likewise, the origin of *c*-P(3-HB) is unknown; no enzymes have been identified which might be responsible for *c*-P(3-HB) synthesis in *E. coli* or in any of the higher organisms, such as plants and mammals, in which *c*-P(3-HB) has been identified [133]. Much work needs to be done in a highly interdisciplinary effort to elucidate the origin and the function of *c*-P(3-HB). Biochemists, biologists, and medical experts will have to join in. We as chemists can synthesize hydroxyalkanoic acid derivatives of known, uniform composition, and we can study their properties and provide information about structure and reactivity at the molecular and supramolecular level. From this, models for the much more complex environments of living cells may be derived.

We would not be surprised, if PHAs would have to be added to the list of physiologically important biooligomers and -polymers as done in Table 9 [22] (in this list polyphosphates and lignin are not included).

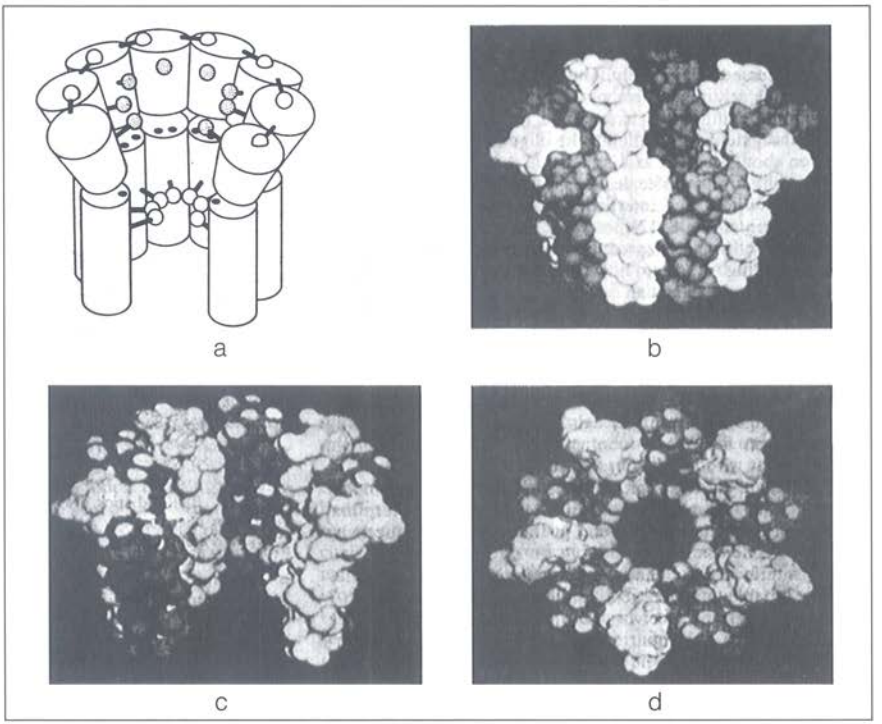

Fig. 74: Schematic and computer graphics representations of the proposed pore constructed from 10 alamethicin monomer units. (Figure taken from [184]).

Finally, the question arises as to whether (*R*)-3-hydroxybutyric acid and its oligomers and polymers might have been present in the prebiotic broth on earth before amino acids, peptides and proteins. Thus, the P(3-HB) complexes with inorganic salts, including polyphosphates, might constitute the primordial ion channels, and, in fact, one of the proposed models [136] for the structure of such channels looks very similar to a prototypical protein ion channel like alamethicin [184] (compare Figs. 71b and 74). Simple experiments can be thought of to test this idea in the context of *Wächtershäuser's* theory of the origin of life on our planet [185].

Acknowledgements

We thank Dr. Jennifer Matthews for polishing our English, the ZENECA Bio Products (Billingham, G.B.) for generous gifts of P(3-HB) and P(3-HB/3-HV), and the FMC Co., Lithium Division (Gastonia, N.C., USA) for supplies of chlorosilanes. Continuing financial support by Sandoz Pharma (Basel) is gratefully acknowledged.

References

1. Doudoroff M, Stanier RY (1959). Nature (London) 183:1440
2. Schlegel HG (1985). Allgemeine Mikrobiologie. Thieme, Stuttgart, 6th ed
3. Doi Y (1990). Microbial Polyesters. VCH Publishers, Weinheim
4. ZENECA Bio Products, PO Box 2, Belasis Avenue, Billingham, Cleveland, TS23 1YN, England
5. Schurz J (1988). Nachr Chem Tech Lab. 36:388
6. Zoebelein H (1992). Chem unserer Zeit 26:27
7. The New York Times (1985). May 3
8. Neue Zürcher Zeitung (1986). December 12
9. (1991). Geo 3:80
10. (1995). Der Spiegel 2:151
11. Frankfurter Allgemeine Zeitung, Blick durch die Wirtschaft (1995). January 2
12. Schlegel HG, Gottschalk G (1962). Angew Chem 74:342
13. Dawes EA, Senior PJ (1973). Adv Microb Physiol 10:135
14. Dawes EA (1986). Microbial Energetics. Blackie & Son, London, chap 11, 12
15. Lafferty RM, Korsatko B, Korsatko W (1988). In: Rehm HJ (ed) Biotechnology. Vol 6b, VCH, Weinheim, p 135
16. Holmes PA (1988). In: Bassett DC (ed) Developments in Crystalline Polymers-2. Elsevier, Barking, New York, p 1
17. Anderson AJ, Dawes EA (1990). Microbiol Rev 54:450
18. Brandl H, Gross RA, Lenz RW, Fuller RC (1990). Adv Biochem Engin Biotechnol 41:77
19. Glass JE, Swift G (eds) (1990). Agricultural and Synthetic Polymers, Biodegradability and Utilization. ACS symposium series; 433, American Chemical Society, Washington, DC, p 433
20. Steinbüchel A (1991). Nachr Chem Tech Lab 39:1112
21. Steinbüchel A (1991). In: Byrom D (ed) Biomaterials. Stockton Press, New York, p 123
22. Müller H-M, Seebach D (1993). Angew Chem Int Ed Engl 32:477
23. Hocking PJ, Marchessault RH (1994). In: Griffin GJL (ed) Chemistry and Technology of Biodegradable Polymers. Blackie Academic & Professional, Glasgow, p 48
24. Lemoigne M (1925). Ann Inst Pasteur (Paris) 39:144
25. Lemoigne M (1927). Ann Inst Pasteur (Paris) 41:148
26. Peoples OP, Sinskey AJ (1989). J Biol Chem 264:15298
27. Gilbert P, Brown MRW (1978). J Bacteriol 133:1062

28. Ellar D, Lundgren DG, Okamura K, Marchessault RH (1968). J Mol Biol 35:489

29. Griebel R, Smith Z, Merrick JM (1968). Biochemistry 7:3676

30. Merrick JM, Doudoroff M (1964). J Bacteriol 88:60

31. Kawaguchi Y, Doi Y (1990). FEMS Microbiol Lett 70:151

32. Amor SB, Rayment T, Sanders JKM (1991). Macromolecules 24:4583

33. Bonthrone KM, Clauss J, Horowitz DM, Hunter BK, Sanders JKM (1992). FEMS Microbiol Rev 103:269

34. Horowitz DM, Clauss J, Hunter BK, Sanders JKM (1993). Nature 363:23

35. de Koning GJM, Lemstra PJ (1992). Polymer 33:3292

36. Doi Y, Kunioka M, Nakamura Y, Soga K (1986). Macromol Chem Rapid Commun 7:661

37. Haywood GW, Anderson AJ, Williams DR, Dawes EA, Ewing DF (1991). Int J Macromol 13:83

38. de Koning GJM, Lemstra PJ (1993). Polymer 34:4089

39. Poirier Y, Dennis DE, Nawrath C, Somerville C (1993). Adv Mater 5:30

40. de Koning GJM, van Bilesen HMM, Lemstra PJ, Hazenberg W, Witholt B, Preusting H, van der Galien JG, Schirmer A, Jendrossek D (1994). Polymer 35:2090

41. Cornibert J, Marchessault RH (1972). J Mol Biol 71:735

42. Cornibert J, Marchessault RH (1975). Macromolecules 8:296

43. Bailey JE (1991). Science 252:1668

44. Slater SC, Voige WH, Dennis DE (1988). J Bacteriol 170:4431

45. Schubert P, Steinbüchel A, Schlegel HG (1988). J Bacteriol 170:5837

46. Schubert P, Krüger N, Steinbüchel A (1991). J Bacteriol 173:168

47. Poirier Y, Nawrath C, Somerville C (1995). Bio/Technology 13:142

48. Marchessault RH (1995). Chemistry & Engineering News, 1:29

49. Kemmish D (1993). In: Ching C, Kaplan D, Thomas E (eds) Biodegradable Polymers and Packaging. Technomic Publishing Company, Lancaster, Basel, p 225

50. ICI (1984). European Patent, 0145233

51. Byrom D (1987). Trends Biotechnol 5:246

52. Byrom D (1992). FEMS Microbiol Rev 103:247

53. Page WJ (1992). FEMS Microbiol Rev 103:149

54. Page WJ, Cornish A (1992). Appl Environ Microbiol 59:4236

55. Bourque D, Pomerleau Y, Groleau D (1992). In: Vert M, Feijen J, Albertsson A, Scott G, Chiellini E (eds) Biodegradable Polymers and Plastics. The Royal Society of Chemistry, Cambridge, p 229

56. Bourque D, Ouellette B, André G, Groleau D (1992). Appl Microbiol Biotechnol 37:7

57. Hrabak O (1992). FEMS Microbiol Rev 103:251

58. BIOMER biodegradable polymers, Forst-Kasten-Str. 15, 82152 Krailling, Germany

59. Wynne F (1991). ICI, at a workshop on biodegradable plastics at Zürich University, November 27

60. Brandl H, Gross RA, Lenz RW, Lloyd R, Fuller RC (1991). Arch Microbiol 155:337

61. Preusting H, Nijenhuis A, Witholt B (1990). Macromolecules 23:4220

62. Taber DF, Silverberg LJ (1991). Tetrahedron Lett 32:4227

63. Noyori R (ed) (1992). Asymmetric Hydrogenation. Kagaku Dozin, Tokyo, p 301

64. Hoke JB, Hollis LS, Stern EW (1993). J Organomet Chem 455:193

65. Curlee TR, Das S (eds) (1991). Plastic wastes: management, control, recycling, and disposal. US Environmental Protection Agency, Noyes Data Corp, Park Ridge NJ

66. Rafler G (1995). Spektrum der Wissenschaft 2:81

67. Evans JD, Sikdar SK (1990). Chemtech 1:38

68. Ching C, Kaplan D, Thomas E (eds) (1993). Biodegradable Polymers and Packaging. Technomic, Lancaster, Basel

69. de Koning GJM (1993). Thesis, Technische Universiteit Eindhoven

70. ICI, A Guide for Processors

71. Reeve MS, McCarthy S, Gross RA (1990). Polym Prepr (Am Chem Soc Div Polym Chem) 31(1):437

72. Avella M, Martuscelli E (1988). Polymer 29:1731

73. Holmes PA (1985). Phys Technol 16:32

74. Rieker C (1990). Thesis, Universität Stuttgart

75. (1994). Chemie Plus 12:37

76. Yalpani M (1992). PCT Int Appl, WO 9209,211 (CA: 1992, 117, 190663y)

77. Yalpani M (1992). PCT Int Appl WO 9209,210 (CA: 1992, 117, 149843u)

78. Koch BPG (1993). Thesis, 10237. ETH Zürich

79. Chowdhury AA (1963). Arch Mikrobiol 47:167

80. Tanio T, Fukui T, Shirakura Y, Saito T, Tomita K, Kaio T, Masamune S (1982). Eur J Biochem 124:71

81. Shirakura Y, Fukui T, Tanio T, Nakayama K, Matsuno R, Tomita K (1983). Biochim Biophys Acta 748:331

82. Fukui T, Narikawa T, Miwa K, Shirakura Y, Saito T, Tomita K (1988). Biochim Biophys Acta 952:164

83. Shirakura Y, Fukui T, Saito T, Okamoto Y, Narikawa T, Koide K, Tomita K, Takemasa T, Masamune S (1986). Biochim Biophys Acta 880:46

84. Delafield FP, Doudoroff M, Palleroni NJ, Lusty CJ, Cantopoulos R (1965). J Bacteriol 90:1455

85. Delafield FP, Cooksey KE, Doudoroff M (1965). J Bacteriol 240:4023

86. Lusty CJ, Doudoroff M (1966). Biochem 56:960

87. Stinson MW, Merrick JM (1974). J Bacteriol 119:152

88. Nakayama K, Saito T, Fukui T, Shirakura Y, Tomita K (1985). Biochim Biophys Acta 827:63

89. Mulzer J (1993). Das Phänomen der Chiralität – Laune oder Fundamentalprinzip der Natur?, Schering Lecture, Schering Forschungsgesellschaft, Berlin, 17:36

90. Seebach D, Kalinowski HO (1976). Nachr Chem Tech Lab 24:415

91. Seebach D, Hungerbühler E (1980). In: Scheffold R (ed) Modern Synthetic Methods 1980. Vol 2, Salle & Sauerländer, Interlaken, Switzerland, p 91

92. Schnurrenberger P, Seebach D, Züger MF (1982). Helv Chim Acta 65:1197

93. Seebach D, Züger M (1982). Helv Chim Acta 65:495

94. Seebach D, Züger MF (1984). Tetrahedron Lett 25:2747

95. Vanlautem N, Jacques G (1982). Eur Pat Appl, EP 43 620 A1 (CA: 1982, 96, 163397f)

96. Akita S, Einaga Y, Miyaki Y, Fujita H (1976). Macromolecules 9:774

97. Seebach D, Beck AK, Breitschuh R, Job K (1992). Org Synth 71:39

98. Seebach D, Chow HF, Jackson RFW, Sutter MA, Thaisrivongs S, Zimmermann J (1986). Liebigs Ann Chem 1281

99. Curtis NR, Holmes AB, Looney MG, Pearson ND, Slim GC (1991). Tetrahedron Lett 32:537

100. Otha K, Mitsunobu O (1991). Tetrahedron Let 32:517

101. Braun M, Mahler U, Houben S (1990). Liebigs Ann Chem p 513

102. Hintermann S, ETH Zürich (unpublished)

103. Breitschuh R, Seebach D (1990). Chimia 44:216

104. Seebach D (1990). Angew Chem 102:1363

105. Seebach D (1990). Angew Chem Int Ed Engl 29:1320

106. Seebach D, Müller H-M, Bürger HM, Plattner DA (1992). Angew Chem 104:443

107. Müller H-M (1992). Thesis 9685. ETH Zürich

108. Sakurada Y (1926). Chem Zentralblatt 97:1273

109. Pfaltz A (1993). Acc Chem Res 26:339

110. Karpishin TB, Raymond KN (1992). Angew Chem 104:486

111. Lundgren DG, Bott KF (1963). J Bacteriol 86:462

112. Stevenson LH, Socolofsky MD (1973). J Microbiol Serol 39:341

113. Schulz S, Toft S (1993). Science 260:1635

114. Reusch R, Sadoff H (1983). J Bacteriol 156:778

115. Wenzel W, Amann MJ (1985). Lexikon der Gentechnologie. Springer, Heidelberg

116. Reusch R, Hiske T, Sadoff H, Harris R, T. Beveridge (1987). Can J Microbiol 33:435

117. Reusch R, Hiske T, Sadoff H (1986). J Bacteriol 168:553

118. Stryer L (1990). Biochemie. 3. Auflage, Spektrum der Wissenschaften, Heidelberg

119. Voet D, Voet JG (1992). Biochemie. VCH Verlagsgesellschaft mbH, Weinheim, New York, Basel, Cambridge

120. Reusch RN, Sadoff HL (1988). Proc Natl Acad Sci USA 85:4176

121. Reusch RN (1989). Proc Soc Exp Biol Med 191:377

122. Hanahan D (1983). J Mol Biol 166:557

123. Dower WJ, Miller JF, Ragsdale CW (1988). Nucleic Acids Res 16:6127

124. Taketo A (1988). Biochim Biophys Acta 949:318

125. Reusch R, Sparrow A, Gardiner J (1992). Biochim Biophys Acta 1123:33

126. Reusch RN (1992). FEMS Microbiol Rev 103:119

127. Buddecke E (1977). Grundriß der Biochemie. Walter de Gruyter, Berlin, New York, 5. Auflage, p 201

128. Owen OE, Morgan AP, Kemp HG, Sullivan JM, Herrera MG, Cahill GF (1967). J Clin Invest 46:1589

129. McGarry JD, Foster DW (1980). Ann Rev Biochem 49:395

130. Pawan GLS, Semple SJG (1983). The Lancet 1:15

131. Karr DB, Waters JK, Emerich DW (1983). Appl Environ Microbiol 46:1339

132. Braunegg G, Sonnleitner B, Lafferty RM (1978). Eur J Appl Microbiol Biotechnol 6:29

133. Seebach D, Brunner A, Bürger HM, Schneider J, Reusch RN (1994). Eur J Biochem 224:317

134. Inkeles S, Eisenberg D (1981). Medicine (Baltimore) 60:110

135. Ross R (1986). N Engl J Med 314:488

136. Seebach D, Bürger HM, Müller H-M, Lengweiler UD, Beck AK, Sykes KE, Barker PA, Barham PJ (1994). Helv Chim Acta 77:1099

137. Bürger HM (1993). Thesis 10436. ETH Zürich

138. Seebach D, Beck AK, Brändli U, Müller D, Przybylski M, Schneider K (1990). Chimia 44:112

139. Bürger HM, Müller H-M, Seebach D, Börnsen KO, Schär M, Widmer HM (1993). Macromolecules 26:4783

140. Ohlsen I, Merrick JM, Goldstein IJ (1965). Biochemistry 4:453

141. Plattner DA, Brunner A, Dobler M, Müller H-M, Petter W, Zbinden P, Seebach D (1993). Helv Chim Acta 76:2004

142. Seebach D, Brändli U, Schnurrenberger P, Przybylski M (1988). Helv Chim Acta 71:155

143. Keller A (1968). Reports on Progress in Physics. Vol 31, The Institute of Physics and the Physical Society, London, p 632

144. Blundell DJ, Keller A, Connor TM (1967). J Polym Sci A-2 5:991

145. Williams T, Blundell DJ, Keller A (1968). J Polym Sci A-2 6:1613

146. Keller A, Martuscelli E, Priest DJ, Udagawa Y (1971). J Polym Sci A-2 9:1807

147. Welland EJ, Stejny J, Halter A, Keller A (1989). Polym Commun 30:302

148. Sykes KE, McMaster TJ, Miles MJ, Barker PA, Barham PJ, Seebach D, Müller H-M, Lengweiler UD (1995). J Mat Science 30:623

149. Seebach D, Hoffmann T, Kühnle FNM, Lengweiler UD (1994). Helv Chim Acta 77:2007

150. Inanaga J, Hirata K, Saeki H, Katsuka T, Yamaguchi M (1979). Bull Chem Soc Jpn 52:1989

151. Shanzer A, Libman J, Frolow F (1981). J Am Chem Soc 103:7339

152. Lageveen RG, Huisman GW, Preusting H, Ketelaar P, Eggink G, Witholt B (1988). Appl Environ Microbiol 54:2924

153. Yokouchi M, Chatani Y, Tadokoro H, Tani H, Teranishi K (1973). Polymer 14:267

154. Yokouchi M, Chatani Y, Tadokoro H, Tani H (1974). Polymer Journal 6:248

155. Weast RC (ed) (1975). Handbook of Chemistry and Physics. 56th ed, CRC Press, Cleveland, Ohio

156. Dietrich B, Viout P, Lehn J-M (1993). Macrocyclic Chemistry. VCH, Weinheim

157. Dobler M (1981). Ionophores and their Structure. Wiley & Sons, New York

158. Seebach D, Bürger HM, Plattner DA, Nesper R, Fässler T (1993). Helv Chim Acta 76:2581

159. Bürger HM, Seebach D (1993). Helv Chim Acta 76:2570

160. Cox BG, Schneider H (1992). Coordination and Transport Properties of Macrocyclic Compounds in Solution. Vol 76, Elsevier Science Publishers, Amsterdam

161. Tajima I, Okada M, Sumitomo H (1981). J Am Chem Soc 103:4096

162. Izatt RM, Clark GA, Bradshaw JS, Lamb JD, Christensen JJ (1986). Sep Purif Meth15:21

163. Hashimoto H, Kakuchi T, Yokota K (1991). J Org Chem 56:6470

164. McLaughlin SGA, Szabo G, Ciani S, Eisenman G (1972). J. Membrane Biol 9:3

165. Cole KS, Curtis HJ (1939). J Gen Physiol 22:649

166. Curtis HJ, Cole KS (1940). J Cell Comp Physiol 15:147

167. Hodgkin AL, Huxley AF (1939). Nature (London) 144:710

168. Miller C (ed) (1986). Ion Channel Reconstitution. Plenum Press, New York and London

169. Miller C (1983). Physiol Rev 63:1209

170. Alvarez O (1986). In: Miller C (ed) Ion Channel Reconstitution. Plenum Press, New York and London, p 115

171. Lynn AR, Rosen BP (1987). In: Rosen BP, Silver S (eds) Ion Transport in Prokaryotes. Academic Press, San Diego, p 181

172. Brey RN, Rosen BP (1979). J Bacteriol 139:824

173. Ambudkar SV, Zlotnick GW, Rosen BP (1984). J Biol Chem 259:6142

174. Reusch RN, Bramble LL, Huang R, Michigan State University (unpublished)

175. Tsien RW (1983). Ann Rev Physiol 45:341

176. Hagiwara S, Byerly L (1981). Ann Rev Neurosci 4:69

177. Schlieper P, de Robertis E (1977). Arch Biochem Biophys 184:204

178. Tanaka JC, Furman RE, Barchi RL (1986). In: Miller C (ed) Ion Channel Reconstitution. Plenum Press, New York and London, p 277

179. Antonov VF, Petrov VV, Molnar AA, Predvoditelev DA, Ivanov AS (1980). Nature 283:585

180. Kobuke Y, Ueda K, Sokabe M (1992). J Am Chem Soc 114:7618

181. Brückner S, Meille SV, Malpezzi L, Cesàro A, Navarini L, Tombolini R (1988). Macromolecules 21:967

182. Lauzier C, Marchessault RH, Smith P, Chanzy H (1992). Polymer 33:823

183. Aeberli B, Brandl H, Schwegler I, Bürger HM, Müller H-M, Hoffmann T, Lengweiler UD, Seebach D (1995). Can J Microbiology (in press)

184. Fox RO, Richards FM (1982). Nature 300:325

185. Wächtershäuser G (1992). Prog Biophys Molec Biol 58:85

Curriculum Vitae

Name	Dieter Seebach Dipl. Chem., Dr. rer. nat., Dr. h. c. Professor of Chemistry
Ad Personam	
Born	October 31, 1937, in Karlsruhe, Germany
Married	with Ingeborg Seebach-Reichling since 1961
Children	two sons, born 1964 and 1971 one daughter, born 1968
Resident	of Switzerland, CH 8044 Zürich, Orellistrasse 3 Telephone 0041-1-262 43 80
Citizen	of Germany

Education

1943–1947	Elementary Schools at Karlsruhe, Annweiler, Bad Dürrheim, Germany
1947–1956	Secondary School, classical type, Bismarck Gymnasium, Karlsruhe
1956–1961	University studies at the Technische Hochschule (University) of Karlsruhe as chemistry major; degree of Diplomchemiker
1961–1964	Graduate School, Ph. D. thesis work with Professor R. Criegee, University of Karlsruhe (TH)

Professional Career

1964	Private assistant to Professor R. Criegee Technische Hochschule, Karlsruhe, Germany
1965	Postdoctoral Fellow with Professor E. J. Corey, Harvard University, Cambridge, Mass., USA
1965/1966	Lecturer on Chemistry at Harvard University, Cambridge, Mass., USA
1966-1969	Habilitation, University of Karlsruhe (independent research)
1969-1971	Privatdozent, University of Karlsruhe
1971-1977	Professor of Organic Chemistry, University of Gießen, Germany
since 1977	Professor of Chemistry, Eidgenössische Technische Hochschule (ETH), Zürich, Switzerland

Professional Activities

1971	Author of the Houben-Weyl, volume 4/4 on Carbocyclic Four-Membered Rings
1971-1977	Director of the Institut für Organische Chemie der Universität Gießen, Germany
1975/1976	Chairman of the Fakultät für Chemie, Universität Gießen
1976-1978	Committee, Fachgutachterausschuß Chemie der Deutschen Forschungsgemeinschaft, Bonn
since 1977	Consultant to Sandoz AG, Basel, Switzerland (Pharma and Agro Division)
since 1981 since 1988	Board of Directors to Lonza AG, Basel, Switzerland Board of Directors to Sandoz Inc.
1977-1981	Board of Organic Syntheses, USA, as foreign editor
1981-1992	Board of the Schweizerischer Chemiker-Verband
since 1983	Editorial Board of "Organic Nitro Chemistry", published by Verlag Chemie International, Inc., USA, Managing Editor: Dr. Henry Feuer
1984/1985 and 1991/1992	Director of the Laboratorium für Organische Chemie, ETH, Zürich, Switzerland
since 1984	Editorial Advisory Board of Synthesis, Georg Thieme Verlag, Stuttgart/New York
since 1985	Advisory Board of Chimia, Birkhäuser AG, Basel, Switzerland, Schweizerischer Chemiker-Verband (Association of Swiss Chemists)
1985-1994	Editorial Board (Kuratorium), Angewandte Chemie, Verlag Chemie, Weinheim, Germany
1986-1991	Editorial Committee of Helvetica Chimia Acta, Schweizerische Chemische Gesellschaft
1987	President of the 23rd EUCHEM Conference on Stereochemistry, Bürgenstock, Switzerland, May 3-9, 1987
October 1987–March 1995	Board of the Schweizerische Chemische Gesellschaft and Neue Schweizerische Chemische Gesellschaft (Swiss Chemical Society)
1991-1996	Canvassing Committee for the Roger Adams Award in Organic Chemistry (Am. Chem. Soc.)
1994-1996	Chairman of the Department of Chemistry, ETH, Zürich, Switzerland

Memberships of Chemical Societies

- Gesellschaft Deutscher Chemiker (GDCh)
- Schweizerische Chemische Gesellschaft (SCG) (1977 – 1993)
- Schweizerischer Chemiker-Verband (SChV) (1977 – 1993)
- American Chemical Society
- Deutsche Gesellschaft für chemisches Apparatewesen (DECHEMA)
- The Society of Synthetic Organic Chemistry, Japan
- The Royal Society of Chemistry, Great Britain
- The Chemical Society of Japan
- Göttinger chemische Gesellschaft Museum der Chemie e.V. Göttingen
- Neue Schweizerische Chemische Gesellschaft (NSCG) and of the Sections
  "Medizinische Chemie"
  "Chemische Forschung"
  "Industrielle Chemie"
- Liebig-Vereinigung für Organische Chemie und
  Wöhler-Vereinigung für Anorganische Chemie der Gesellschaft Deutscher Chemiker

Prizes, Awards, and Academies

1964	Wolf-Preis for the Ph.D. thesis, University of Karlsruhe, Germany
1969–1971	Dozentenpreis, Fonds der Chemischen Industrie, Germany
1984	FRSC, Fellow of the Royal Society of Chemistry, Great Britain
1984	Leopoldina, Elected Member of the Deutsche Akademie der Naturforscher, Halle, DDR
1985	Havinga Medal, Stichting Havinga Fonds, Leiden, The Netherlands
1987	Karl Ziegler-Preis, Gesellschaft Deutscher Chemiker
1987	First Fluka-Prize for the Reagent of the Year 1987
1989	Dr. h.c. of the University of Montpellier, France
1989	Member of the Academia Europea
1990	Corresponding Member, Akademie der Wissenschaften und der Literatur in Mainz, Germany
1992	ACS Award for Creative Work in Organic Synthesis
1992	Member of the New York Academy of Sciences
1994	Merck-Schuchardt Chair at the 5th Belgian Organic Synthesis Symposium in Namur

Visiting Professorships

September 1969–February 1970	University of Wisconsin, Madison, USA
January–June 1974	California Institute of Technology, Pasadena, USA
May/June 1977	Rand Afrikaans University, Johannesburg, South Africa
March 1978	Polish Academy of Sciences, lectures in Warsaw and Lodz, Poland
March 1980	Australian National University, Canberra, Australia
April/Mai 1980	Imperial College, London, Great Britain
March 1981	The Weizmann Institute of Science, Rehovot, Israel
1981/1982	Carl Ziegler Visiting Professorship, Max-Planck-Institut für Kohlenforschung, Mülheim an der Ruhr, Germany
March/April 1985	JSPS Fellowship for Research in Japan. Visiting Japan as lecturer and guest of the Japanese Society for the Promotion of Science
May/June 1987	Université Louis Pasteur, Strasbourg, France
May and October 1989	Walter Hieber-Gastprofessur der Wacker-Chemie GmbH, Chemiegebäude, Technische Universität München, Garching
October 1992	BASF-Gastprofessur, Universität Kaiserslautern, Germany

Special Lectureships

September/October 1972	DuPont Travel Grantee, USA 15 lectures at universities and companies
October/November 1977	Pacific Coast Lectureship, USA/Canada Lectures at universities and companies along the USA west coast
October 1981	Kolthoff Lecturer, University of Minnesota, Minneapolis, USA
September 1982	Vorhees Memorial Lecturer, University of Illinois, Urbana-Champaign, USA
September 1982	First Atlantic Coast Lecturer, USA 6 lectures at universities of the south-east USA
October 1982	Organic Synthesis Lecturer, Princeton University, Princeton, USA
February/March 1984	The Greater Manchester Lectureship, University of Manchester, U.K. Lectures in the Greater Manchester Area
September 1984	Syntex Distinguished Lectureship in Organic Chemistry, Colorado State University, Fort Collins, USA
September/October 1984	UNIDEL Lectureship, University of Delaware, Newark, USA
September 1985	5th HAVINGA Lecture, University of Leiden, The Netherlands

November 1985	Distinguished Visiting Lecturer, The University of Texas at Austin, USA
February 1986	The 1986 Morris S. Kharasch Memorial Lecturer, The University of Chicago, USA
May 1986	The Werner E. Bachmann Memorial Lecturer 1986, The University of Michigan, Ann Arbor, Michigan, USA
May 1986	The 1986 Organic Syntheses Lectureship, The University of California, Berkeley, USA
September 1987	The 1987 Barré Lecturer, The University of Montréal, Canada
November 1987	The Musgrave Lecturer, The University of Durham, Durham, Great Britain
February 1988	The 4th Burroughs-Wellcome Lecturer, The Research Laboratories Burroughs Wellcome, Research Triangle Park (first lecture) and The University of North Carolina at Chapel Hill, USA (second lecture)
February/ March 1988	The Ralph Hirschmann Lecturer, The University of Wisconsin, Madison, USA
September 1988	The Weissberger-Williams Lecture Series, Eastman Kodak Company, Research Laboratories, Rochester, USA
November 1988	The Thirteenth Annual "McNeil-Ortho-Chemistry Lecture", McNeil Pharmaceutical, Chemical Process Research, Spring House, Pennsylvania, USA
November 1988	Jeremy Musher Memorial Lecture, The Hebrew University of Jerusalem, Israel
March 1989	1989 George Büchi Visiting Lecturer in Organic Chemistry, Massachusetts Institute of Technology, Cambridge, Mass., USA
July 1989	The Reuben Benjamin Sandin Lecturer, University of Alberta, Edmonton, Canada
March 1990	Pfizer Lecturer, Ohio State University, Columbus, Ohio, USA
March 1990	Organic Syntheses Lecturer, University of California, Irvine, CA, USA
July/ August 1990	The Andrews Lectures, The University of New South Wales, Australia
October 1990	The 1990 Max Tishler Prize Lecturer, Harvard University, Cambridge, USA
November 1990	The Forty-Third Annual Falk-Plaut Lecturer, Columbia University, New York, USA
March–May 1991	Centenary Lecturer, The Royal Society of Chemistry, Great Britain Lectures at different universities in Great Britain
October 1991	Syntex Distinguished Lecturer, Fall 1991, University of Colorado, Boulder, USA

October 1991	1991 Syntex Lecturer, University of California, Berkeley, USA
February 1992	The Firth Lectureship, University of Sheffield, Sheffield, Great Britain
March 1992	GLAXO Lecturer, Duke University, Durham, NC, USA
April 1992	Carl Shipp Marvel Lecturer, University of Illinois at Urbana-Champaign, Urbana, USA
May 1992	Merck Lecturer, University of Cambridge, Cambridge, Great Britain
November 1992	Bergmann Lecturer, Yale University, New Haven CT, USA
March 1993	The Twelfth Distinguished Warner-Lambert Lecturer, Michigan State University, East Lansing, USA
October 1993	Clemo Lecturer, University of Newcastle upon Tyne, Great Britain
November 1993	The 1993 Bio-Méga-Boehringer-Ingelheim Lecturer, University of Sherbrooke, Sherbrooke, Canada
February 1994	Ligand Pharmaceuticals Lecturer, Lecture Series on "Frontiers in Chemistry", The ScRIPPS Research Institute, La Jolla, USA
July 1994	5th Merck-Schuchardt-Chair in Organic Synthesis, 5th Belgian Organic Synthesis Symposium (BOSS 5), July 11-15, 1994, Namur, Belgium
March 1995	Schering Lecture, Schering Aktiengesellschaft, Berlin, Germany
July 1995	Interdisziplinäre Vorlesungsreihe der Sandoz-Stiftung für therapeutische Forschung und Sandoz-Preis, University of Regensburg, Germany

Curricula Vitae

Andreas Brunner	was born in Brig-Glis (Switzerland) in 1966. He studied chemistry at the ETH Zürich (diploma thesis in 1990 with D. Seebach). Since 1991 he is working as a graduate student on the synthesis of 3-HB derivatives and on the physiological occurrence and properties of 3-HB oligomers in the group of D. Seebach at the ETH Zürich.
Beat Markus Bachmann	was born in Zürich (Switzerland) in 1968. He studied chemistry at the University of Zürich (diploma thesis in 1993 with A. Vasella). Since 1993 he is working as a graduate student on the enzymatic degradation of P(3-HB) with D. Seebach at the ETH Zürich.
Torsten Hoffmann	was born in Cologne (Germany) in 1967. He studied chemistry at the Heinrich-Heine University of Düsseldorf (diploma thesis in 1992 with M. Braun). Since 1993 he is working as a graduate student on the synthesis of cyclic derivatives of 3-HB with D. Seebach at the ETH Zürich.
Florian Nicolas Maximilian Kühnle	was born in Wiesbaden (Germany) in 1968. He studied chemistry at the ETH Zürich (diploma thesis in 1992 with M. Quack). Since 1993 he is working as a graduate student on the structure determination of oligo(3-HB) derivatives with D. Seebach at the ETH Zürich.
Urs Daniel Lengweiler	was born in Basel (Switzerland) in 1968. He studied chemistry at the ETH Zürich (diploma thesis in 1991 with D. Seebach). Since 1992 he is working as a graduate student on the synthesis of monodisperse oligo(3-HB) derivatives with D. Seebach at the ETH Zürich.

ISSN 0940-9300